Exploring the deep interior of giant planets with density functional theory and shock-compression experiments

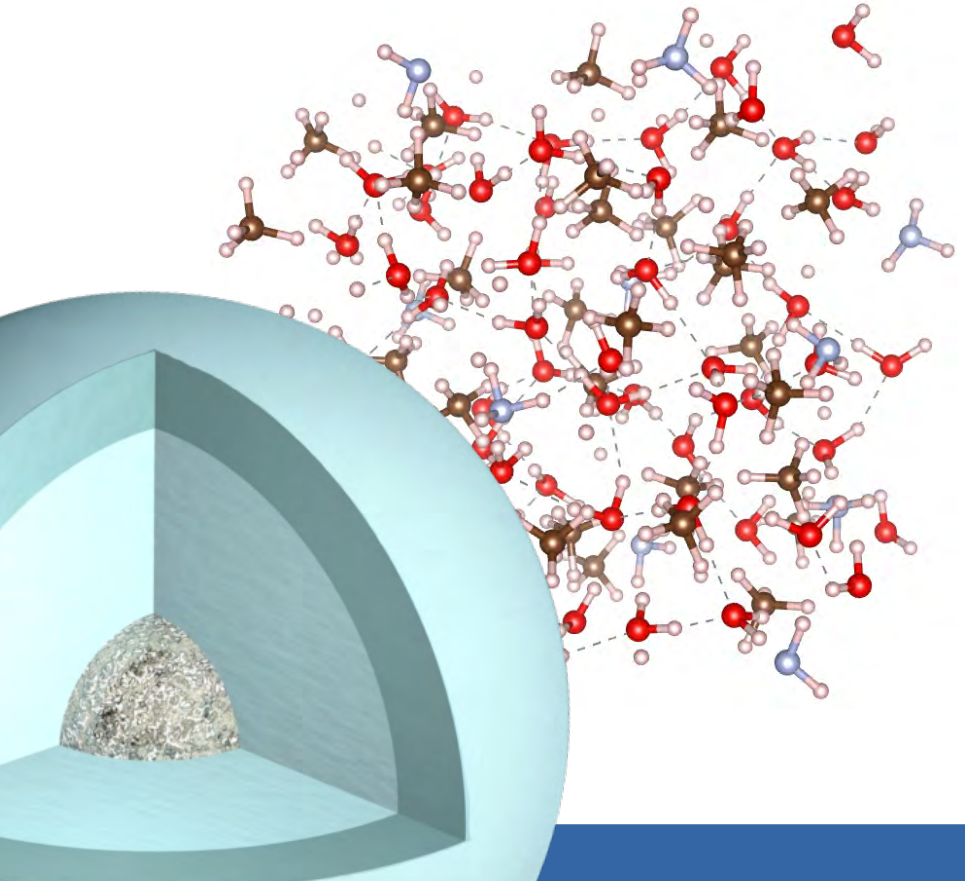

Mandy Bethkenhagen

4th DyCoMaX Workshop

March 13, 2024

Acknowledgement

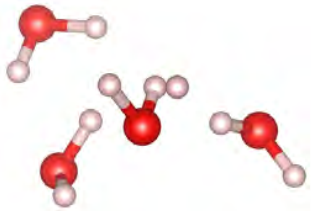

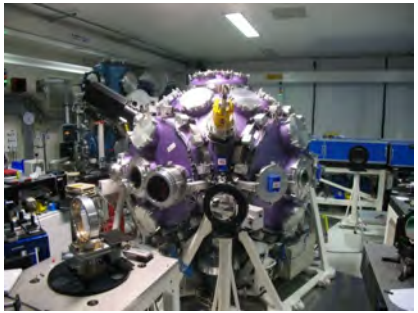

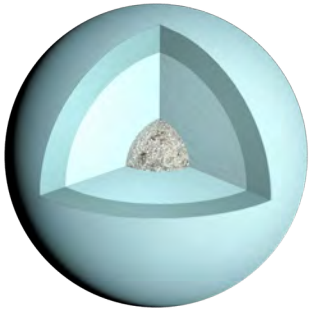

Simulations

Bingqing Cheng, Martin French, Sébastien Hamel, Chris Pickard, Ronald Redmer

Experiments

Alessandra Benuzzi-Mounaix, Federica Coppari, Frédéric Datchi, Marco Guarguaglini, Jean-Alexis Hernandez, Frederic Lefevre, Marius Millot, Alessandra Ravasio, Florent Occelli, Sandra Ninet, Tommaso Vinci

Planetary modeling

Nadine Nettelmann and Ludwig Scheibe

Exoplanet diversity

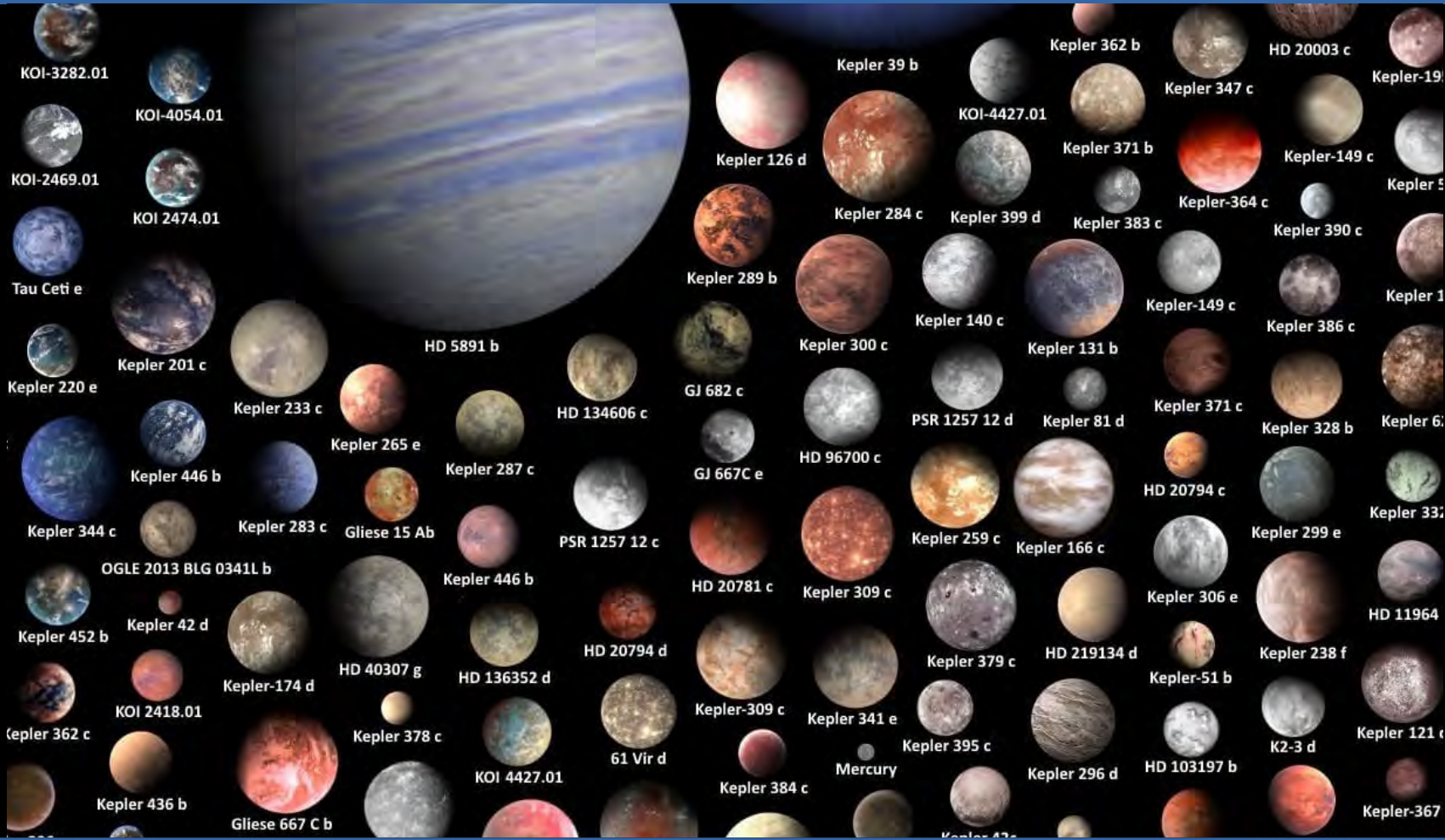

Exoplanet diversity

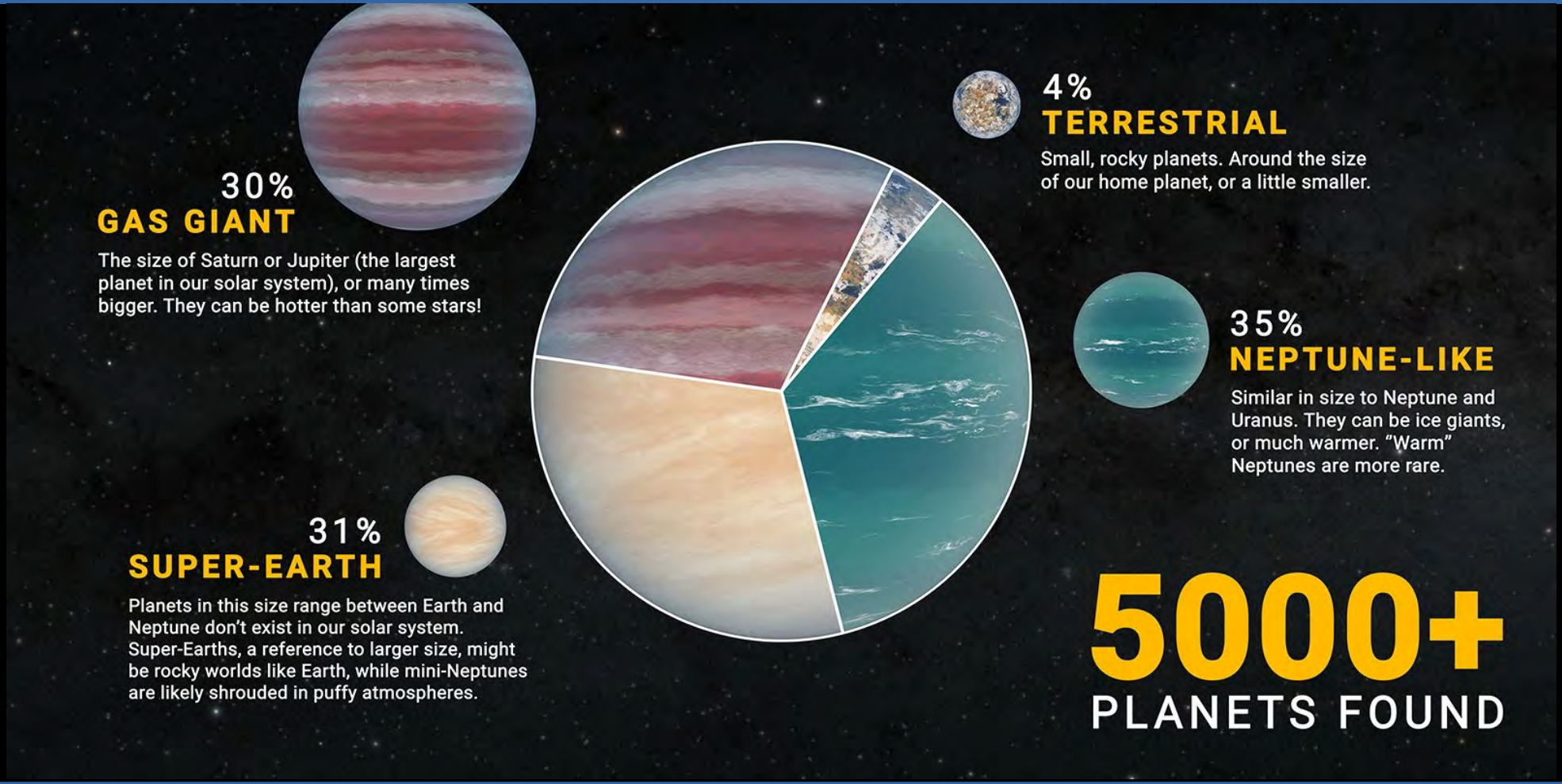

Voyager 2: The last mission to visit the ice giants

Uranus: 1986

Neptune: 1989

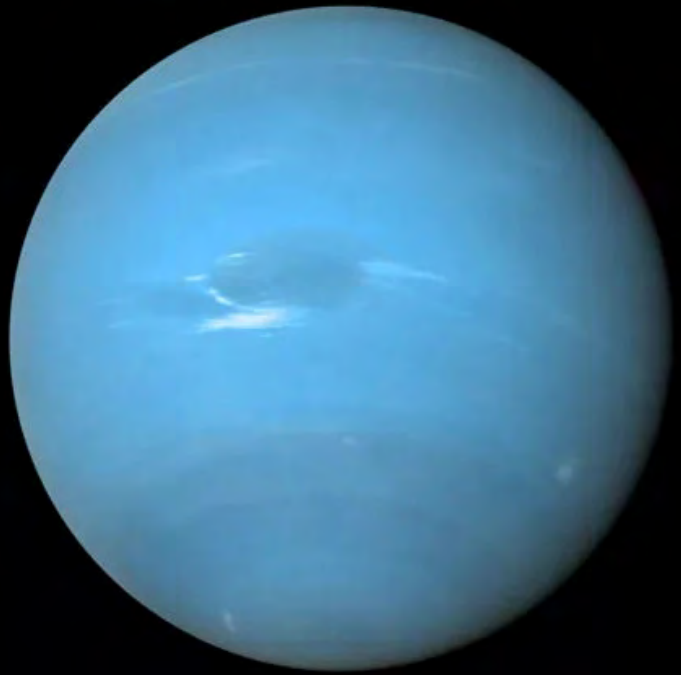

Magnetic field of Uranus

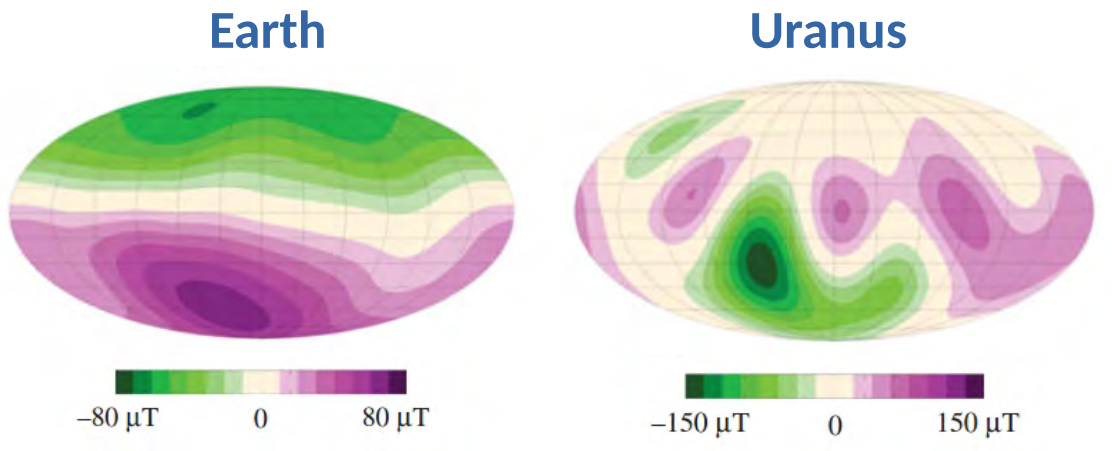

Soderlund & Stanley, Philos. Trans. Royal Soc. A **378**, 20190479 (2020).

Magnetic field of Uranus

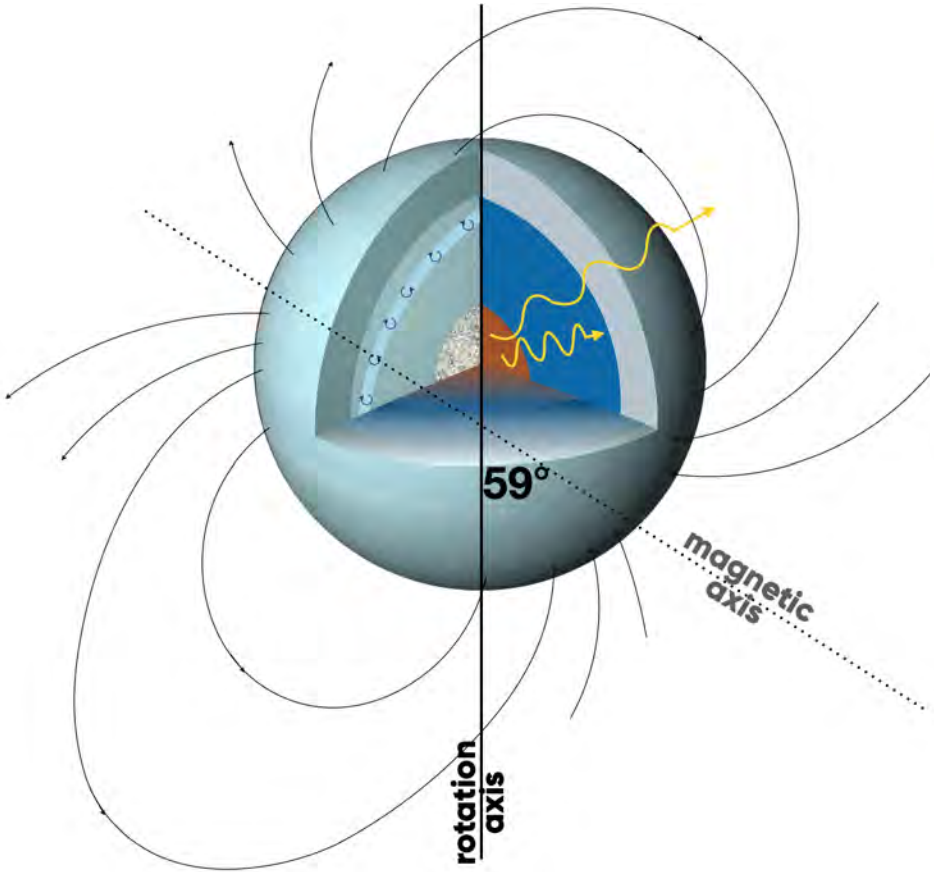

courtesy of A. Ravasio

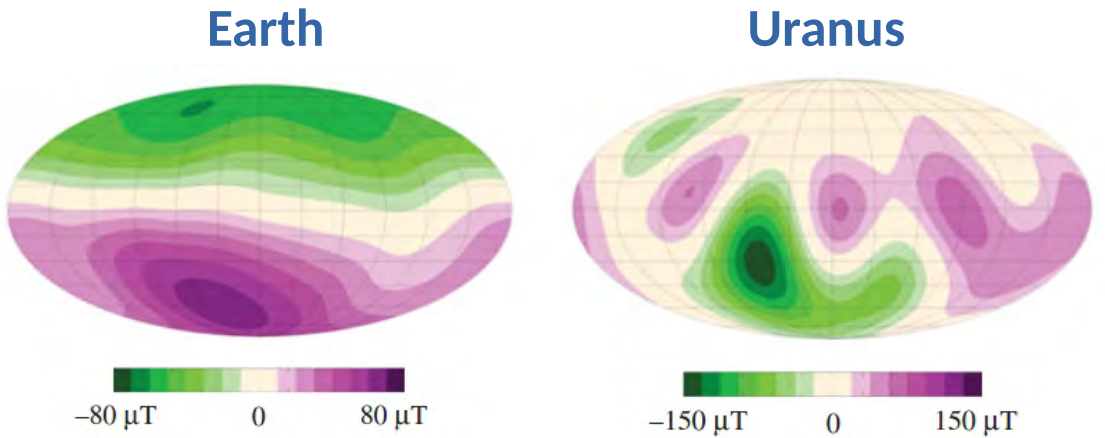

- highly non-axisymmetric non-dipolar magnetic field
  → connection to interior structure?
  → formation and evolution?

Soderlund & Stanley, Philos. Trans. Royal Soc. A **378**, 20190479 (2020).

Interior structure

outer mantle
molecular fluid
(H/He)

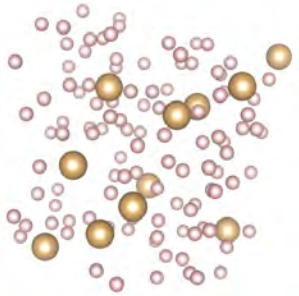

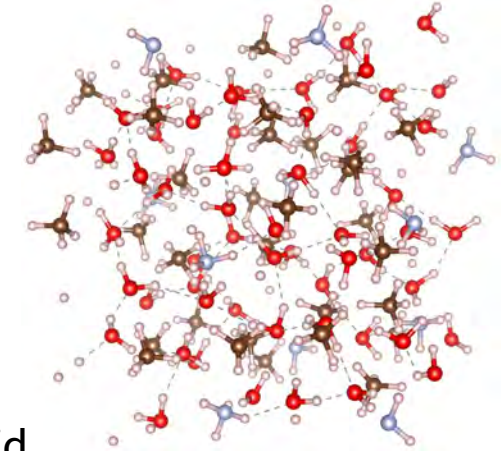

inner mantle
complex ionic fluid
"planetary ices"
(H_2O, NH_3, CH_4)

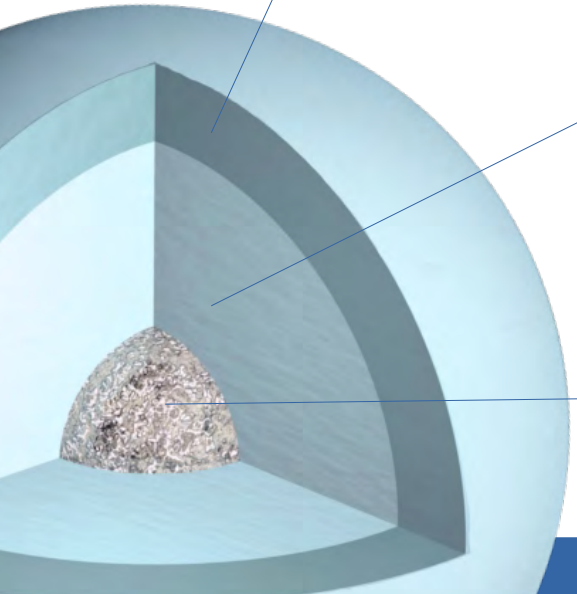

core
rocky solid
(MgO, SiO_2, Fe)

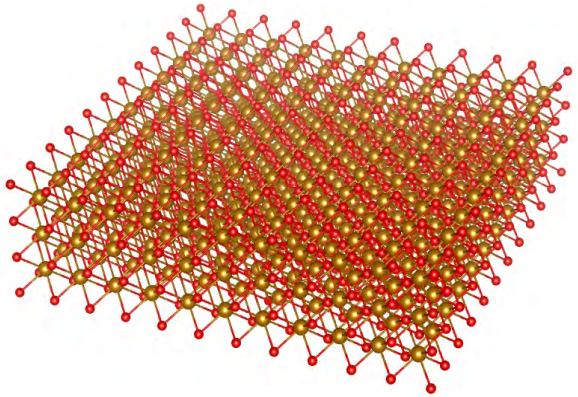

Interior structure

outer mantle
molecular fluid
(H/He)

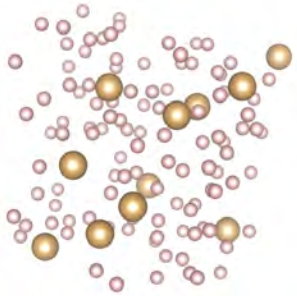

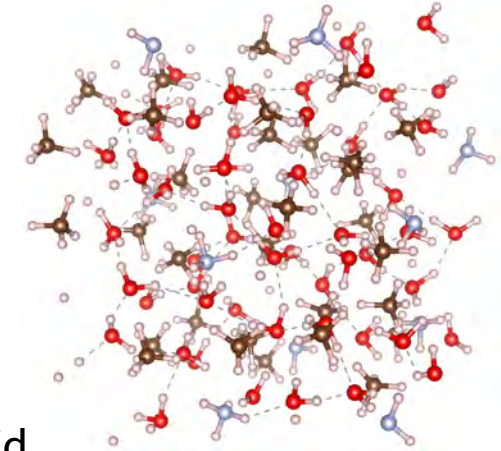

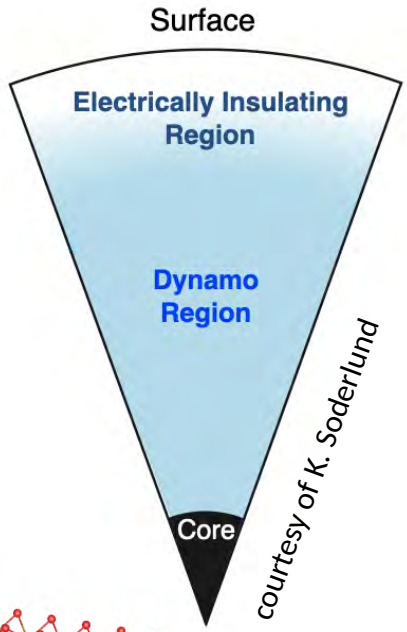

inner mantle
complex ionic fluid
"planetary ices"
(H_2O, NH_3, CH_4)

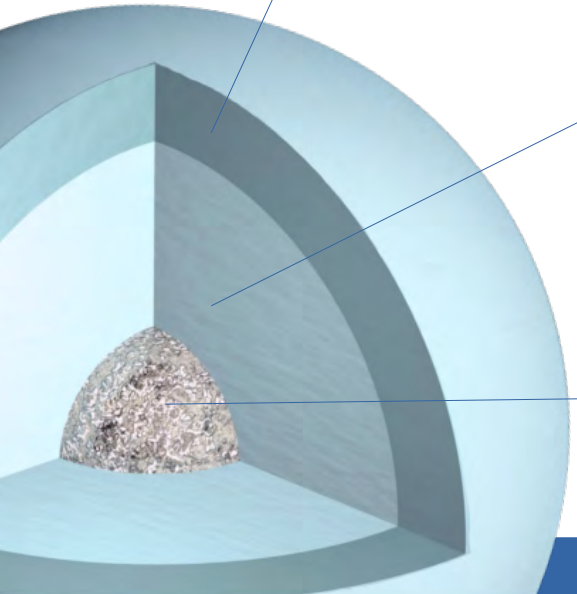

core
rocky solid
(MgO, SiO_2, Fe)

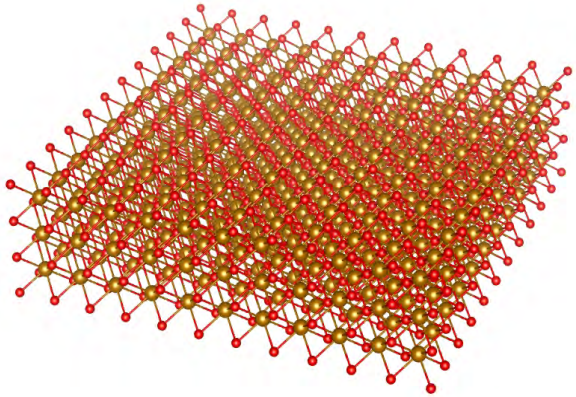

Interior structure

fluid

superionic

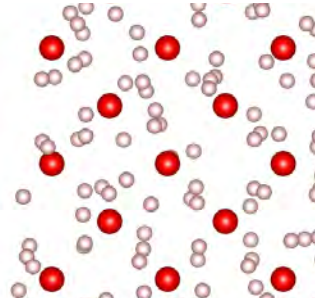

solid

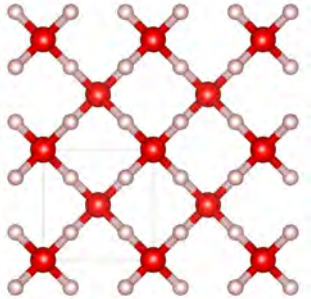

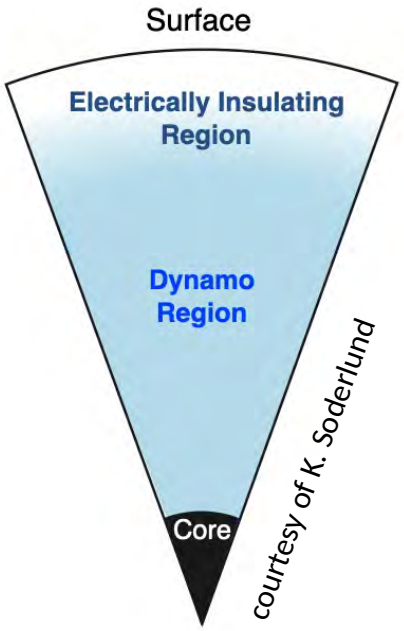

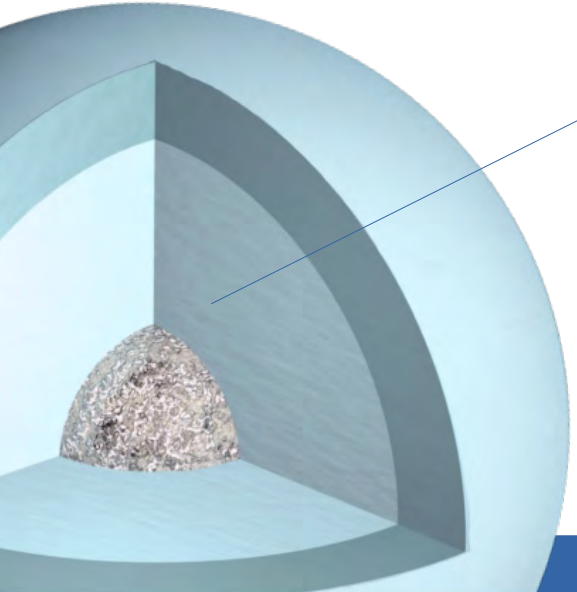

inner mantle
fluid water
and/or
superionic water?

- characteristics of the superionic phase:

  → protons moving freely through the oxygen lattice

  → high ionic conductivity

Ab initio simulations

Molecular dynamics

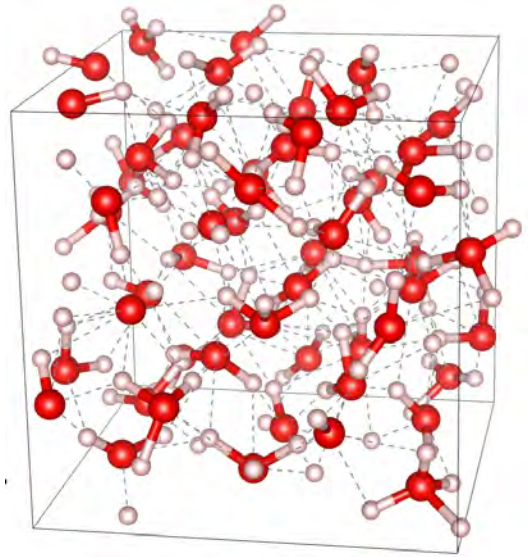

100 - 1000 atoms

- ions are described as classical particles in molecular dynamics framework

Hafner, J. Comput. Chem. **29**, 2045 (2008).
Kresse and Hafner, Phys. Rev. B **47**, 558 (1993).
Perdew et al., Phys. Rev. Lett. **77**, 3865 (1996).

Ab initio simulations

Molecular dynamics + density functional theory

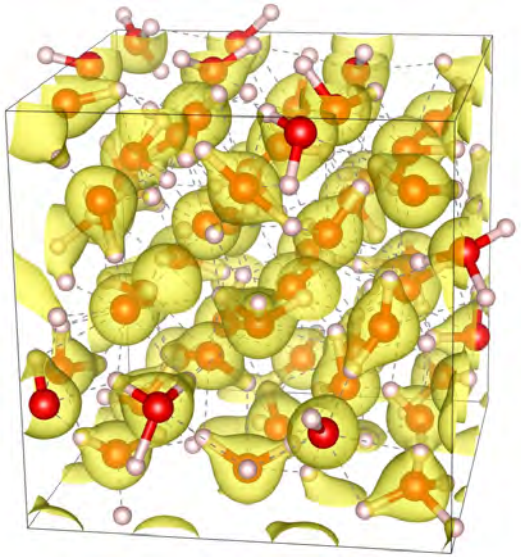

100 - 1000 atoms

- ions are described as classical particles in molecular dynamics framework
- electrons are treated quantum mechanically, where wave functions are replaced by electron density

Hafner, J. Comput. Chem. **29**, 2045 (2008).
Kresse and Hafner, Phys. Rev. B **47**, 558 (1993).
Perdew et al., Phys. Rev. Lett. **77**, 3865 (1996).

Ab initio simulations

Molecular dynamics + density functional theory

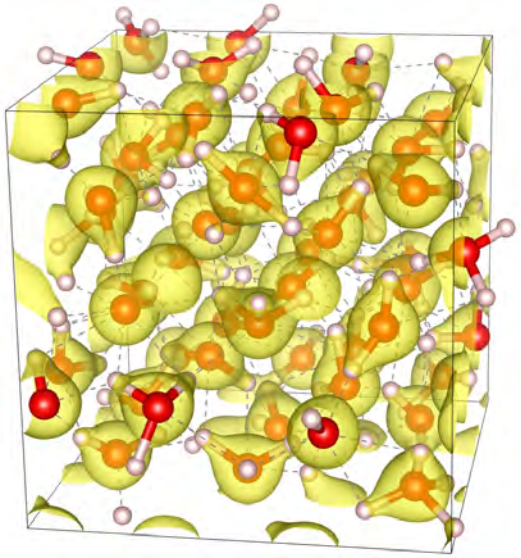

100 - 1000 atoms

- ions are described as classical particles in molecular dynamics framework
- electrons are treated quantum mechanically, where wave functions are replaced by electron density
- exchange-correlation functional determines accuracy of the results

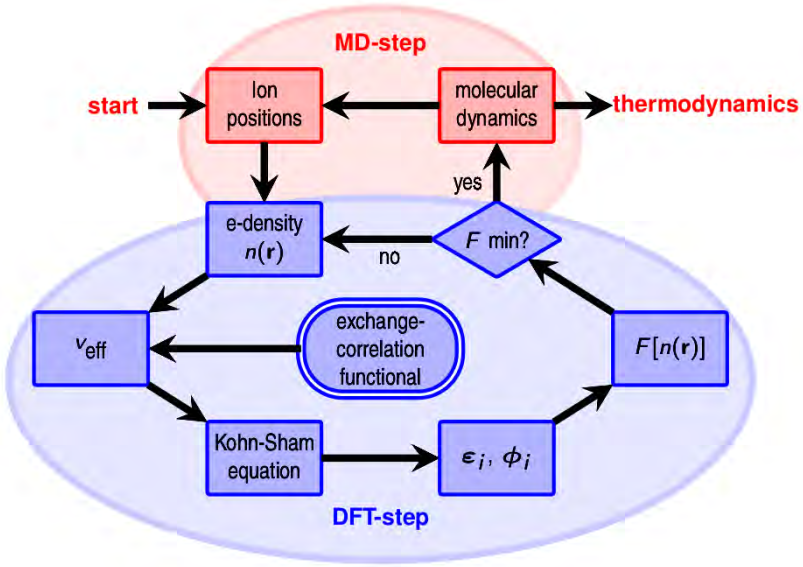

Hafner, J. Comput. Chem. **29**, 2045 (2008).
Kresse and Hafner, Phys. Rev. B **47**, 558 (1993).
Perdew et al., Phys. Rev. Lett. **77**, 3865 (1996).

Ab initio simulations

Molecular dynamics + density functional theory

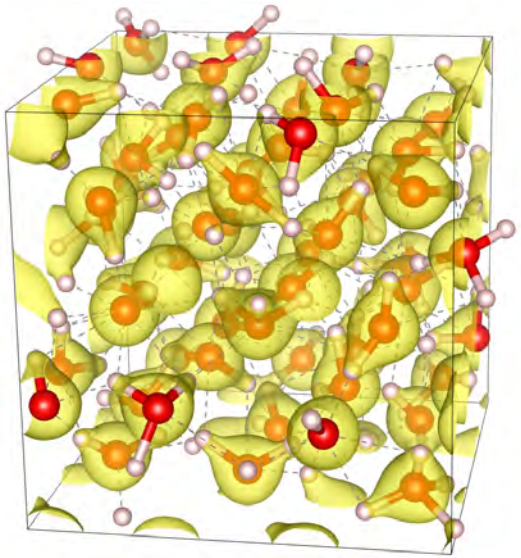

100 - 1000 atoms

... between condensed matter and plasma physics

- solid state densities (up to 10-fold compression)
- high temperatures (several 1000 K)

  → strong correlations

  → metallization, ionization, dissociation

Ab initio simulations

Molecular dynamics + density functional theory

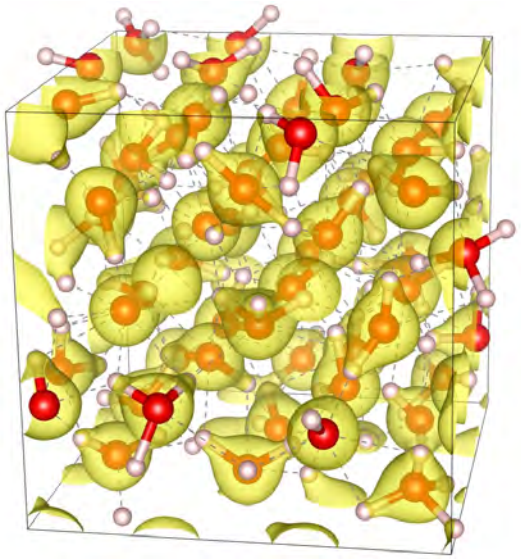

100 - 1000 atoms

… between condensed matter and plasma physics

- solid state densities (up to 10-fold compression)
- high temperatures (several 1000 K)

  → strong correlations

  → metallization, ionization, dissociation

Key quantities

- equations of state → P(ρ,T) & E(ρ,T)
- structure → pair distribution function, bonding
- transport → electrical conductivity, diffusion
- optical properties → reflectivity, opacity

DFT-MD water phase diagram

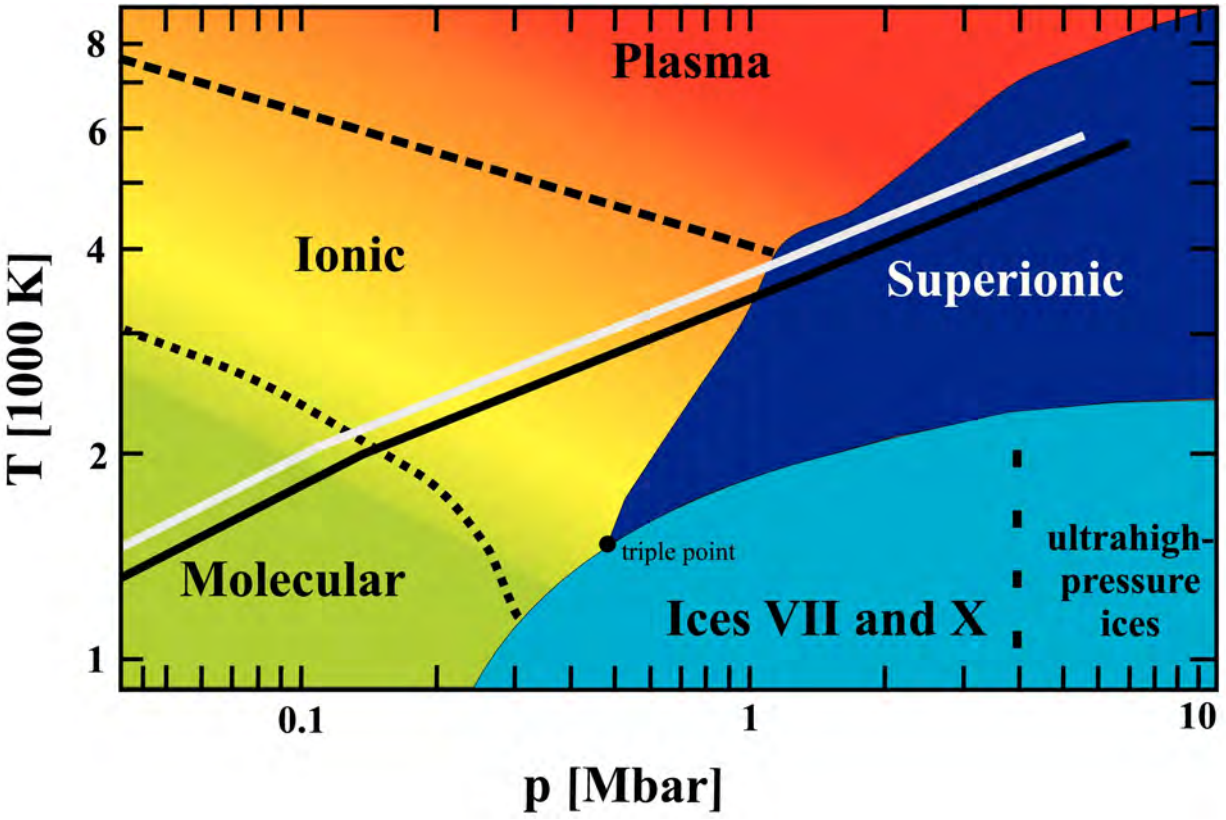

French et al., Phys. Rev. B **79**, 054107 (2009).
Redmer et al., Icarus **211**, 798 (2011).

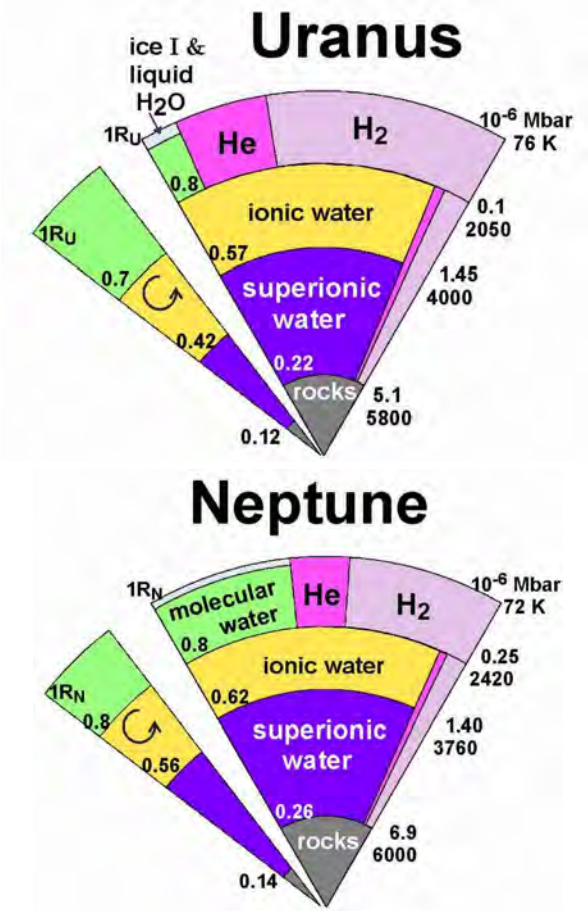

Stanley & Bloxham, Icarus **184**, 556 (2006).

Standard adiabatic models for giant planets

Evolution model

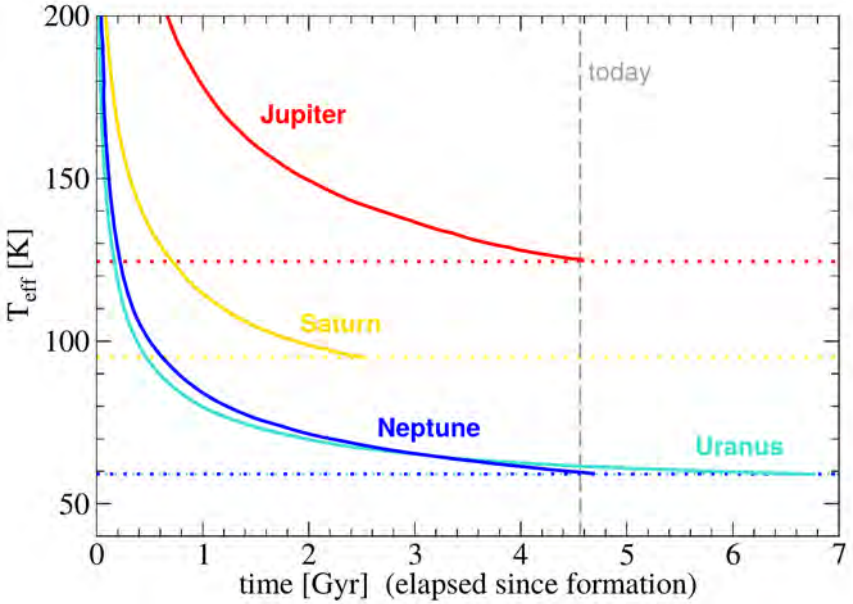

Interior modeling directions

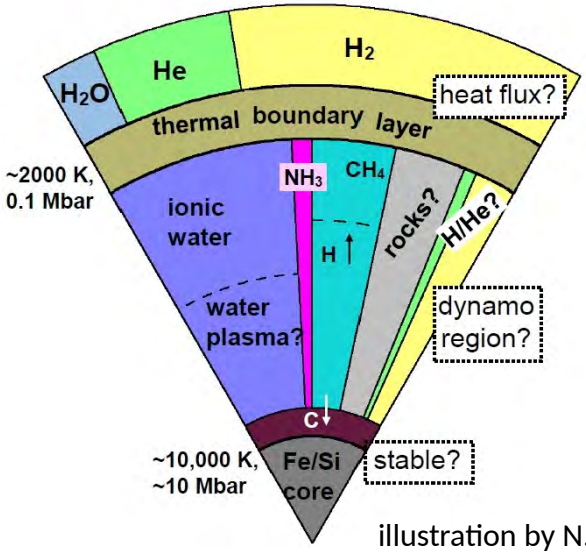

illustration by N. Nettelmann

- Uranus' age cannot be modeled using adiabatic models based on the water EOS only
- need transport and optical properties of water and other materials (e.g. ammonia, methane)

Standard adiabatic models for giant planets

Questions addressed in the following

I. How can we improve the phase diagram and EOS of water?

II. Is it important to consider ammonia?

III. What do we know about high-pressure methane?

Interior modeling directions

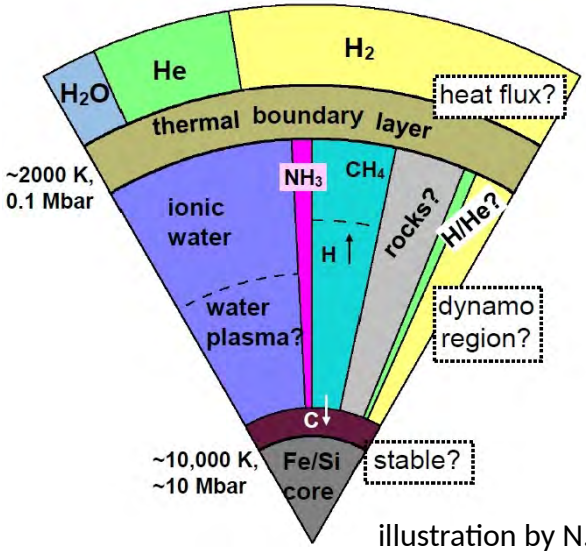

illustration by N. Nettelmann

- Uranus' age cannot be modeled using adiabatic models based on the water EOS only
- need transport and optical properties of water and other materials (e.g. ammonia, methane)

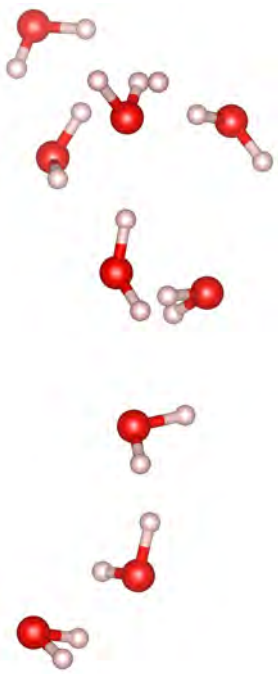

I. How can we improve the phase diagram and EOS of water?

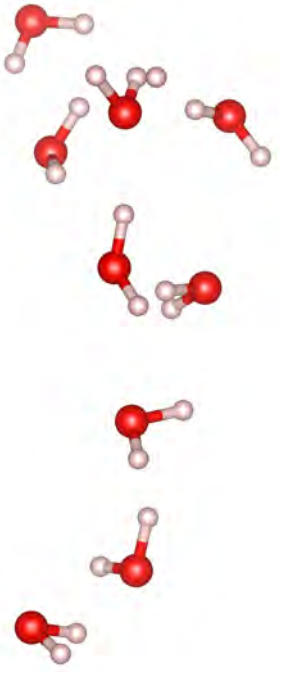

High-pressure experiments: diamond anvil cells

Schematic setup

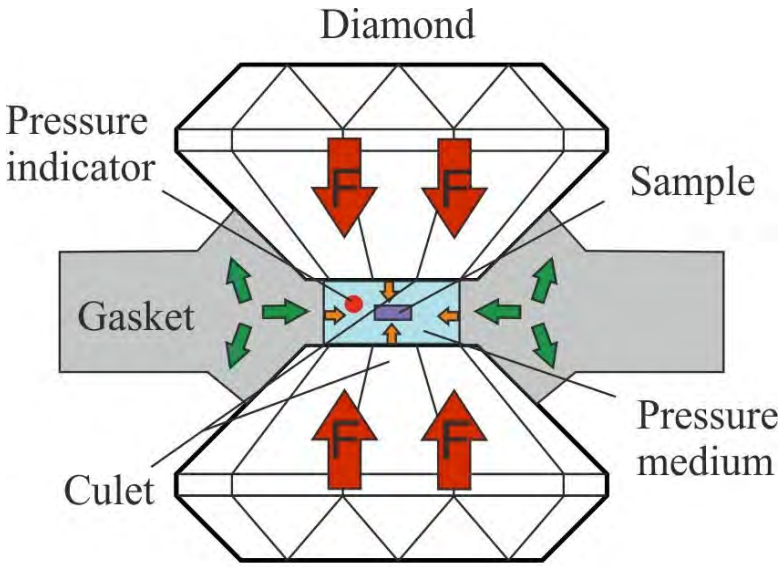

- mostly used at small temperatures (<= 3000 K) and pressures up to 300 GPa

High-pressure experiments: diamond anvil cells

Schematic setup

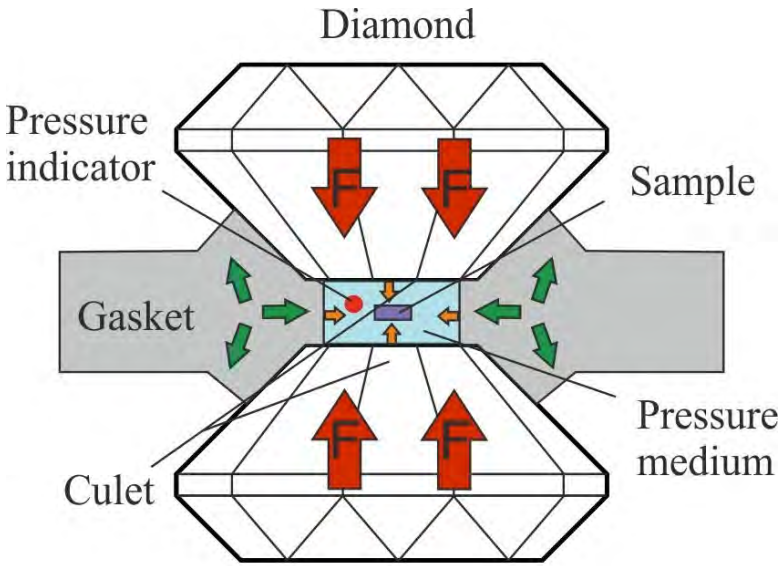

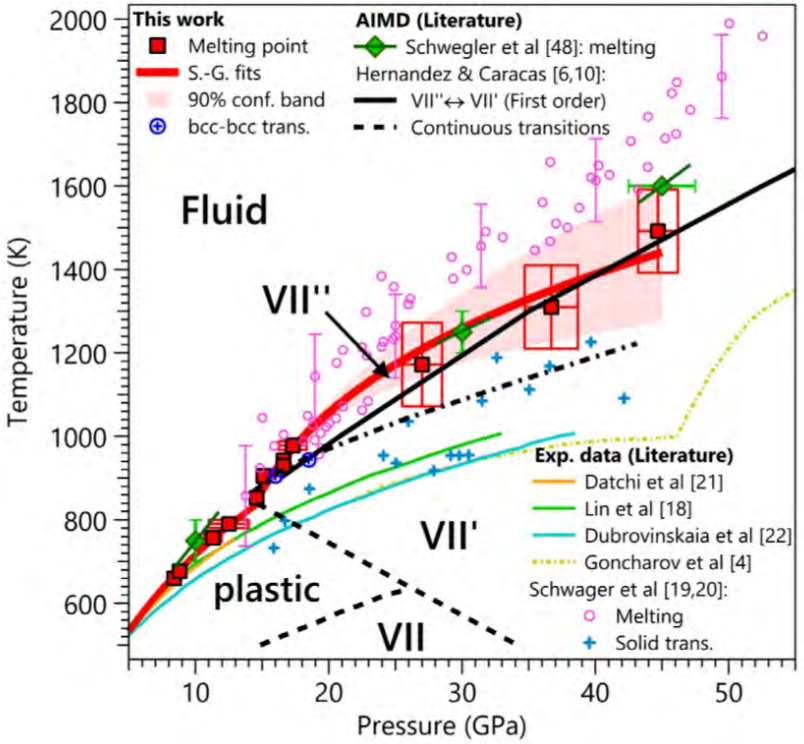

- mostly used at small temperatures (<= 3000 K) and pressures up to 300 GPa

Hernandez & Caracas, J. Chem. Phys. **148**, 214501 (2018).
Queyroux et al., Phys. Rev. Lett. **125**, 195501 (2020).

High-pressure experiments: shock-compression

Schematic setup

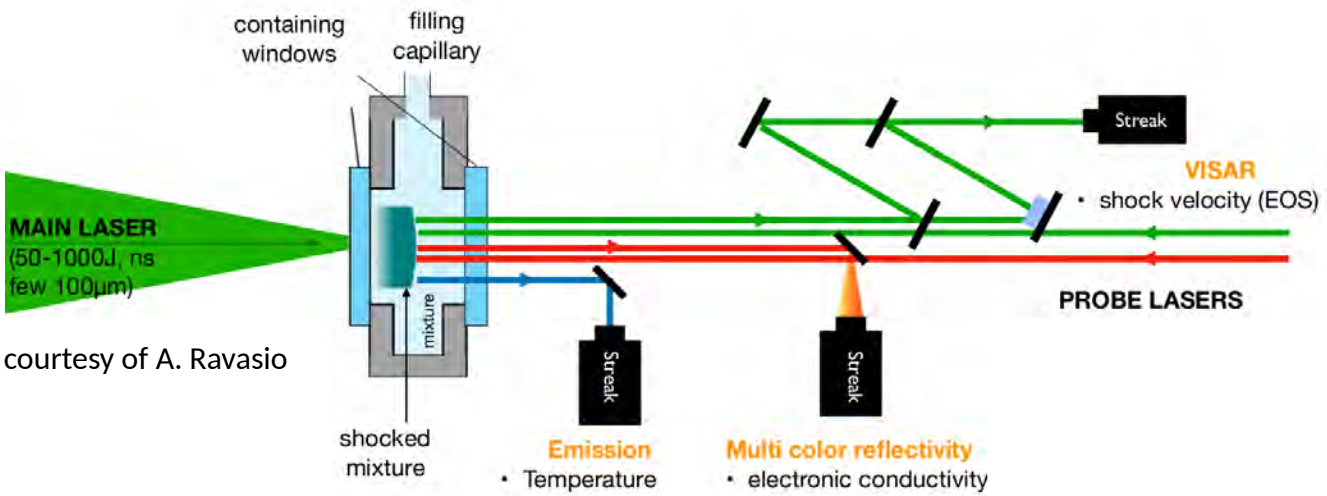

courtesy of A. Ravasio

Hugoniot equation

$$u_1 - u_0 = \frac{1}{2}(p_1 + p_0)\left(\frac{1}{\varrho_0} - \frac{1}{\varrho_1}\right)$$

High-pressure experiments: shock-compression

Schematic setup

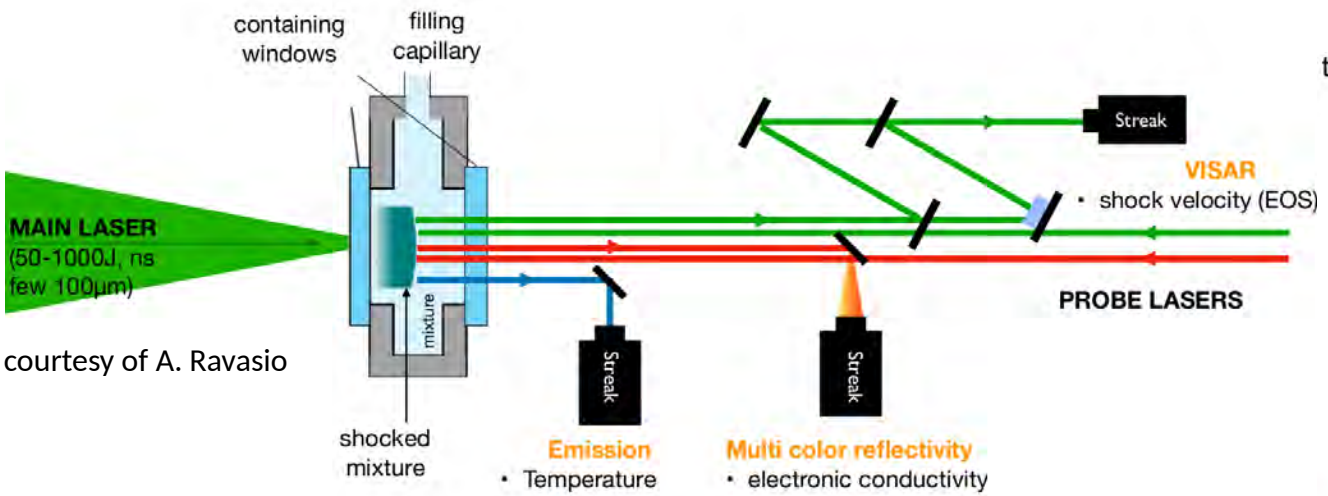

courtesy of A. Ravasio

Shock conditions

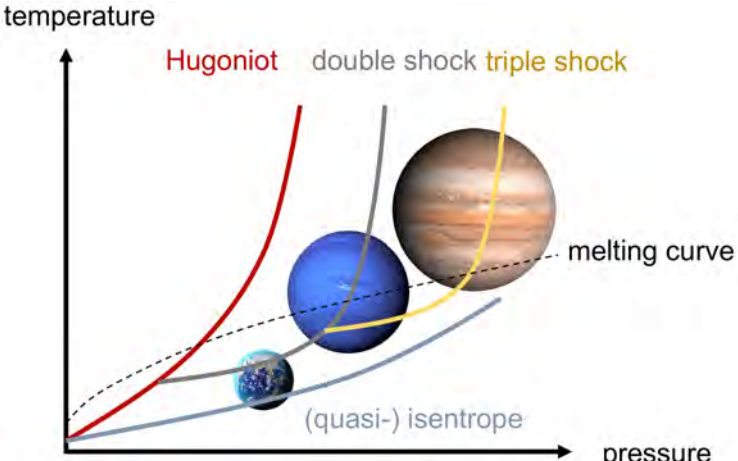

illustration by D. Kraus

Hugoniot equation

$$u_1 - u_0 = \frac{1}{2}(p_1 + p_0)\left(\frac{1}{\varrho_0} - \frac{1}{\varrho_1}\right)$$

- Hugoniot reaches fast high temperatures (e.g. several 10000 K at about 300 GPa for ices)
  → multiple shocks or pre-compression (with DAC) of sample is required to reach ice giant conditions

Shock compression experiments for water

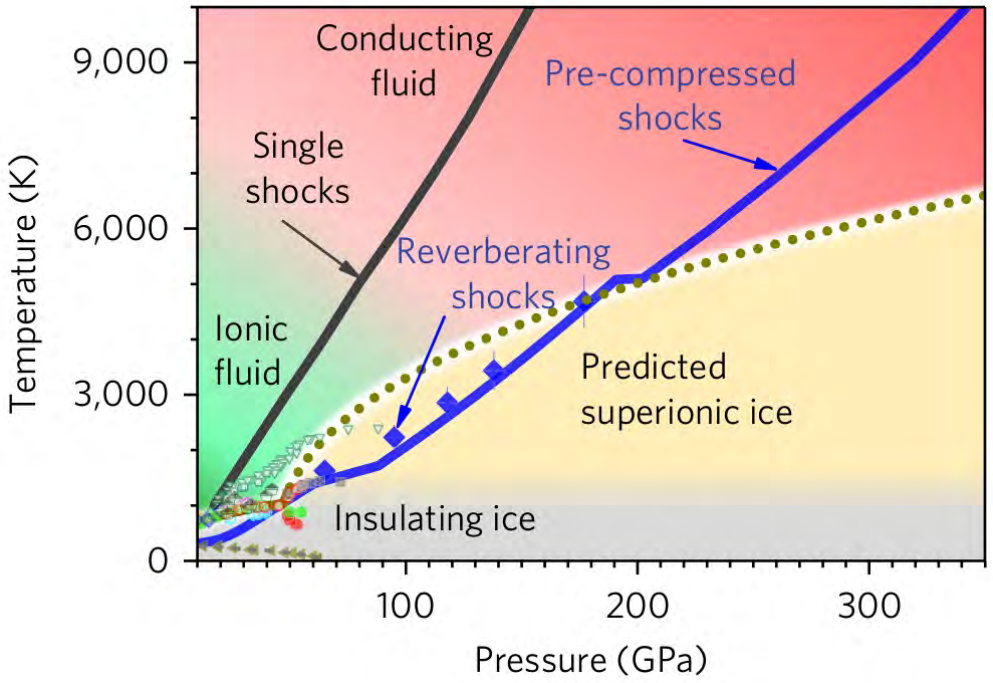

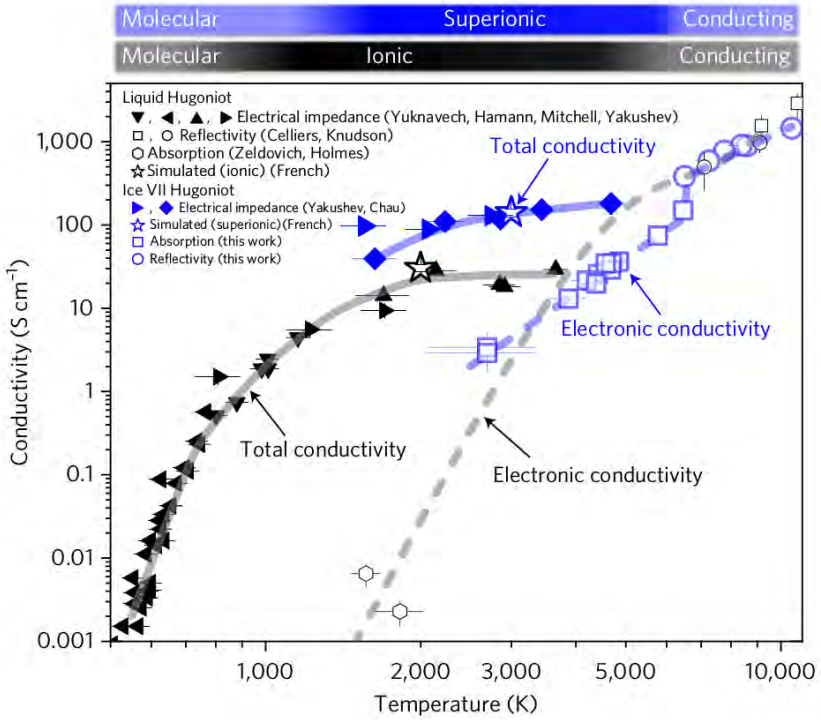

- superionic water identified along the pre-compressed Hugoniot (initial density 1.60 g/cm^3)

Millot et al., Nature Physics **14**, 297 (2018).

Shock compression experiments for water

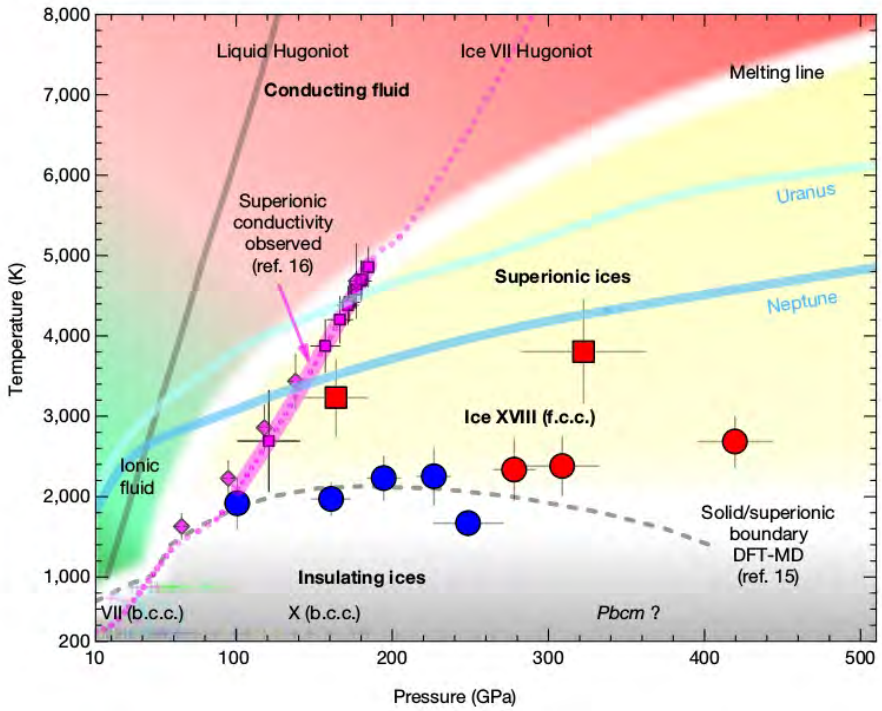

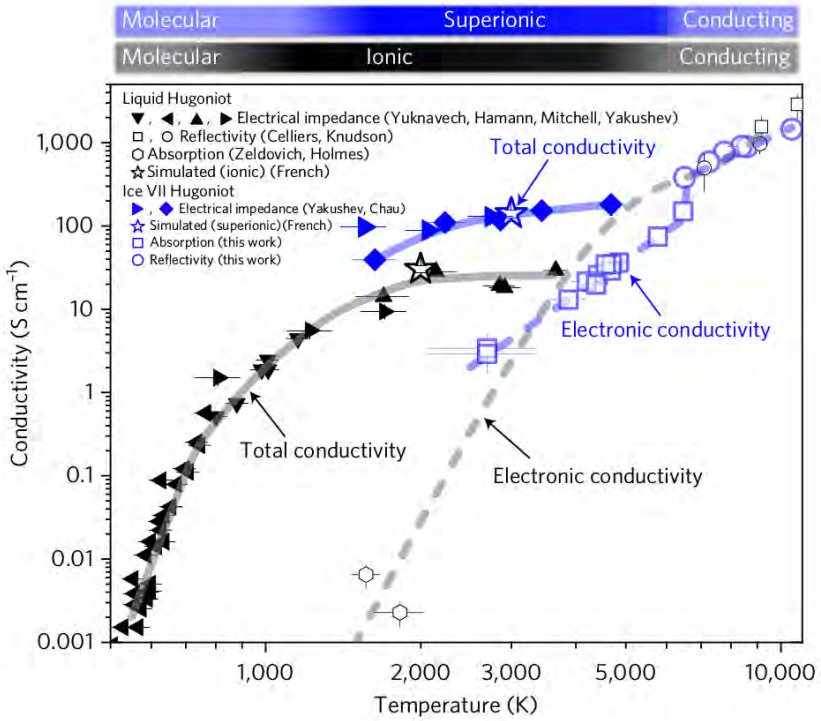

- superionic water identified along the pre-compressed Hugoniot (initial density 1.60 g/cm^3)
- 2 different superionic lattices found (fcc and bcc)

Millot et al., Nature Physics **14**, 297 (2018).
Millot & Coppari et al., Nature **569**, 251 (2019).

Superionic fcc or bcc?

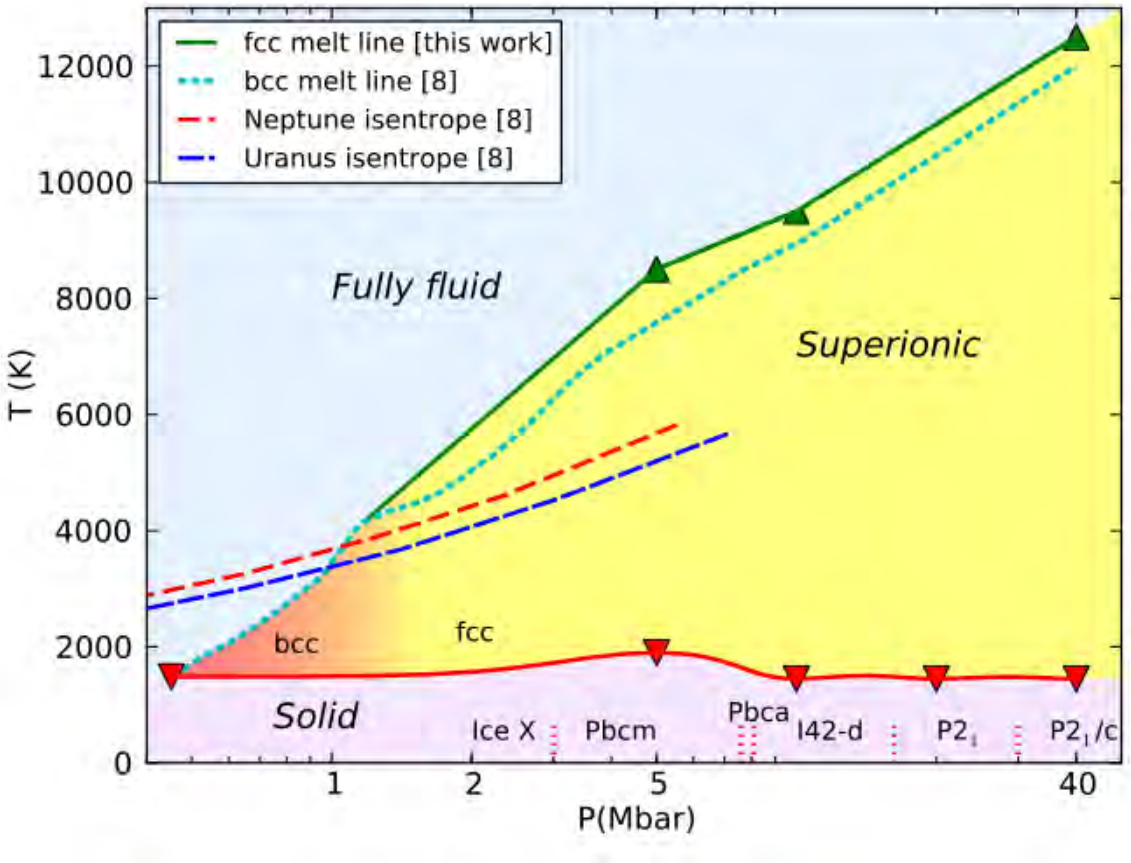

bcc

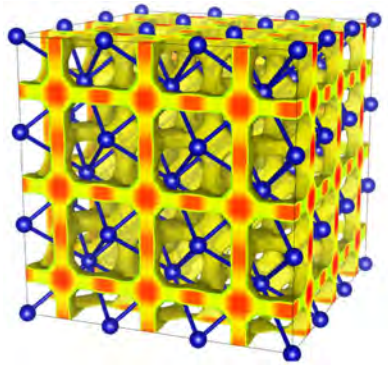

fcc

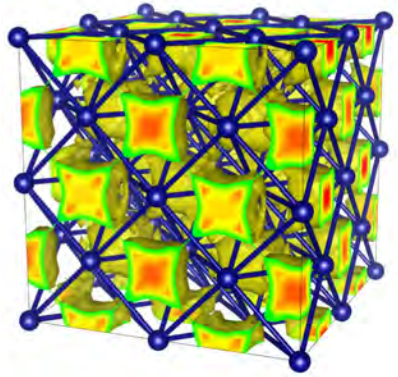

Wilson et al., Phys. Rev. Lett. **110**, 151102 (2013).
Sun et al., Nat. Commun. **6**, 8156 (2015).
French et al., Phys. Rev. E **94**, 125508 (2016).

Ab initio simulations

Molecular dynamics + density functional theory

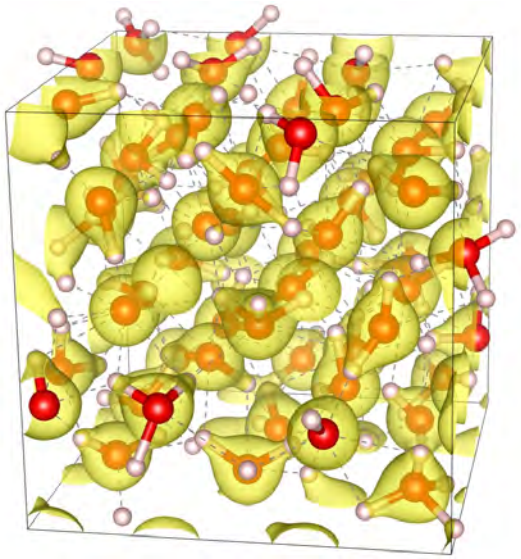

100 - 1000 atoms

… between condensed matter and plasma physics

- solid state densities (up to 10-fold compression)
- high temperatures (several 1000 K)

  → strong correlations

  → metallization, ionization, dissociation

Computational cost limits…

- system size & simulation length
- compositional complexity
- sampling to calculate entropy consistently

Moving towards large-scale simulations

Molecular dynamics + density functional theory

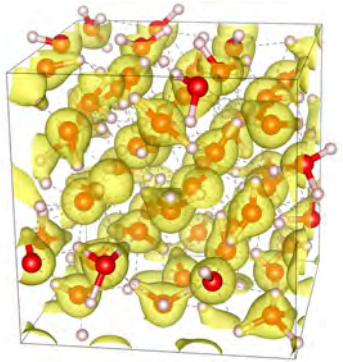

100 - 1000 atoms

machine-learning potential (MLP)

= transfer of ab initio accuracy to large-scale simulations

Large-scale simulations

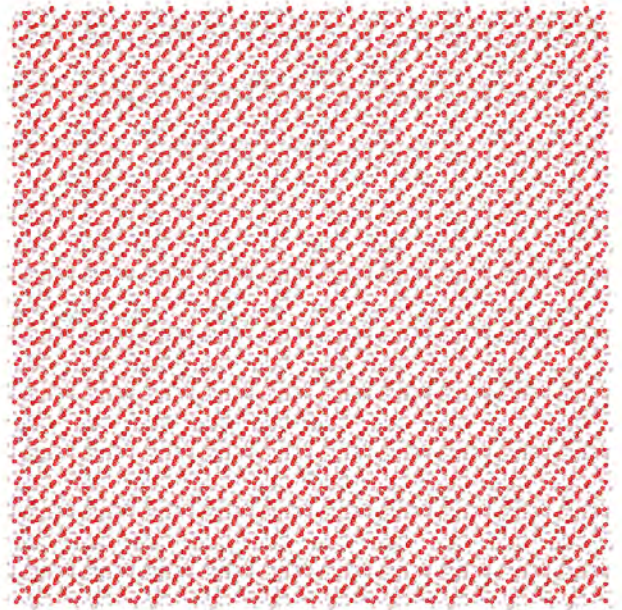

20 000 atoms

Behler & Parrinello, Phys. Rev. Lett. **98**, 146401 (2007).
Singraber et al., J. Chem. Theory Comput. **15**, 3075 (2019).
Cheng, et al., PNAS **116**, 1110 (2019).

Moving towards large-scale simulations

Molecular dynamics + density functional theory

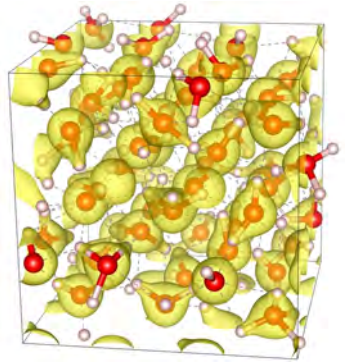

100 - 1000 atoms

machine-learning potential (MLP)

= transfer of ab initio accuracy to large-scale simulations

Large-scale simulations

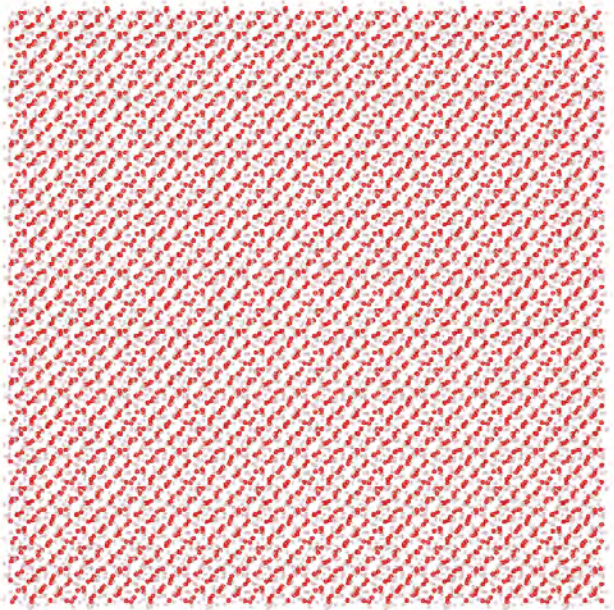

20 000 atoms

Key quantities

- equations of state → P(ρ,T) & E(ρ,T) **+ S(ρ,T) & phase transitions**
- structure → pair distribution function, bonding
- transport → electrical conductivity, diffusion **+ ionic conductivity & viscosity**
- optical properties → reflectivity, opacity
- **(de-)mixing effects, reaction kinetics and interface stabilities**

High-pressure MLP-based phase diagram

- MLP based on artificial neural network architecture built according to framework of Behler & Parrinello
- selected 84 Behler-Parrinello symmetry functions to describe atomic environments
- used the implementation in the n2p2 code

Symmetry functions

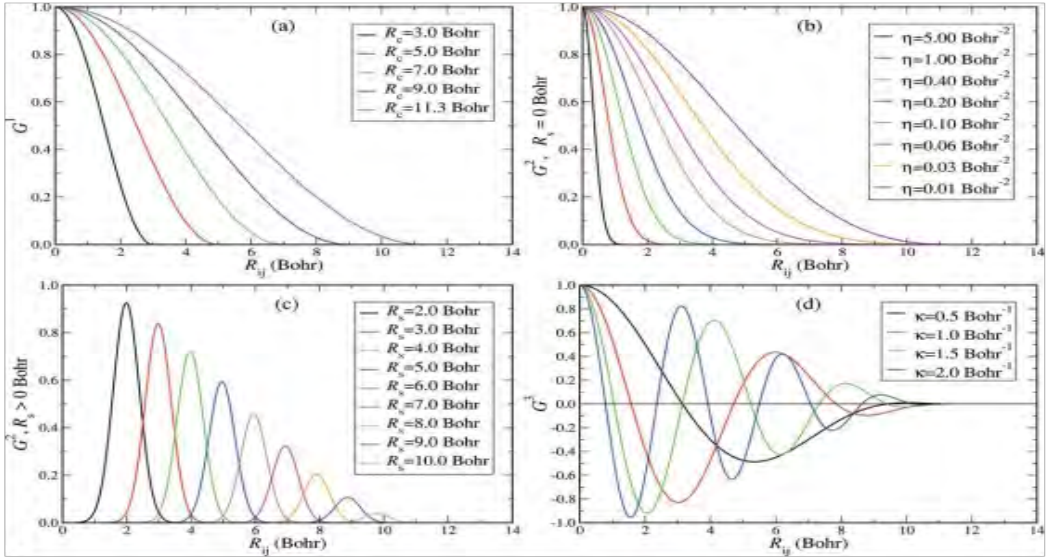

Neural network

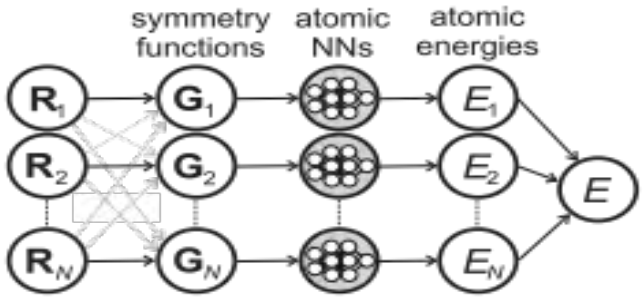

Behler & Parrinello, Phys. Rev. Lett. **98**, 146401 (2007).
Singraber et al., J. Chem. Theory Comput. **15**, 1827 (2019).
Cheng, et al., PNAS **116**, 1110 (2019).
Monserrat et al., Nat. Commun. **11**, 5757 (2020).

Training data set

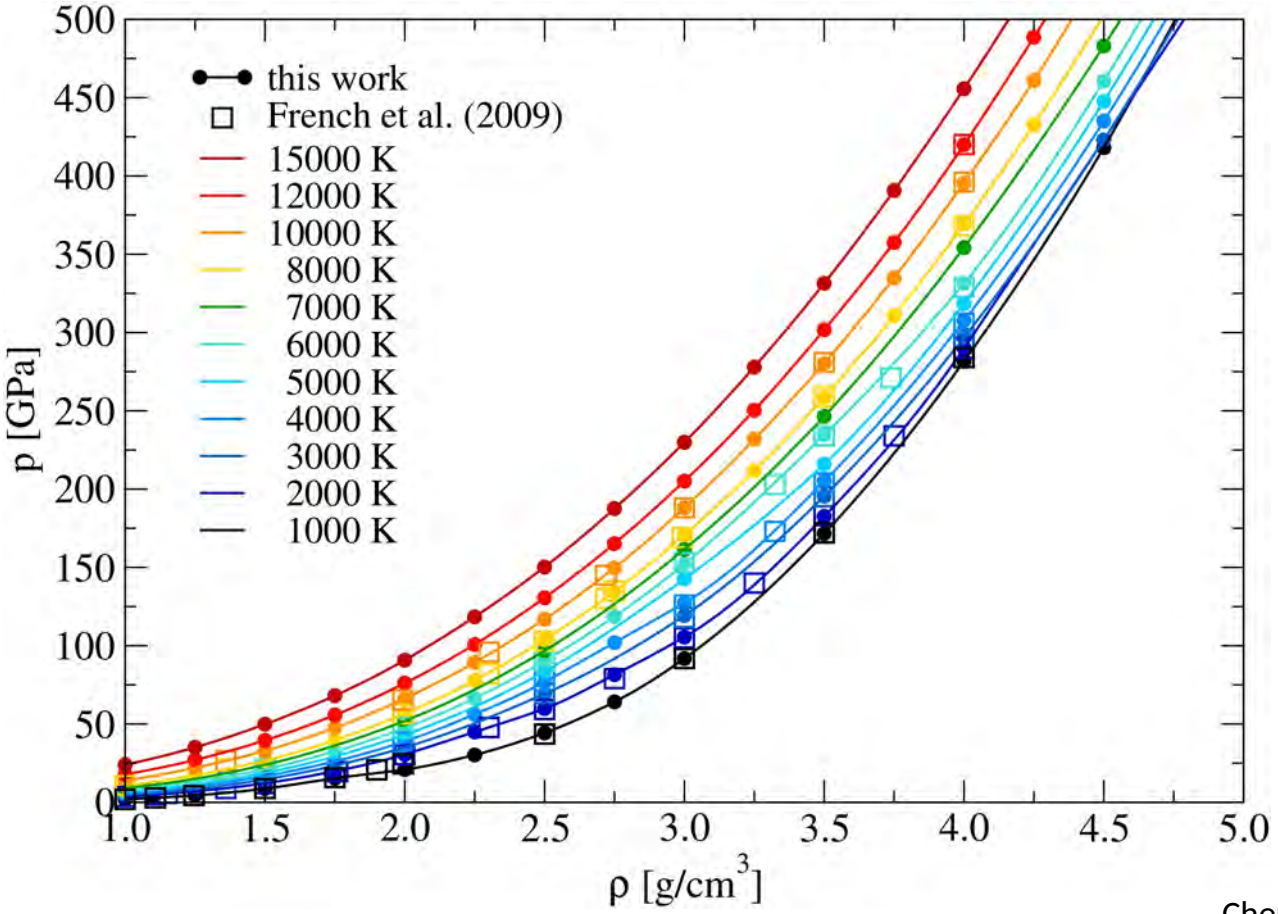

- largest data set contains 54 molecules for wide p-T range (~10600 structures)
- tested different functionals
- added 1000 structures used previously to train MLP for low-pressure phase diagram
- active learning yielded ~5900 additional structures
- total set contains ~17000 structurally diverse configurations (10% taken out for testing set)

French et al., Phys. Rev. B **79**, 054107 (2009).
Cheng, Bethkenhagen et al., Nat. Phys. **17**, 1228 (2021).

Water phase transitions based on MLP

coexistence calculations

liquid

superionic

liquid

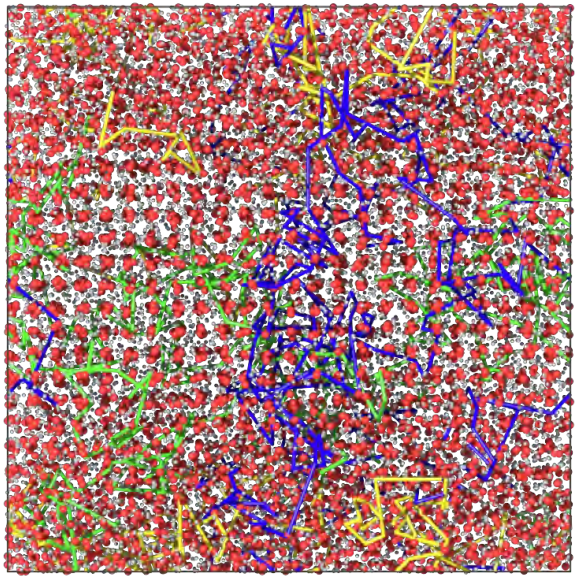

Cheng, Bethkenhagen et al., Nat. Phys. **17**, 1228 (2021).

Water phase transitions based on MLP

coexistence calculations

liquid

superionic

liquid

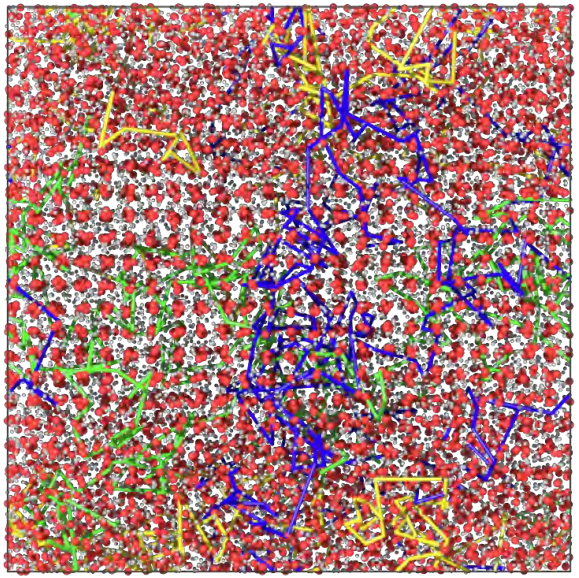

chemical potential

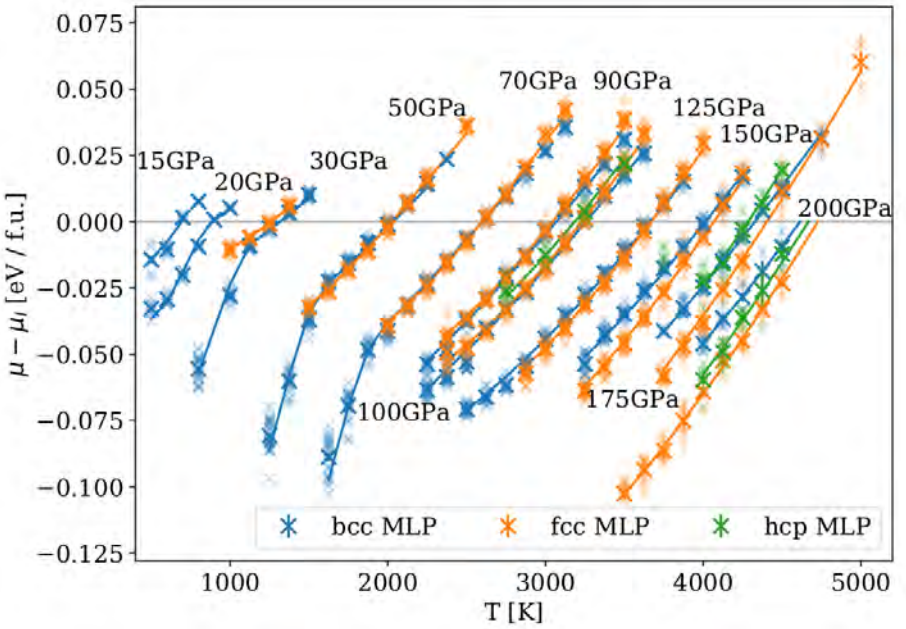

- phase boundaries: interface pinning (PLUMED), thermodynamic integration

Cheng, Bethkenhagen et al., Nat. Phys. **17**, 1228 (2021).

Water phase transitions based on MLP

coexistence calculations

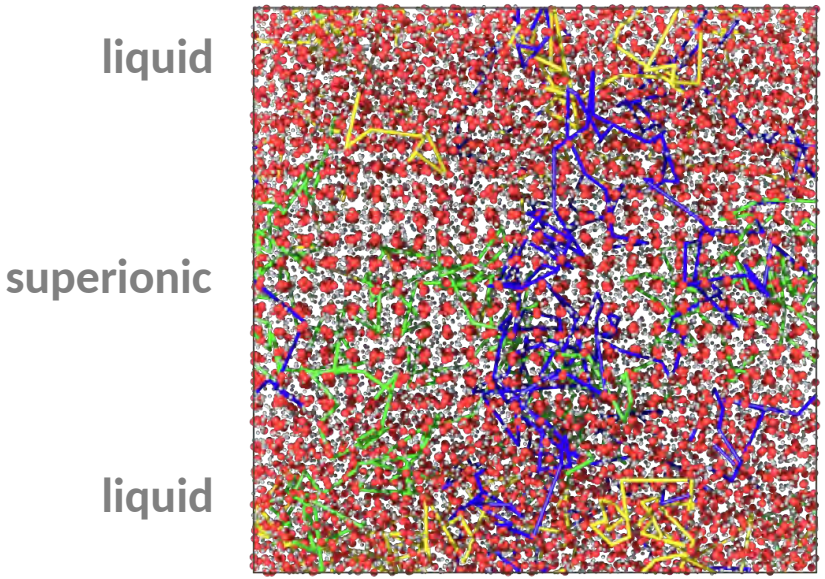

solid – superionic transition

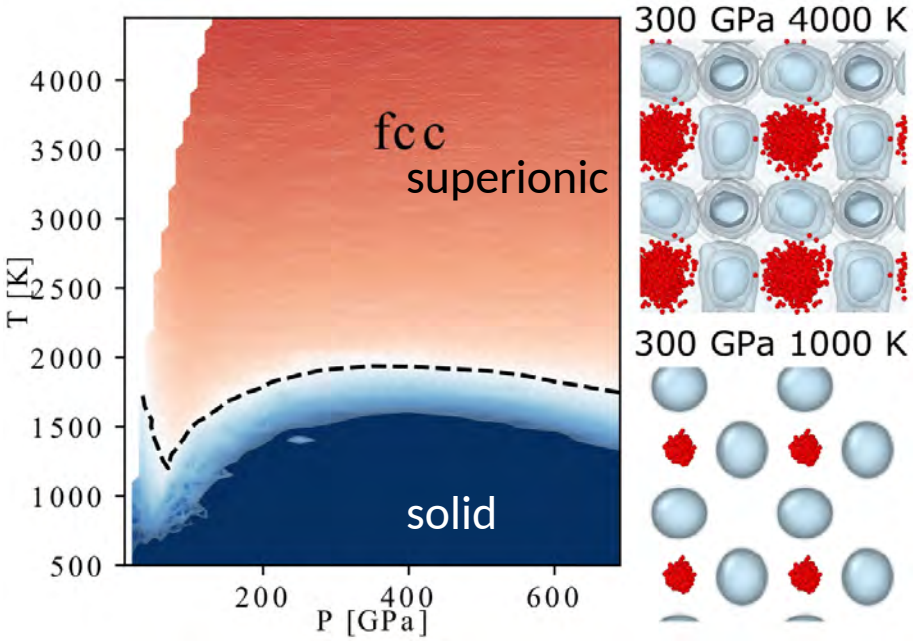

- phase boundaries: interface pinning (PLUMED), thermodynamic integration & diffusion
- resolve hydrogen dynamics in great detail (rotation periods, jumping mechanism)

Cheng, Bethkenhagen et al., Nat. Phys. **17**, 1228 (2021).

Phase diagram for bcc and fcc water

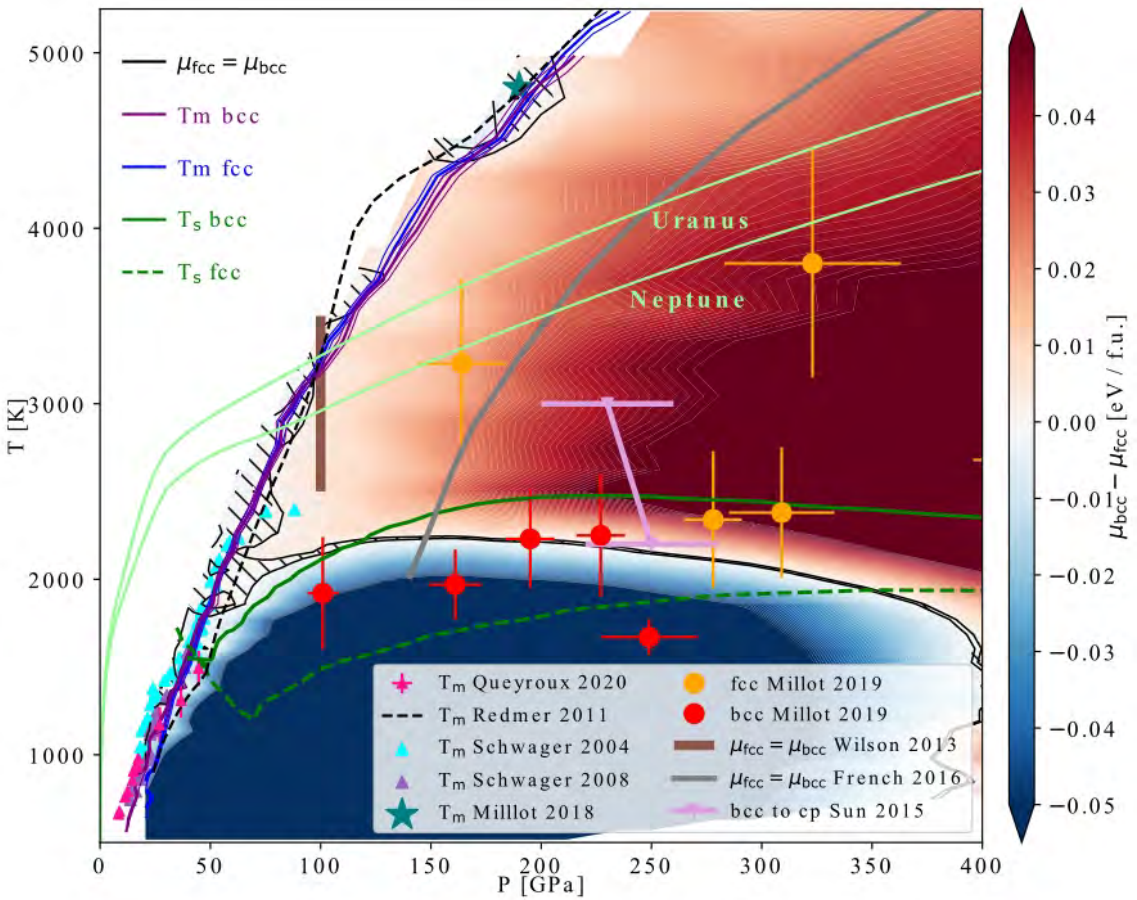

- superionic phase with fcc oxygen lattice is thermodynamically stable at ice giant interior conditions

  → at low pressure bcc possible

  → bcc could be kinetically stablized
- good agreement with XRD measurements of Millot & Coppari et al. (2019)
- melting line deviates from previous DFT-MD work at 4000 K

  → almost identical for bcc and fcc

Scheibe et al., A&A **632**, A70 (2019).
Cheng, Bethkenhagen et al., Nat. Phys. **17**, 1228 (2021).
Reinhardt, Bethkenhagen et al., Nat. Commun. **13**, 4707 (2022).

Mixed stacking in XRD spectra

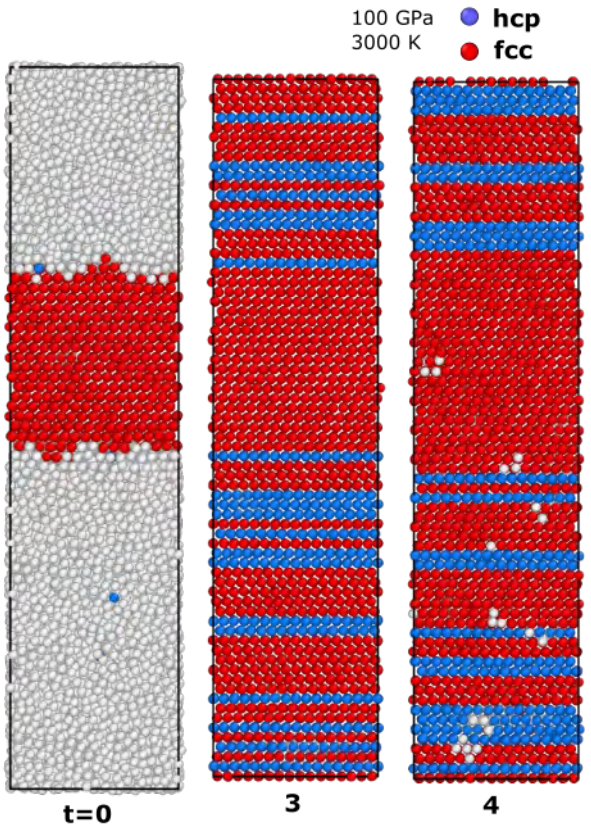

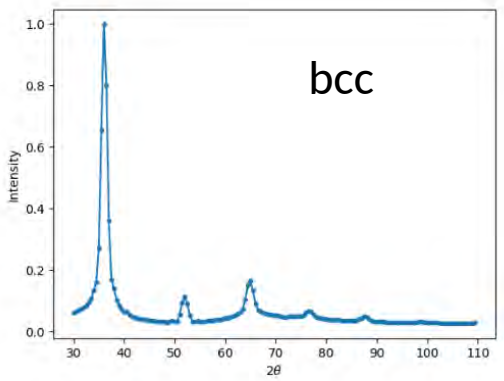

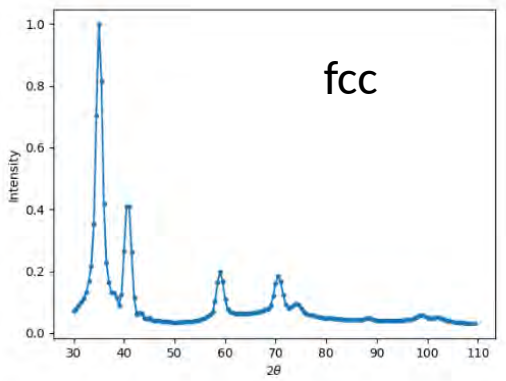

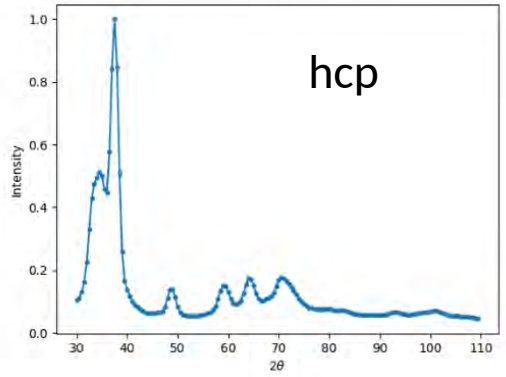

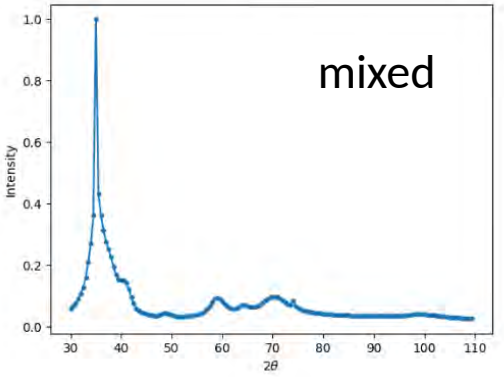

- could be potentially observed in XRD experiments

B. Cheng, M. Bethkenhagen et al., Nat. Phys. **17**, 1228 (2021).



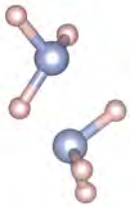
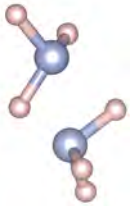

II. Is it important to consider ammonia?

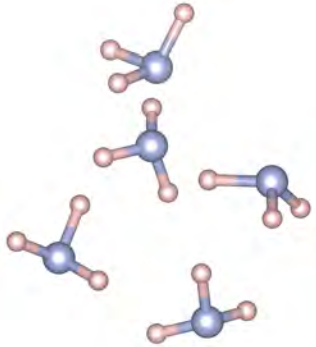
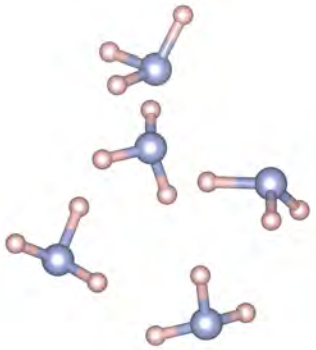

DFT-MD Hugoniot and gas gun data

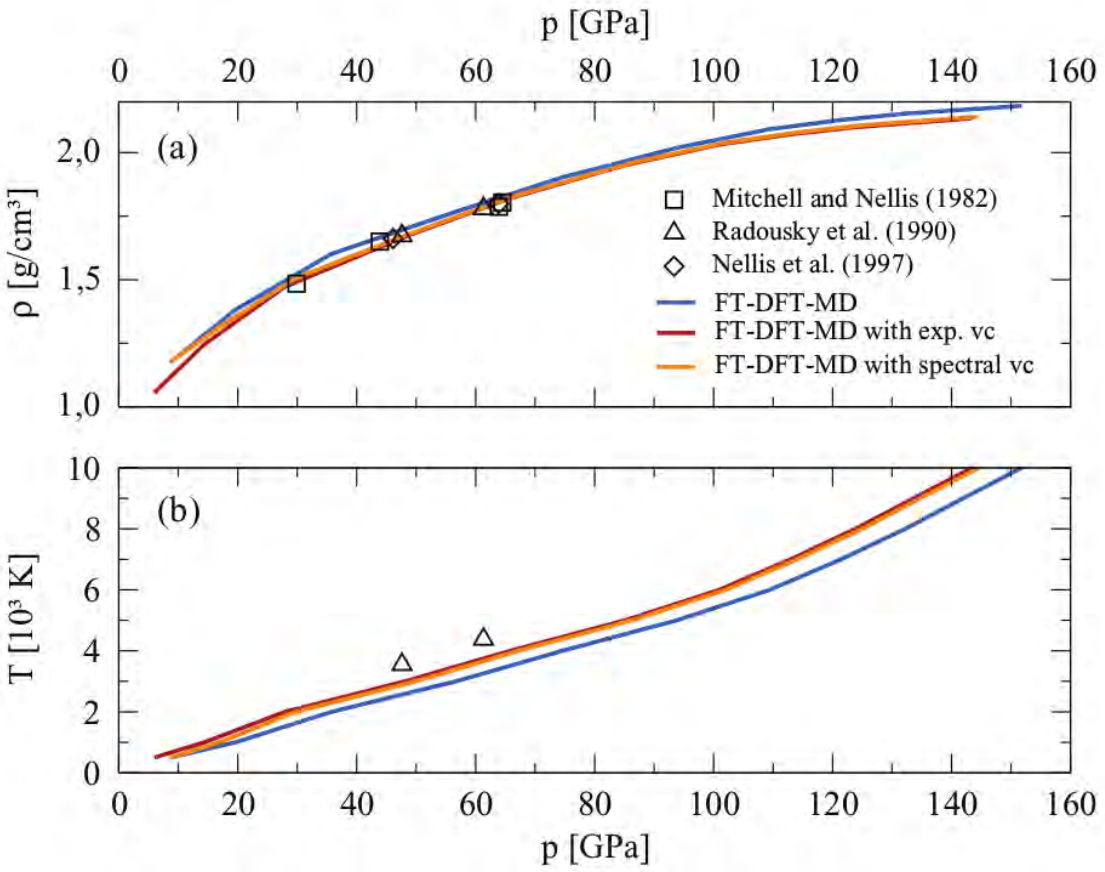

- Hugoniot:

$$u_1 - u_0 = \frac{1}{2}(p_1 + p_0)\left(\frac{1}{\varrho_0} - \frac{1}{\varrho_1}\right)$$

- very sparse shock-compression data obtained with gas guns
- most data for 0.6933 g/cm^3 & 230 K
- pressure data up to 70 GPa and only two points for the temperature available
- no reflectivity data

Mitchell & Nellis, J. Chem. Phys.**76**, 6273 (1982).
Radousky et al., J. Chem. Phys. **93**, 8235 (1990).
Nellis et al., J. Chem. Phys. **107**, 9096 (1997).
Bethkenhagen et al., J. Chem. Phys. **138**, 234504 (2013).

Experimental setup

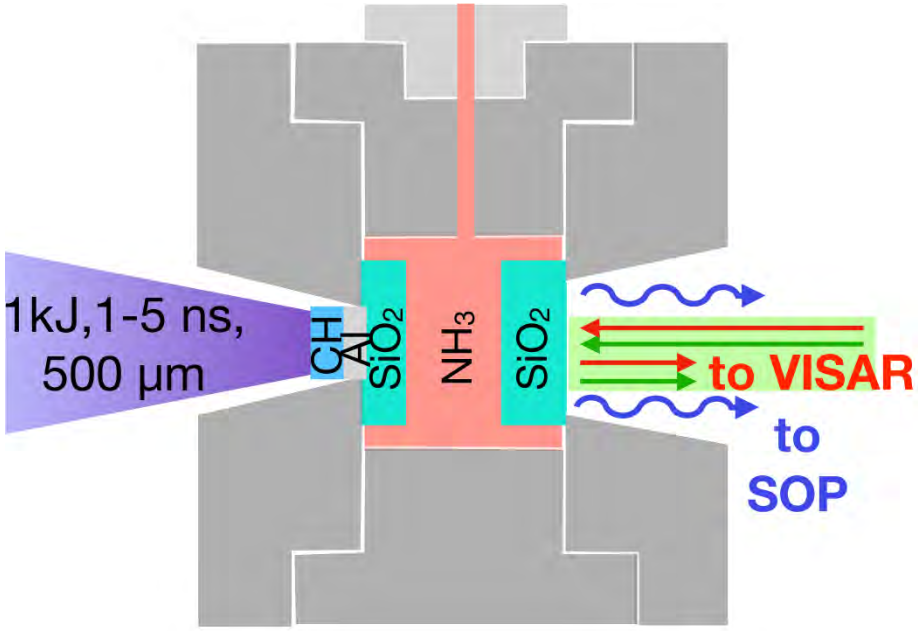

- 3 experimental campaigns at LULI2000 laser facility (Palaiseau, France)
- liquid NH_3 loaded under cryogenic conditions (~ -40°C)
- initial conditions: P_0 = 14 bar, T_0 = 295 K
- diagnositics:
  - velocity interferometer system for any reflector (VISAR) at 532 nm and 1064 nm → EOS & reflectivity
  - streaked optical pyrometer (SOP)

    → self-emission of shocked sample (T)

Ravasio, Bethkenhagen et al., Phys. Rev. Lett. **126**, 025003 (2021).

Experimental setup

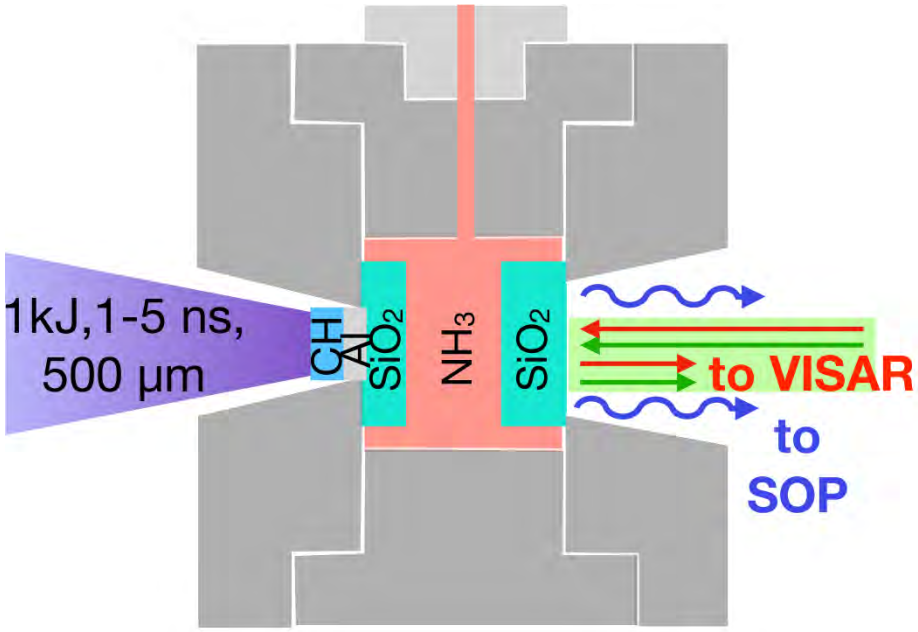

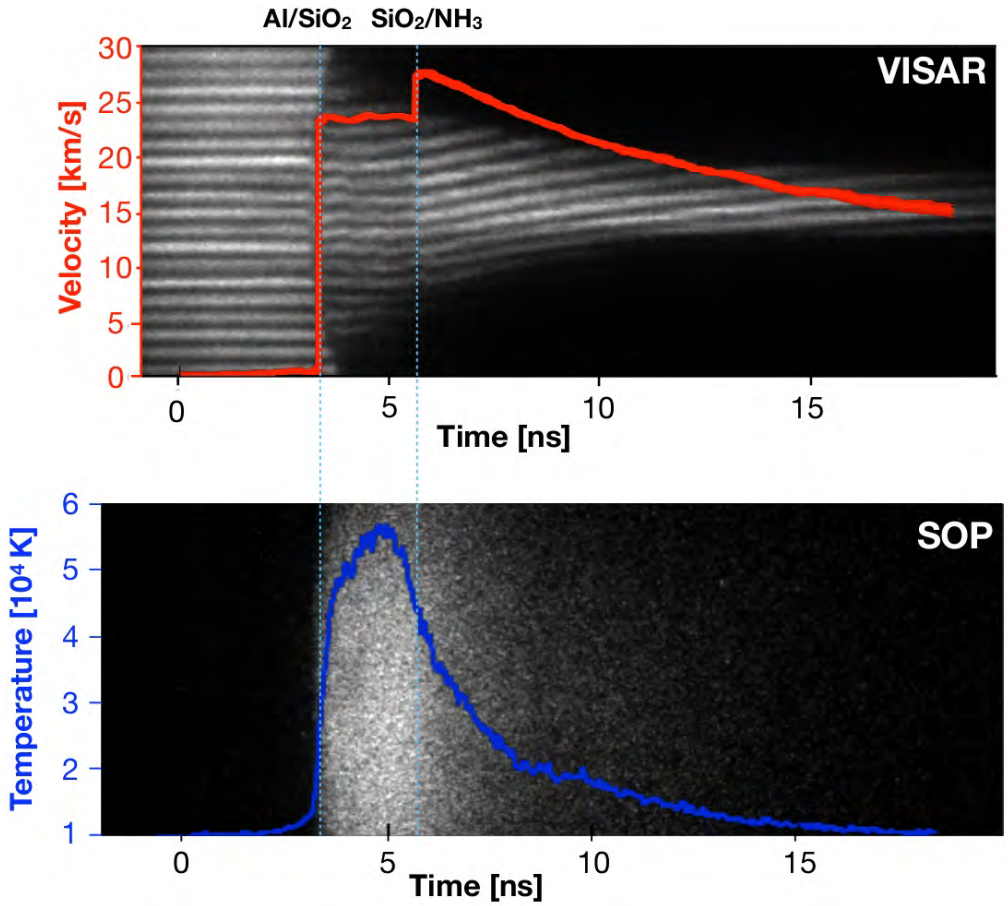

Ravasio, Bethkenhagen et al., Phys. Rev. Lett. **126**, 025003 (2021).

Equation of state

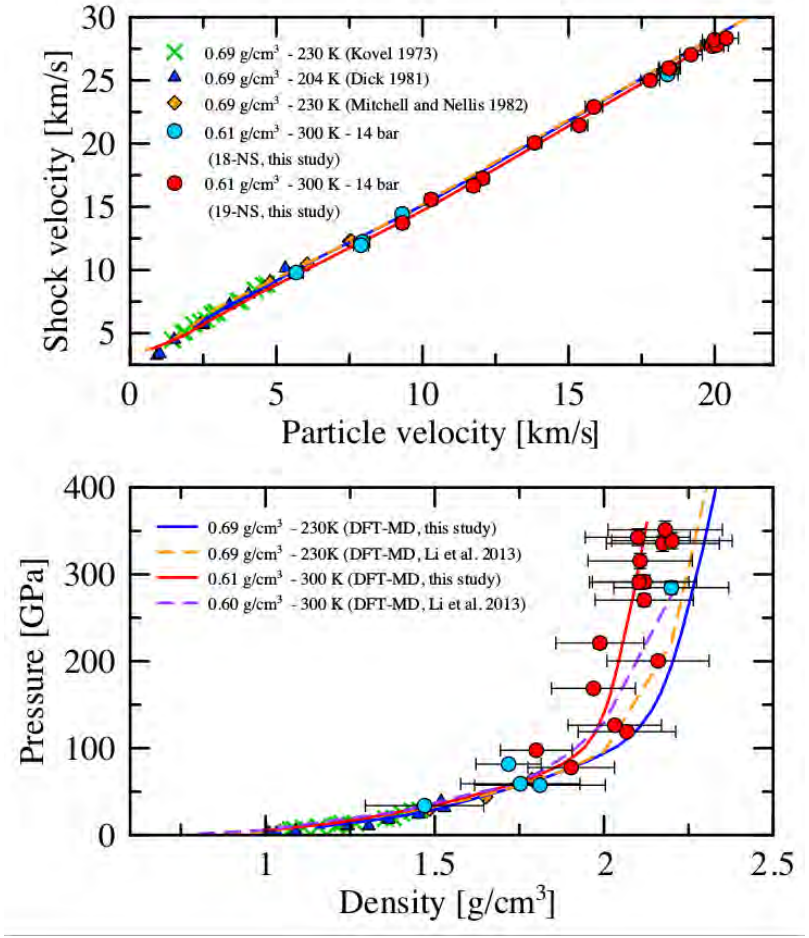

- EOS is measured up to 350 GPa and 40000 K
- consistent with gas gun data
- subtle slope change at 90 GPa and 7000 K

Ravasio, Bethkenhagen et al., Phys. Rev. Lett. **126**, 025003 (2021).

Equation of state

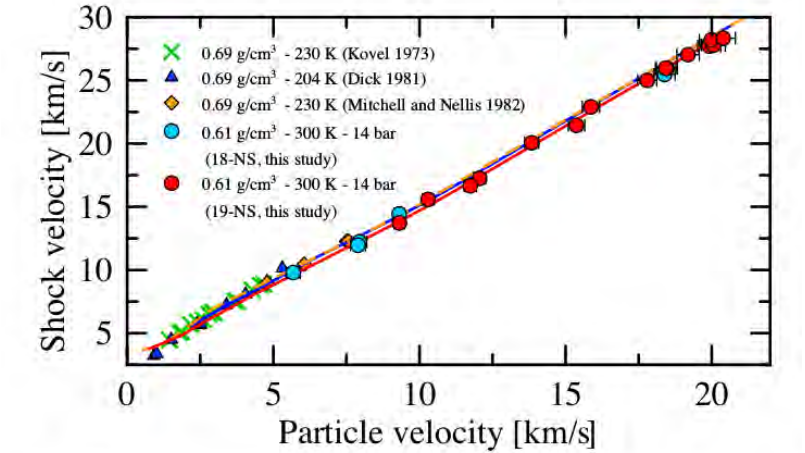

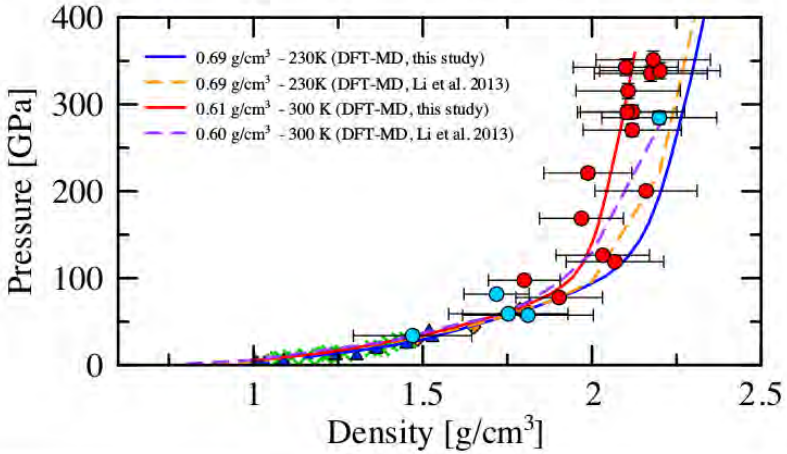

- EOS is measured up to 350 GPa and 40000 K
- consistent with gas gun data
- subtle slope change at 90 GPa and 7000 K

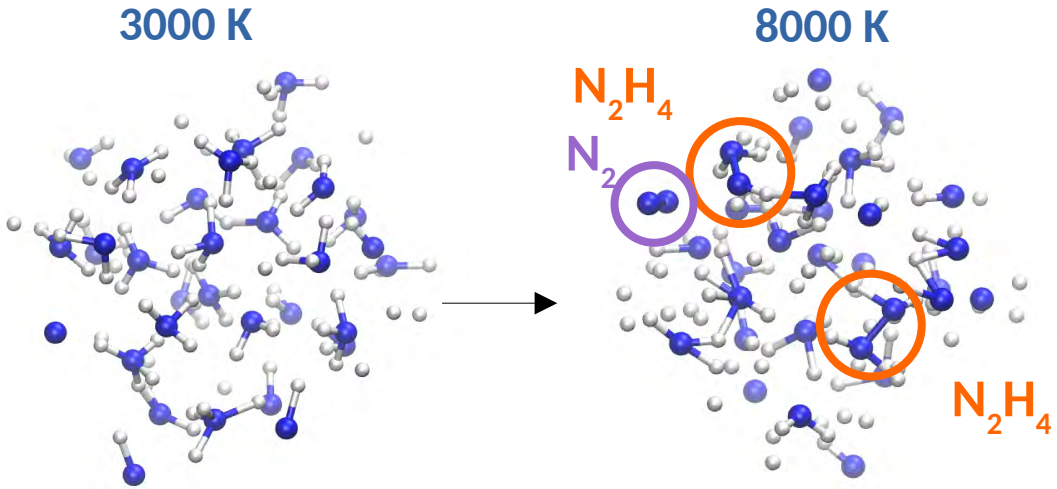

Ravasio, Bethkenhagen et al., Phys. Rev. Lett. **126**, 025003 (2021).

Reflectivity

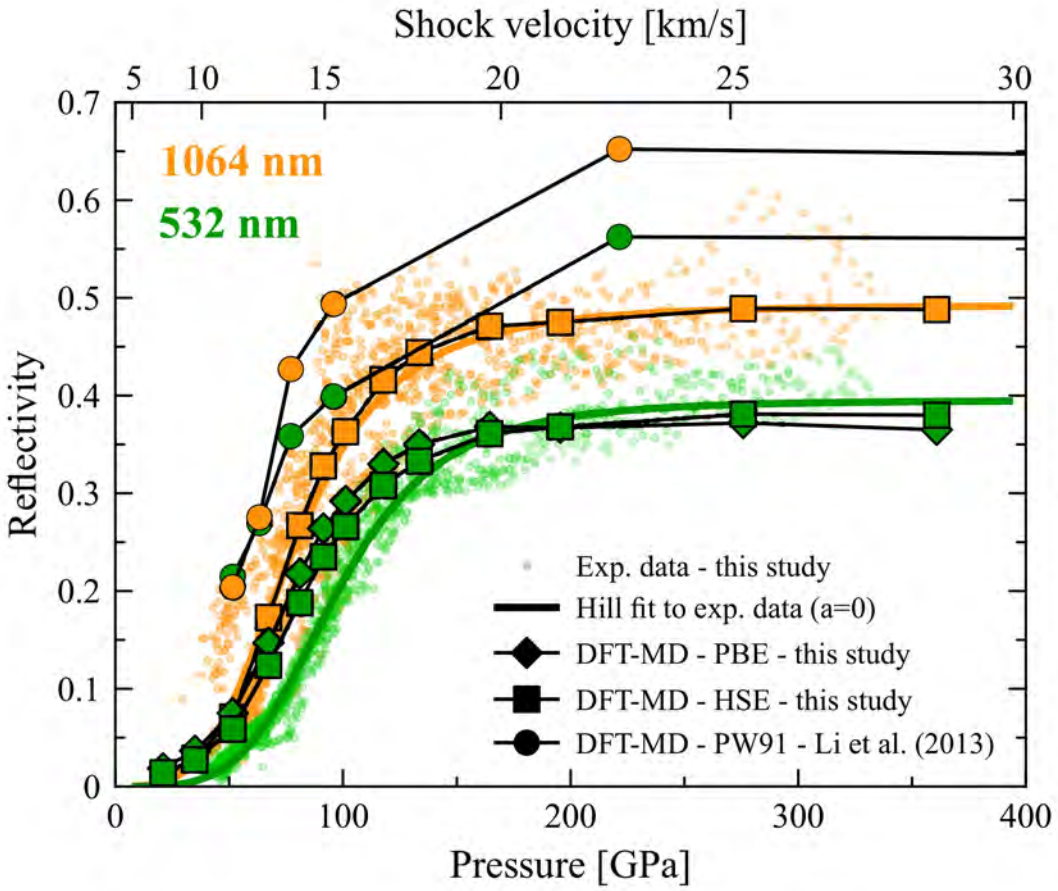

- reflectivity continuously rises above 50 GPa and reaches maximum at about 120 GPa
- measurements and calculations agree remarkably well
- almost no dependence on XC functional except initial state

  exp: $n_{exp} = 1.32$

  DFT: $n_{PBE} = 1.42$ vs. $n_{HSE} = 1.34$
- disagreement with Li et al. (2013) due to $n_{Li} = 1.00$

Ravasio, Bethkenhagen et al., Phys. Rev. Lett. **126**, 025003 (2021).
French, Bethkenhagen et al., Phys. Rev, B **107**,134109 (2023).

Diamond anvil cell data

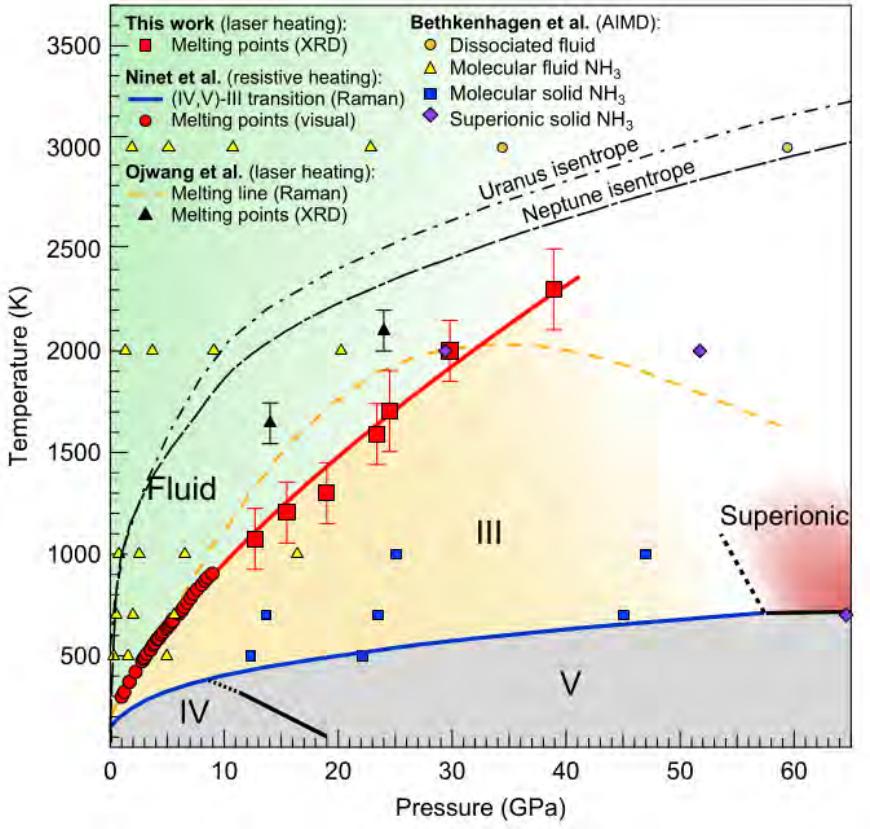

Queyroux et al., Phys. Rev. B **99**, 134107 (2019).

Diamond anvil cell data

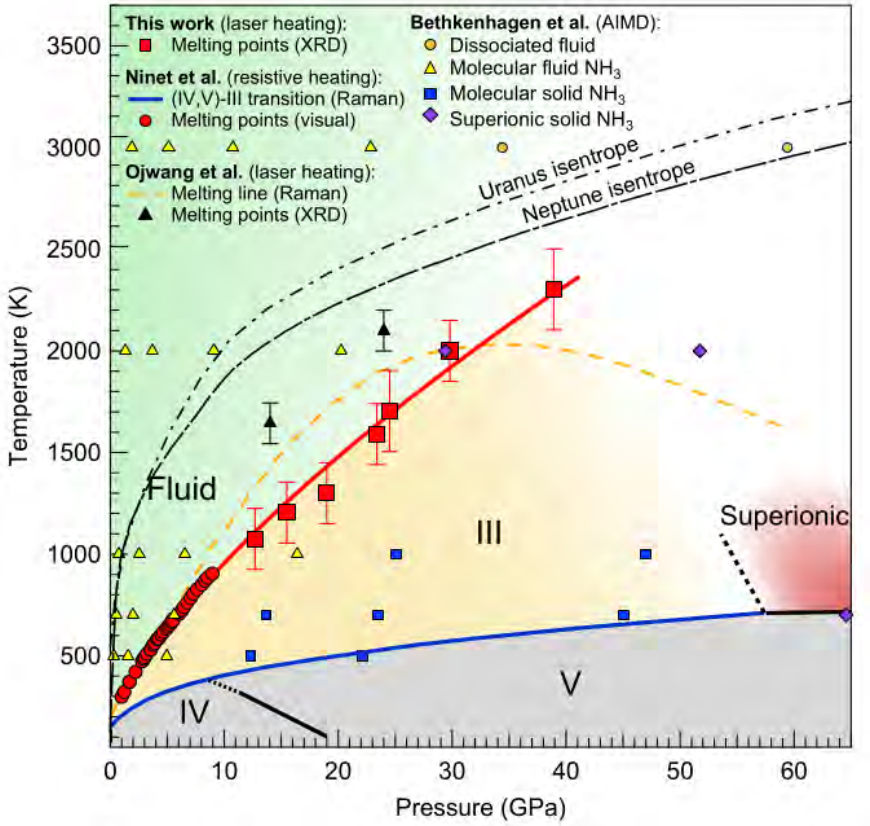

Queyroux et al., Phys. Rev. B **99**, 134107 (2019).

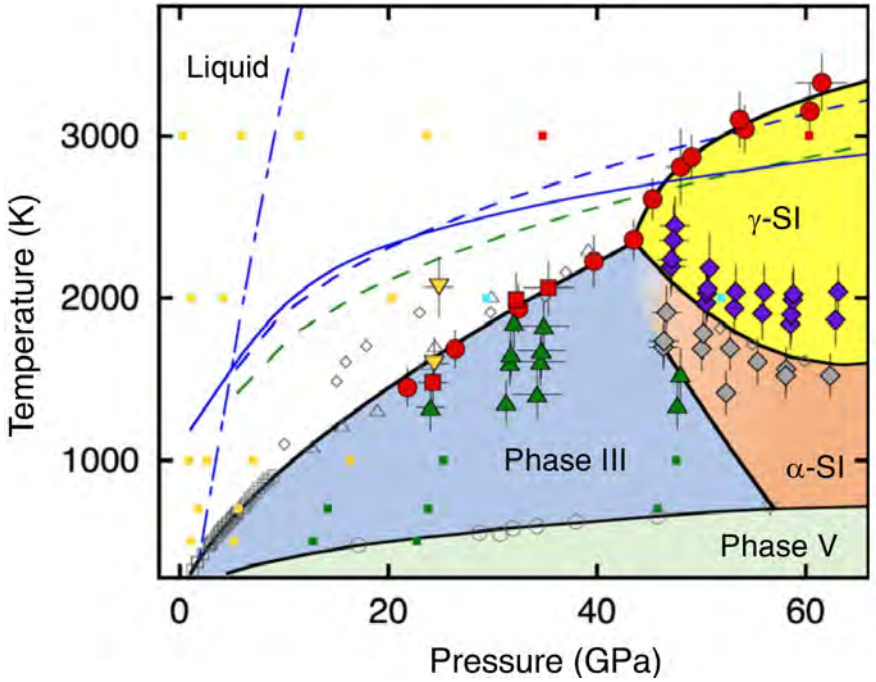

- second superionic phase?
- no structure for the N lattice proposed

Kimura & Murakami, PNAS **118**, e20211810118 (2021).

Experimental setup including DAC

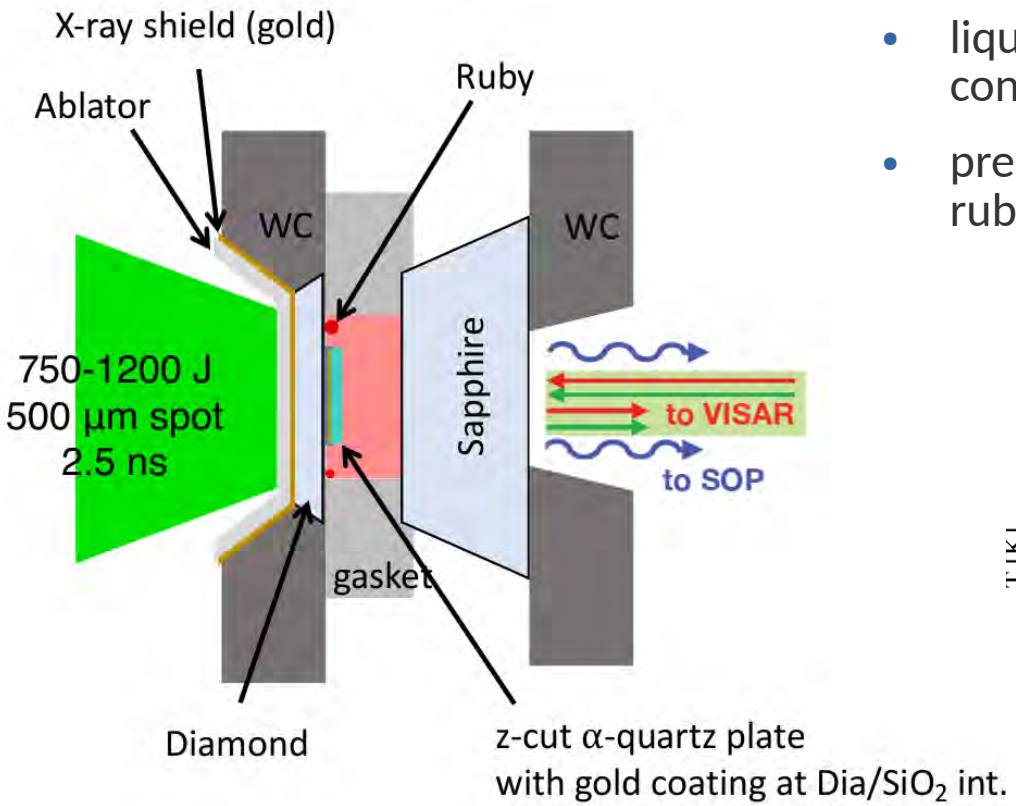

- liquid and solid NH_3 loaded under cryogenic conditions in DAC
- pre-compressions up to 3.1 GPa (measured from ruby fluorescence)

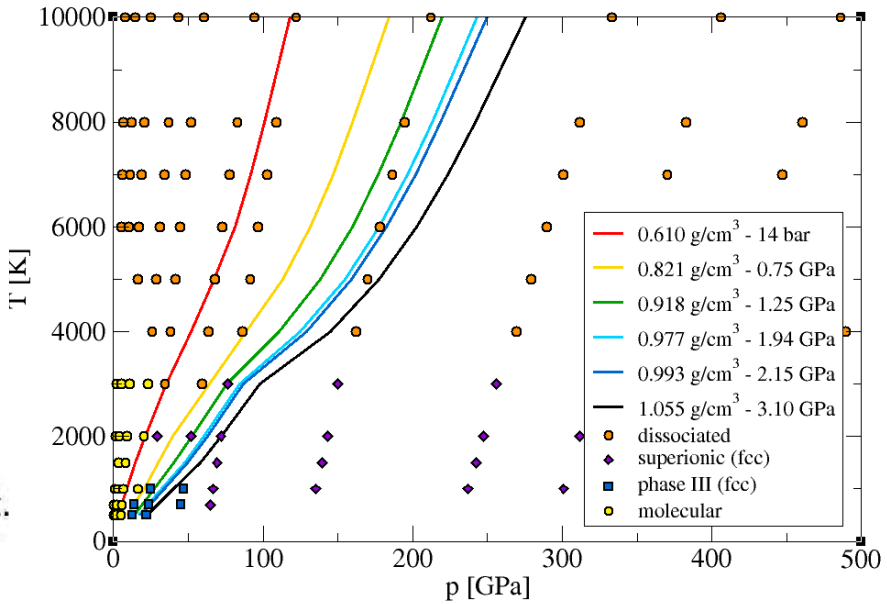

Hernandez, Bethkenhagen et al., Nat. Phys. **19**, 1280 (2023).

Melting curve

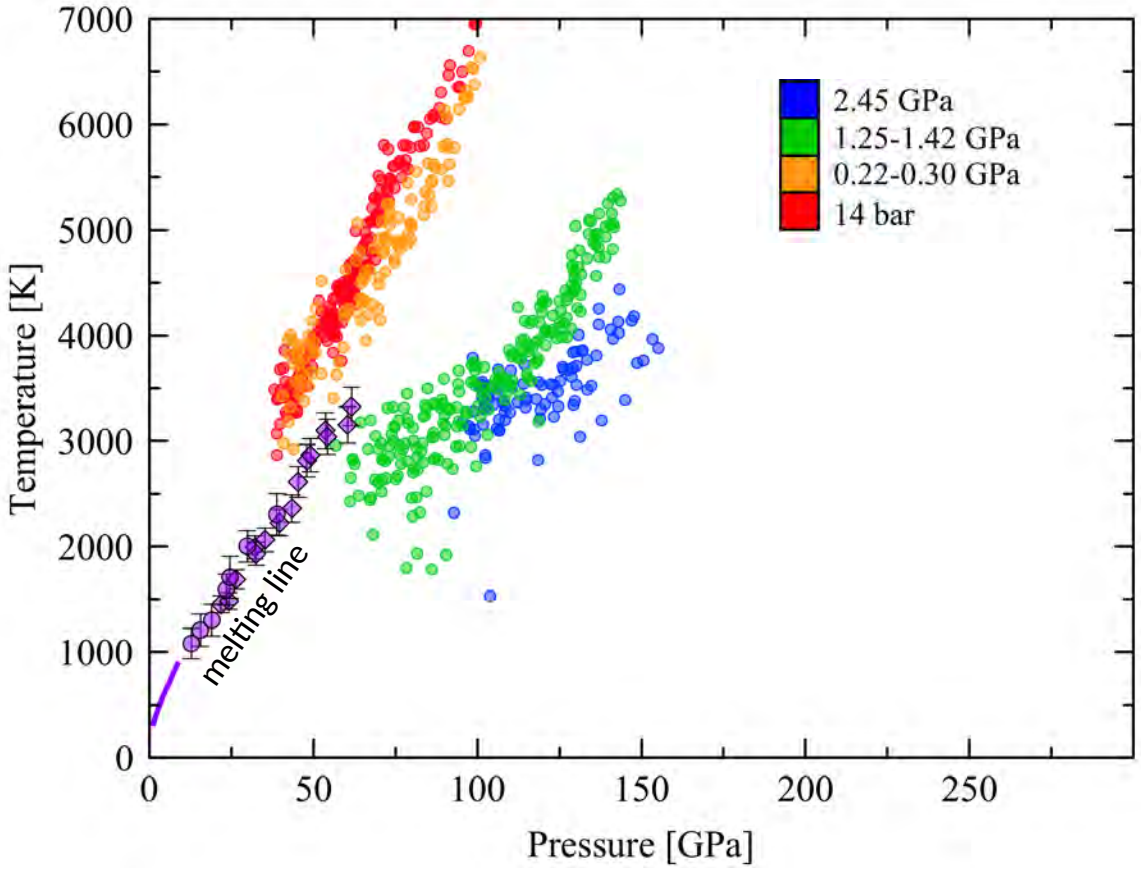

Hernandez, Bethkenhagen et al., Nat. Phys. **19**, 1280 (2023).

Melting curve

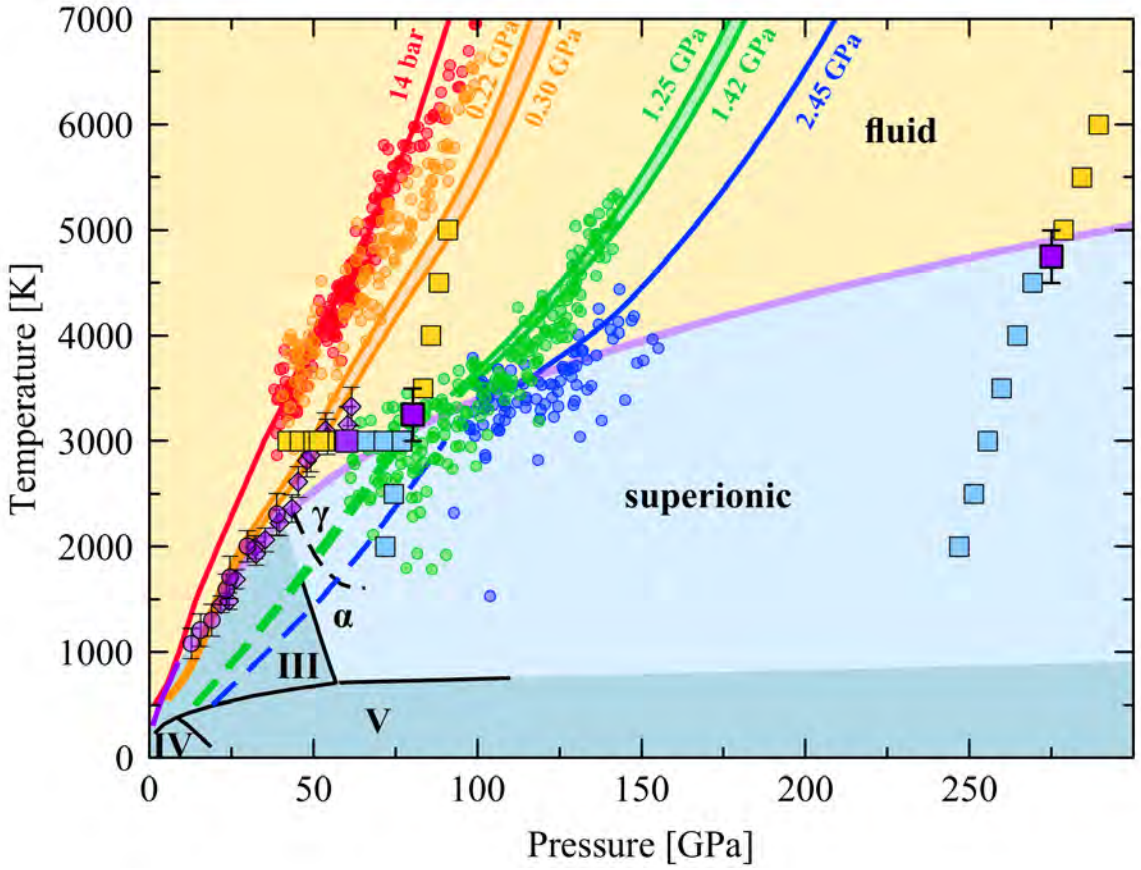

- observed superionic-fluid phase transition for datasets with pre-compressed targets of 1.25 GPa – 2.45 GPa
- performed DFT-MD calculations with 108 molecules:

  → heating/cooling along 2 isochors to constrain melting line

  → expansion calculations at 3000 K favor Queyroux et al. (2019) trend of melting line

  → anchored our fit using their data

Hernandez, Bethkenhagen et al., Nat. Phys. **19**, 1280 (2023).

Electrical conductivity of ammonia and water

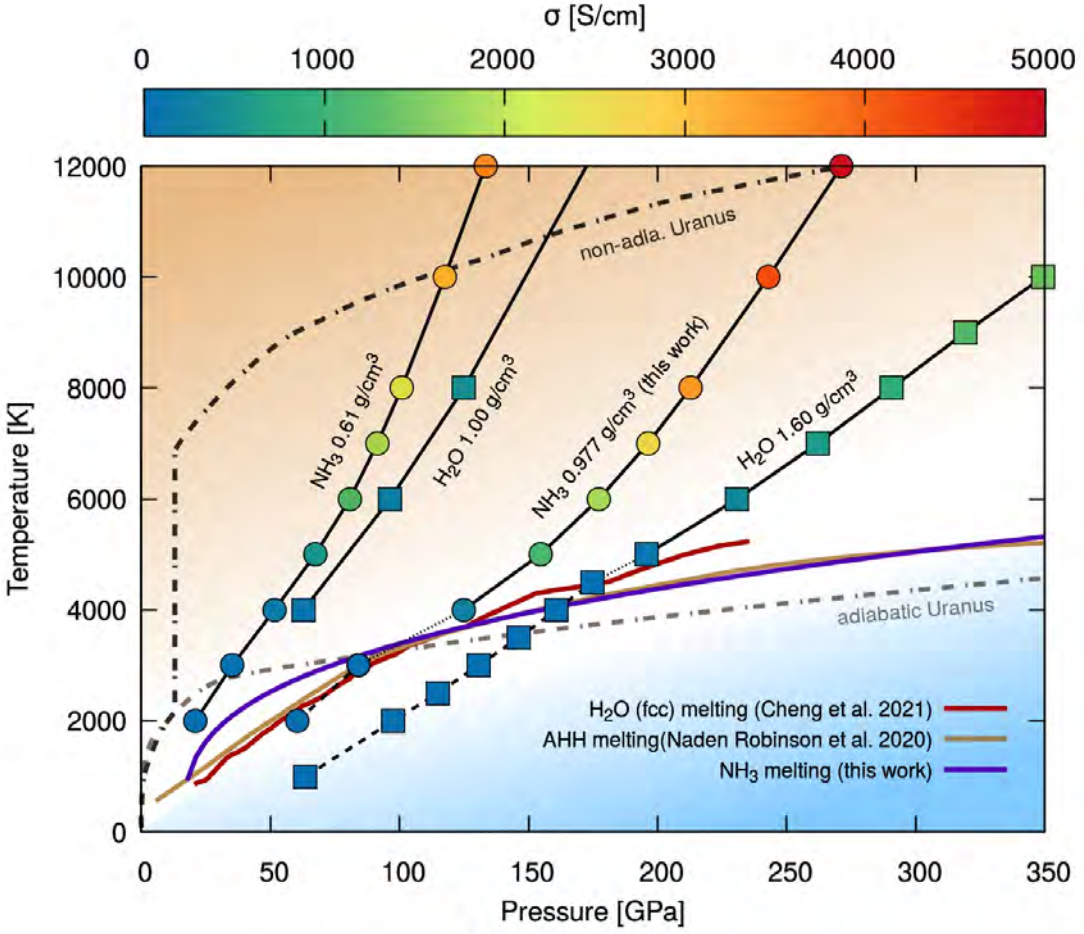

Electrical conductivity of ammonia and water

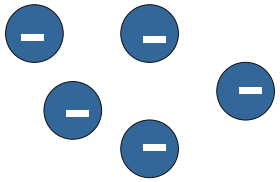

metallic

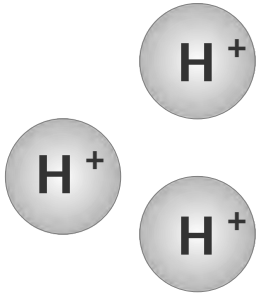

superionic

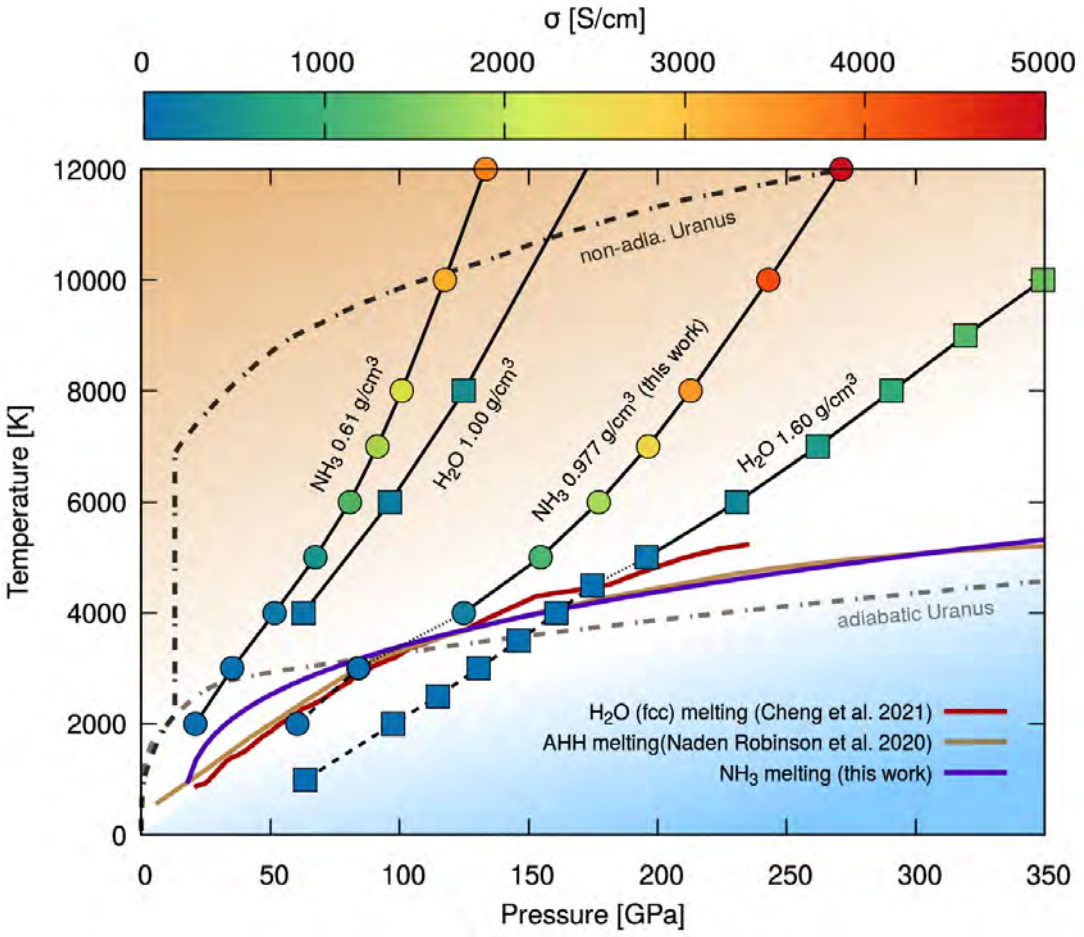

Electrical conductivity of ammonia and water

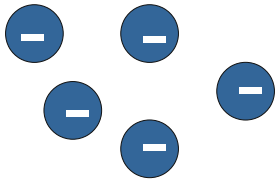

metallic

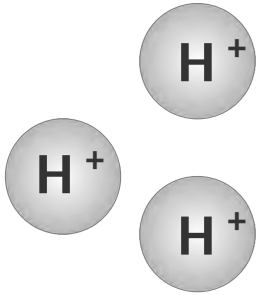

superionic

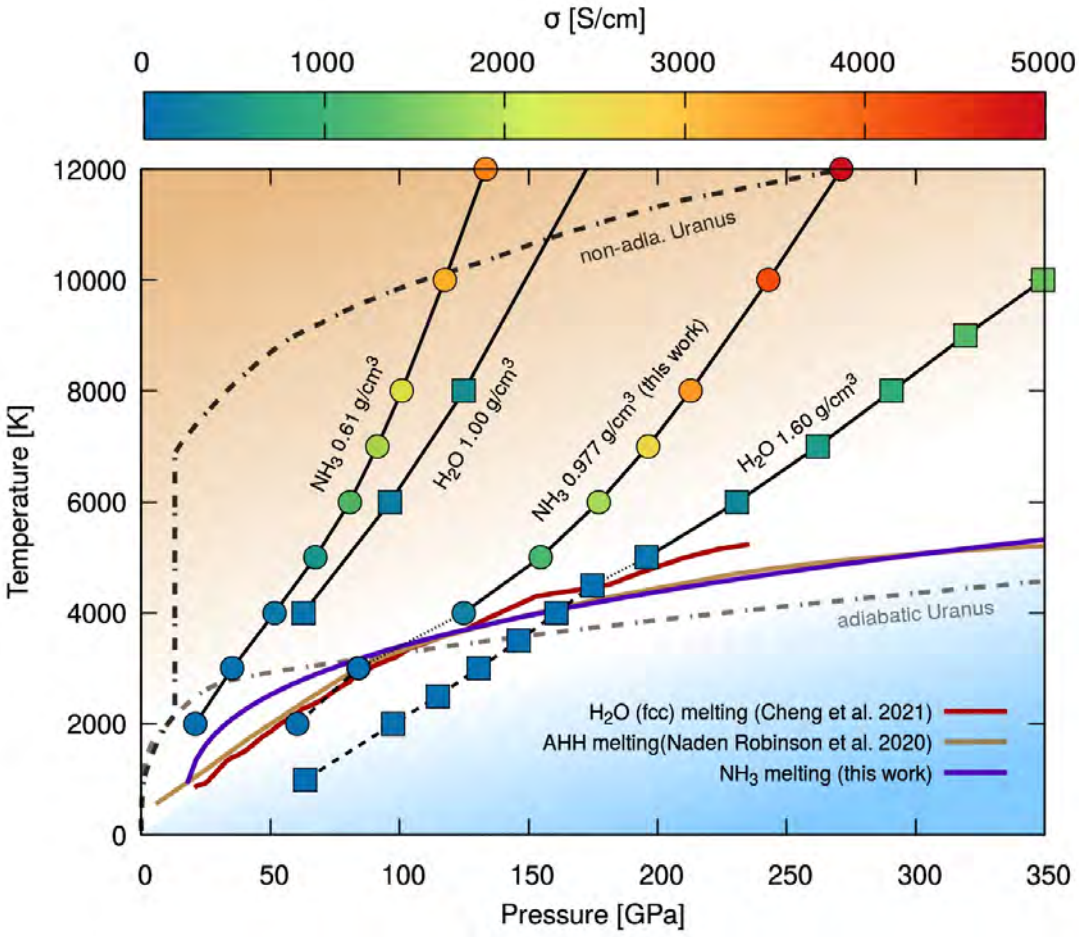

- **non-adiabatic models:**

  → electrical conductivity of ammonia generally found higher than the one of water (one order of magnitude at 100 GPa)

- **adiabatic models:**

  → melting line slope depends on composition, but intersect

  → ammonia-rich layer in ice giants?

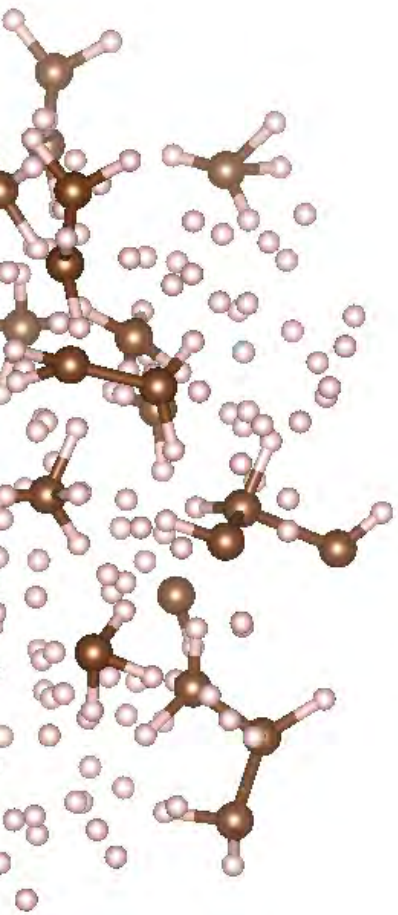

III. What do we know about high-pressure methane?

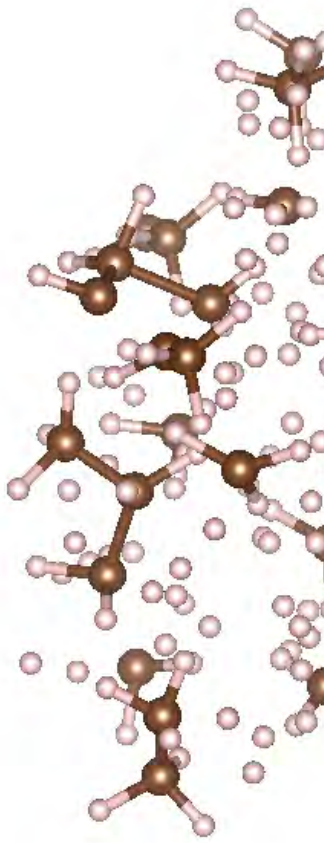

Stability of superionic phases

Hydrocarbons

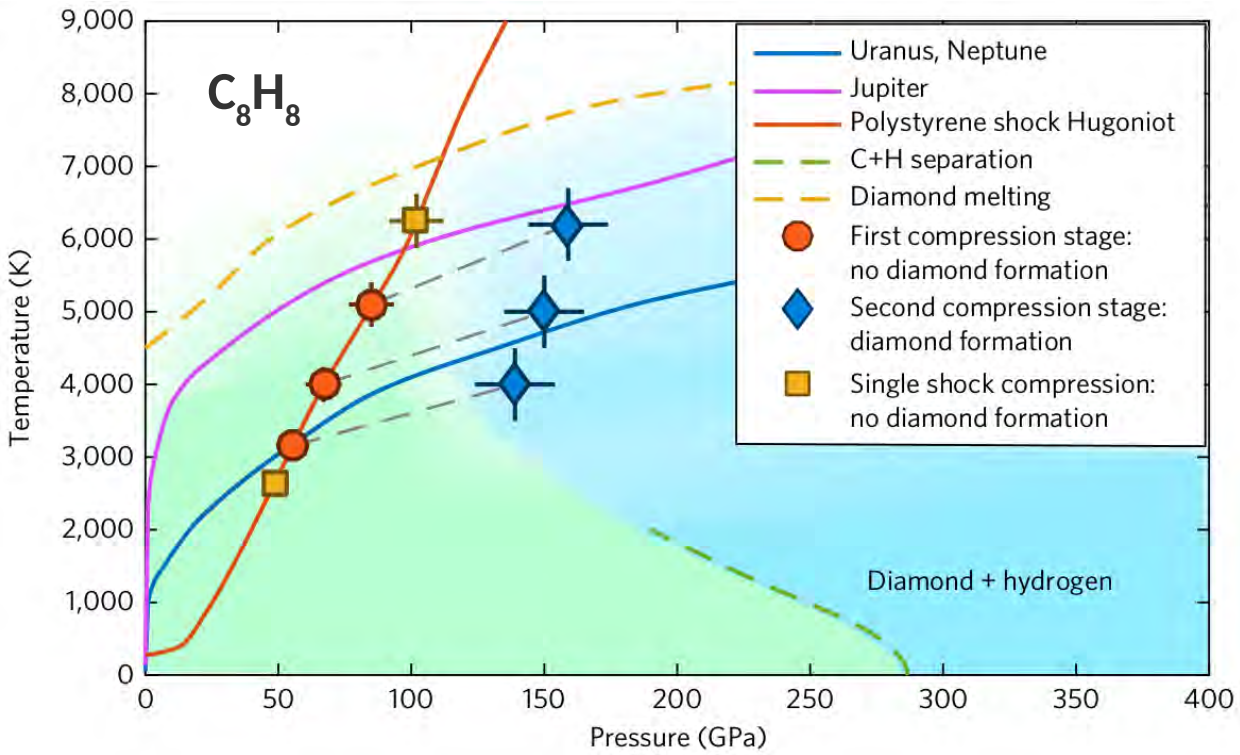

- hydrocarbons do NOT form superionic phases

  → polymerization and diamond formation instead

- study of superionic phases that are potentially stable to the addition of minor carbon concentrations needed

  → however: not even methane alone well understood

Kraus et al., Nat. Astron. **1**, 606 (2017).
He et al., Sci. Adv. **8**, abo0617 (2022).

Phase diagram for C/H mixtures

- recently improved the phase diagram by constructing composition-dependent MLP
- find methane to form diamond throughout both ice giants

  → but probably unrealistic as carbon ratio changes in interior and during evolution
- find a depletion zone above 200 GPa and 3000 K – 3500 K

  → diamond formation is favorable regardless of carbon content

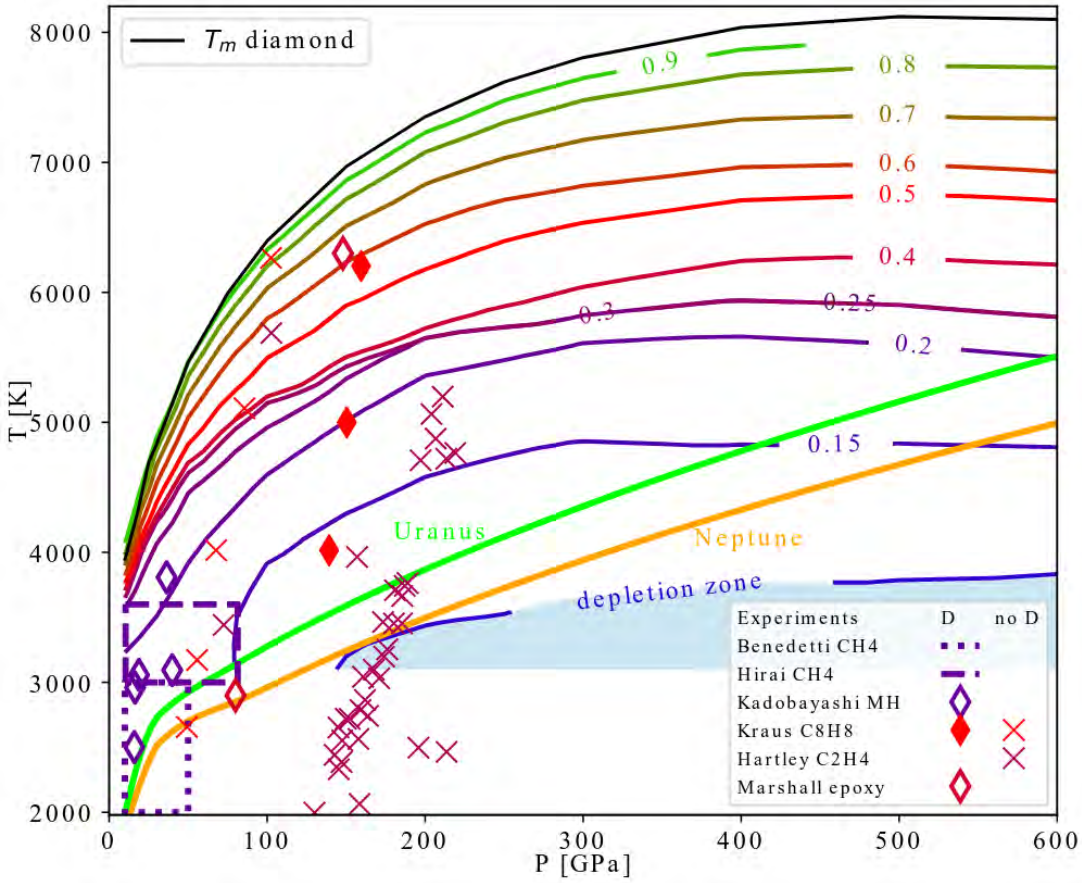

Cheng et al, Nat. Comm. **14**, 1104 (2023).

Conclusions

Uranus

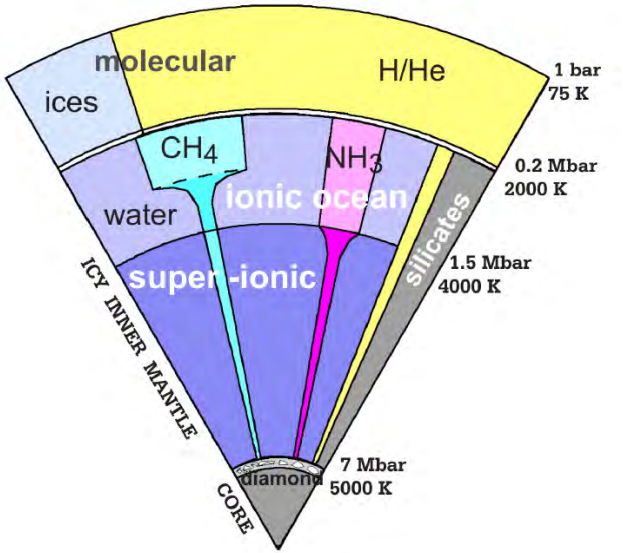

Courtesy by N. Nettelmann.

- interior models for Uranus & Neptune remain challenging

  → more observational data

- ab initio simulations & experiments can support the improvement of models

  → melting lines

  → transport properties (conductivities, diffusion, viscosity)

  → thermodynamic stability of ice-rock mixtures ?

$MgSiO_3$-H_2O (120 GPa)

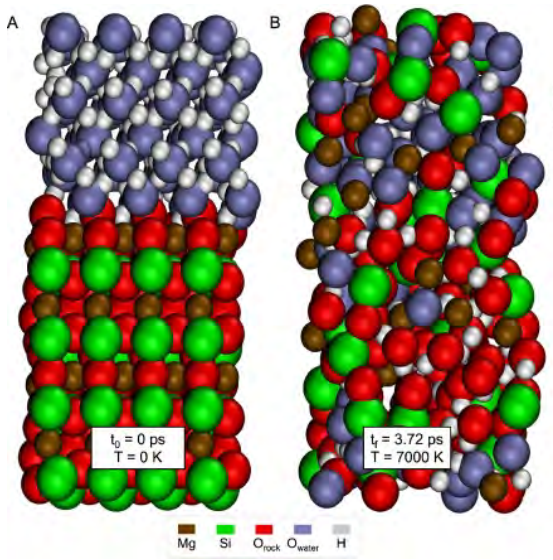

Kovačević et al., Sci. Rep. **12**, 13055 (2022).

A new **Diamond Open-Access Journal** in geoscience?


Mandy Bethkenhagen


Mohammed Gouiza


Maëlis Arnould


Thibault Duretz


Stefano Maffei


Iris van Zelst

GEODYNAMICA

- **From Earth's core to surface**
- **Planets and exoplanets' interior**
- **From geodynamic modeling to mineral physics**
- **…**

eScholarship University of California

Email: geodynamicaj@gmail.com
Keep posted… More to come soon!

Training set vs. testing set error (RSME)

Water

Energy (meV/atom)		Force (meV/Ang.)	
Training set	Test set	Training set	Test set
13	14	750	740

Hydrocarbons

Energy (meV/atom)		Force (meV/Ang.)	
Training set	Test set	Training set	Test set
43	42	865	767
42	45	922	800

Benchmarking the machine learning potential (MLP)

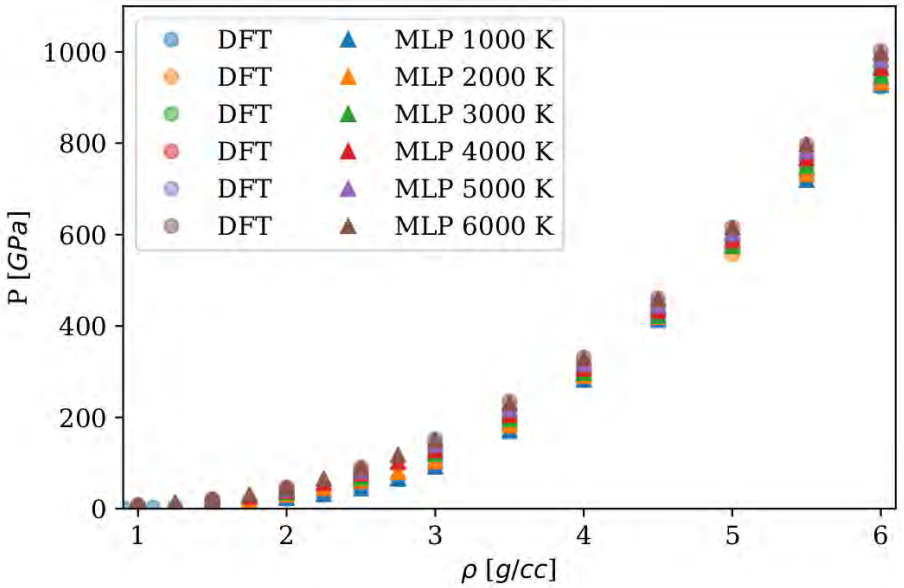

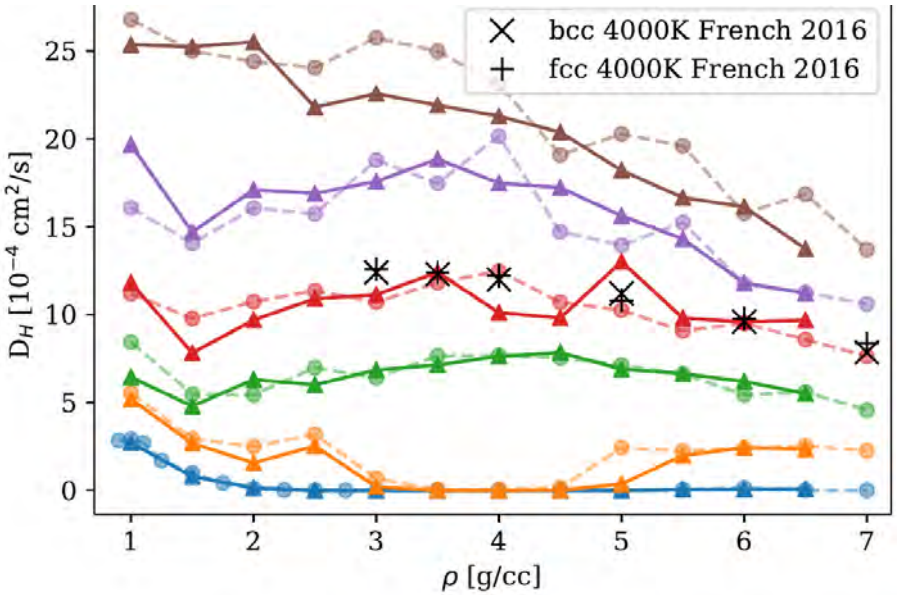

- MLP benchmarked against DFT-MD with respect to EOS, pair distribution functions and diffusion
- potential runs stable up to at least 6000 K and 1000 GPa → covers desired phase space
- find no significant difference for the H diffusion coefficients in bcc and fcc superionic

French et al., Phys. Rev. E **93**, 022140 (2016).
Cheng, Bethkenhagen et al., Nat. Phys. **17**, 1228 (2021).

Thermodynamics of the C/H mixture

- non-ideal mixing effects taken into account
- identify 2 separate liquid-liquid phase separation in the C/H mixture:
  - PS1: A C/H mixture with a carbon fraction that is between the values of χ_C^1 and χ_C^2 will first undergo a liquid-liquid phase separation, and then if diamond forms, it will preferentially nucleate from the carbon-rich liquid phase as it has higher μ_C
  - PS2: For P between 100 and 600 GPa and $T \leq$ 4000 K, C in the C/H mixture will always will always be exposed to a thermodynamic driving force to form diamond, regardless of how low the C fraction is: “depletion zone”

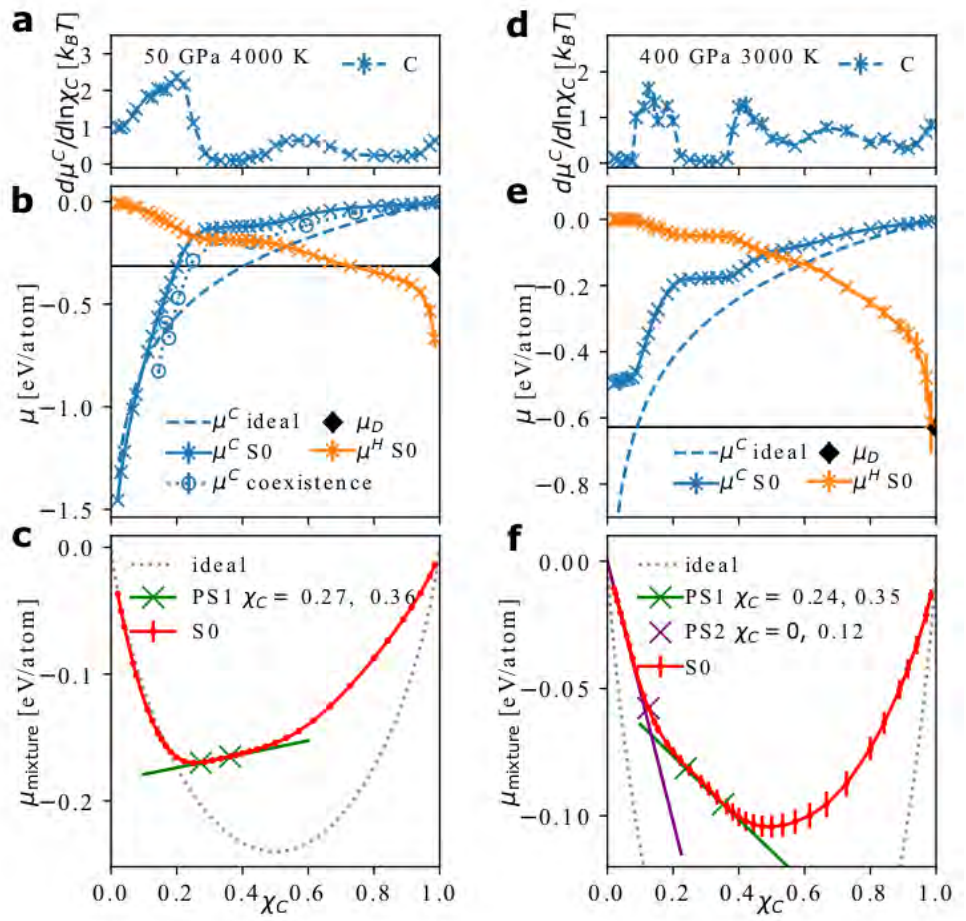

Density Functional Theory Molecular Dynamics

Basic Idea

- replace many-body wavefunction by effective one-electron problem

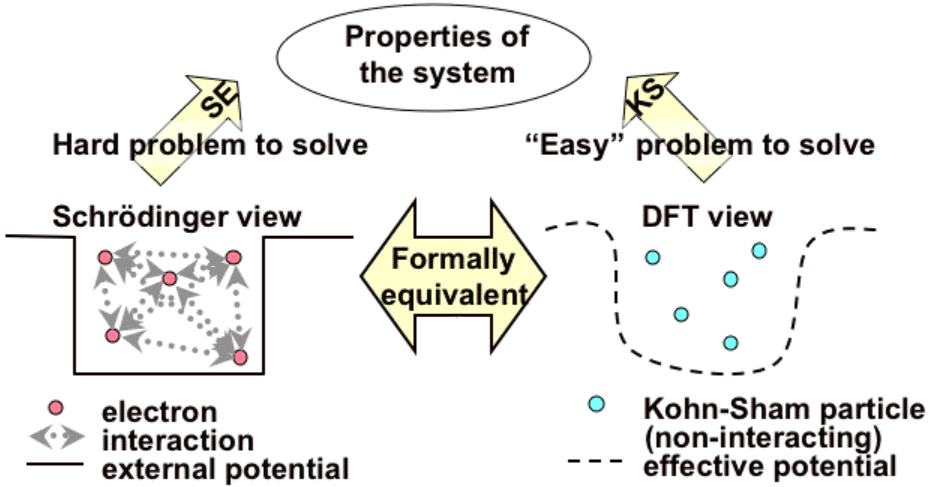

cartoon by Ann E. Mattsson

Workflow of VASP

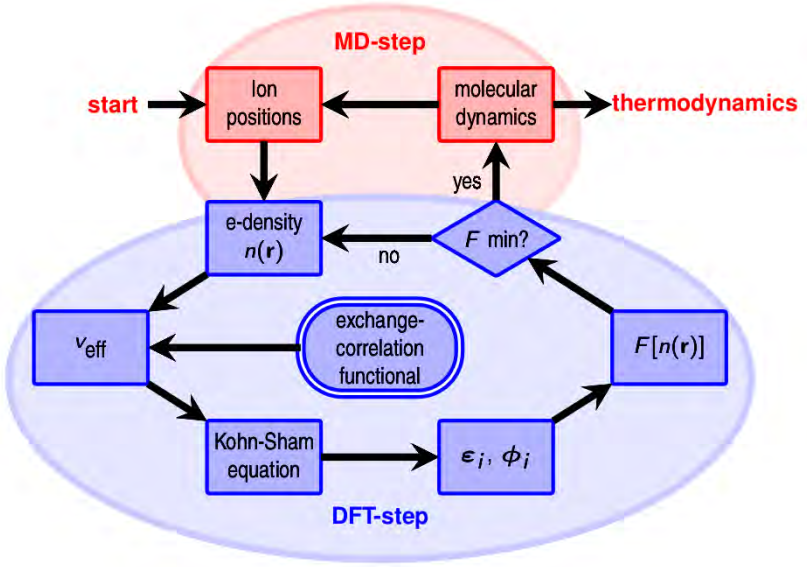

J. Hafner, J. Comput. Chem. **29**, 2045 (2008).
G. Kresse und J. Hafner, Phys. Rev. B **47**, 558 (1993).
J. P. Perdew et al., Phys. Rev. Lett. **77**, 3865 (1996).

Electrical conductivity

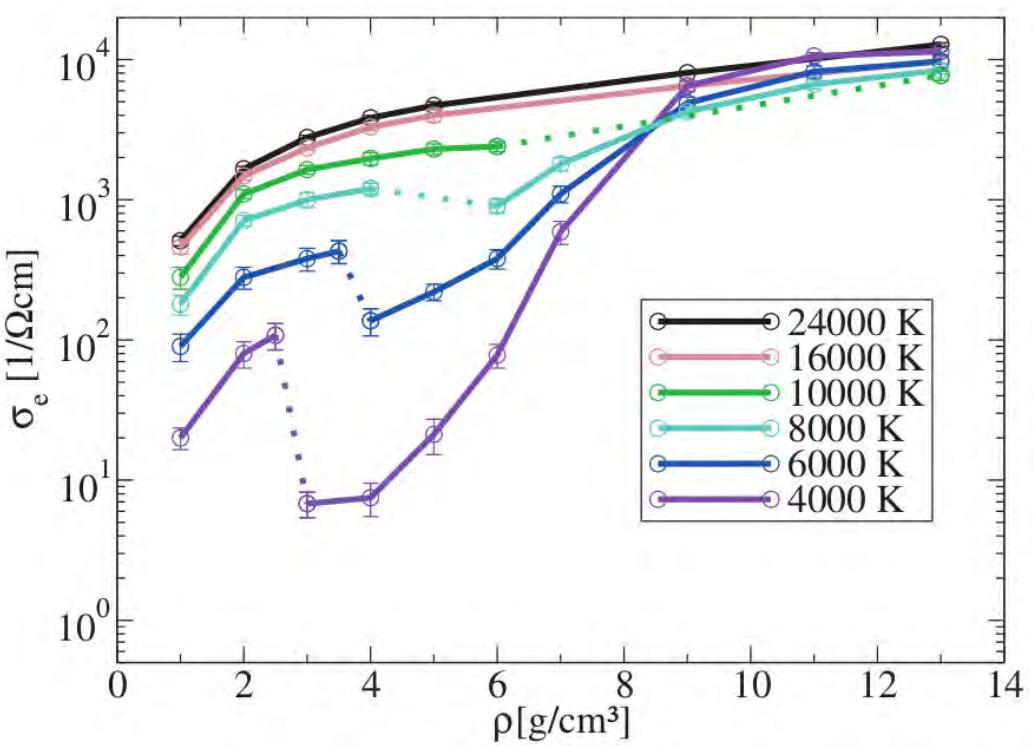

Electronic conductivity

$$L_{mn}(\omega) = \frac{2\pi q^{4-m-n}}{3Vm_e^2\omega} \sum_{\boldsymbol{k}\nu\mu} |\langle \boldsymbol{k}\nu|\hat{\boldsymbol{p}}|\boldsymbol{k}\mu\rangle|^2 (f_{\boldsymbol{k}\nu} - f_{\boldsymbol{k}\mu}) \times \left(\frac{E_{\boldsymbol{k}\mu} + E_{\boldsymbol{k}\nu}}{2} - h_e\right)^{m+n-2} \delta(E_{\boldsymbol{k}\mu} - E_{\boldsymbol{k}\nu} - \hbar\omega)$$

$$\sigma = \lim_{\omega\to 0} L_{11}(\omega)$$

French et al., Phys. Rev. B **82**, 174108 (2010).
French et al., Phys. Rev. Lett. 107, 185901 (2011).

Electronic conductivity

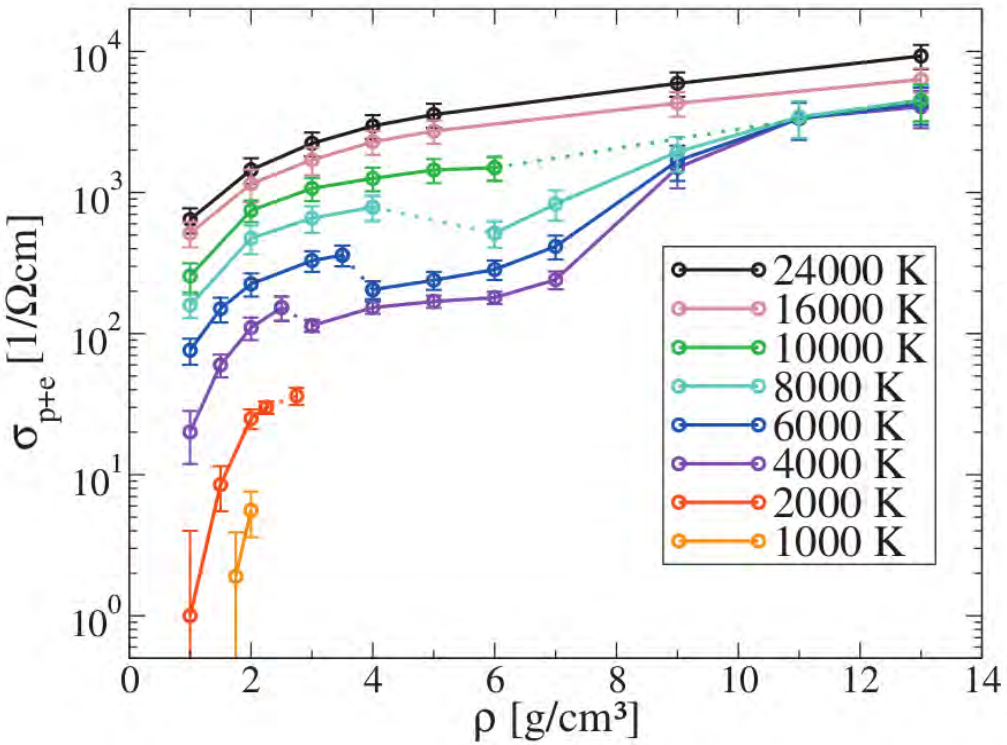

Electronic conductivity

$$L_{mn}(\omega) = \frac{2\pi q^{4-m-n}}{3Vm_e^2\omega} \sum_{\boldsymbol{k}\nu\mu} |\langle \boldsymbol{k}\nu|\hat{\boldsymbol{p}}|\boldsymbol{k}\mu\rangle|^2 (f_{\boldsymbol{k}\nu} - f_{\boldsymbol{k}\mu}) \times \left(\frac{E_{\boldsymbol{k}\mu} + E_{\boldsymbol{k}\nu}}{2} - h_e\right)^{m+n-2} \delta(E_{\boldsymbol{k}\mu} - E_{\boldsymbol{k}\nu} - \hbar\omega)$$

$$\sigma = \lim_{\omega\to 0} L_{11}(\omega)$$

Ionic conductivity

$$\sigma_p = \frac{e^2 n_p}{k_B T}(D_p - \gamma D_O),$$

French et al., Phys. Rev. B **82**, 174108 (2010).
French et al., Phys. Rev. Lett. 107, 185901 (2011).

Optical properties

electrical conductivity

$$\sigma_1(\omega) = \frac{2\pi e^2}{3m^2\omega V}\sum_{\mathbf{k}} w_{\mathbf{k}} \sum_{j=1}^{N_b}\sum_{i=1}^{N_b}\sum_{\alpha=1}^{3}(f_{j,\mathbf{k}} - f_{i,\mathbf{k}}) \times |\langle\Psi_{j,\mathbf{k}}|\hat{p}_\alpha|\Psi_{i,\mathbf{k}}\rangle|^2 \delta(\epsilon_{i,\mathbf{k}} - \epsilon_{j,\mathbf{k}} - \hbar\omega)$$

dielectric function

Holst et al., Phys. Rev. B 83, 235120 (2011).
French & Redmer, Phys. Plasmas 18, 043301 (2011).

$$\varepsilon_1(\omega) = 1 - \frac{\sigma_2(\omega)}{\varepsilon_0\omega} \quad \varepsilon_2(\omega) = \frac{\sigma_1(\omega)}{\varepsilon_0\omega}$$

refractive index

$$n(\omega) + ik(\omega) = \sqrt{\varepsilon_1(\omega) + i\varepsilon_2(\omega)}$$

Optical properties

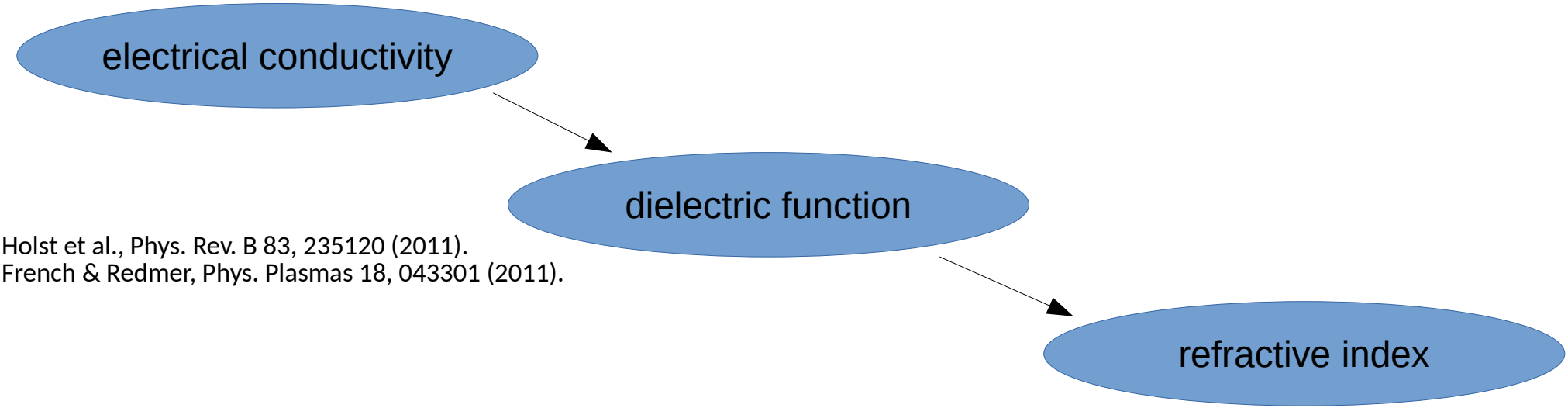

Holst et al., Phys. Rev. B 83, 235120 (2011).
French & Redmer, Phys. Plasmas 18, 043301 (2011).

absorption coefficient

$$\alpha(\omega) = \frac{2\omega}{c} k(\omega)$$

reflectivity

$$R(\omega) = \frac{[n(\omega) - n_0(\omega)]^2 + [k(\omega) - k_0(\omega)]^2}{[n(\omega) + n_0(\omega)]^2 + [k(\omega) + k_0(\omega)]^2}$$

Interior structure modeling

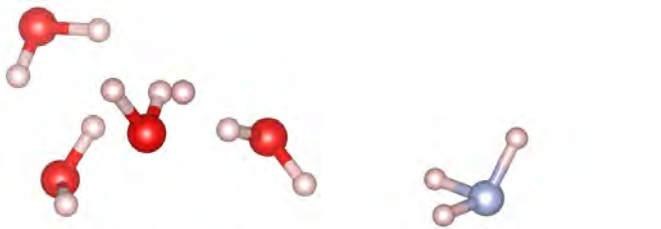

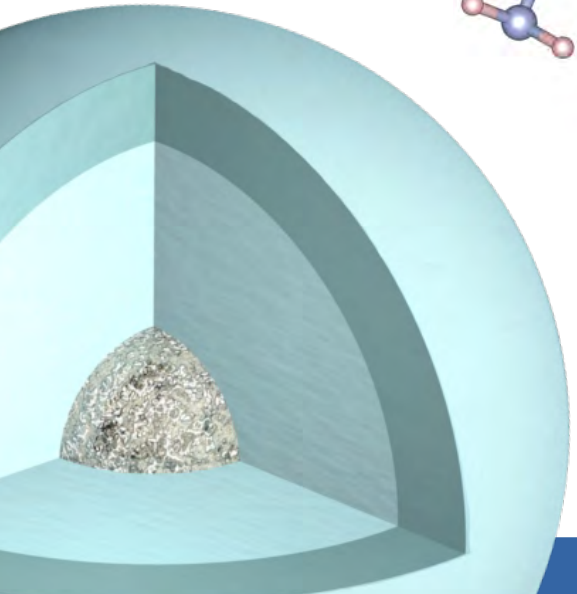

Observational constraints

- mass, radius, rotation, surface temperature
- gravitational moments
- surface and mean composition

Equations and Input

$$dm = 4\pi r^2 \varrho \, dr$$

$$\frac{dV}{dr} = \frac{1}{\varrho}\frac{dp}{dr}$$

- number and properties of layers
- equation of state (EOS)

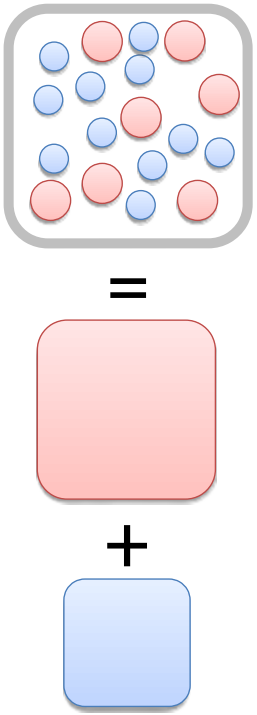

Fortney & Nettelmann, Space Sci. Rev. **152**, 443 (2010).

Linear mixing approximation for planetary ices

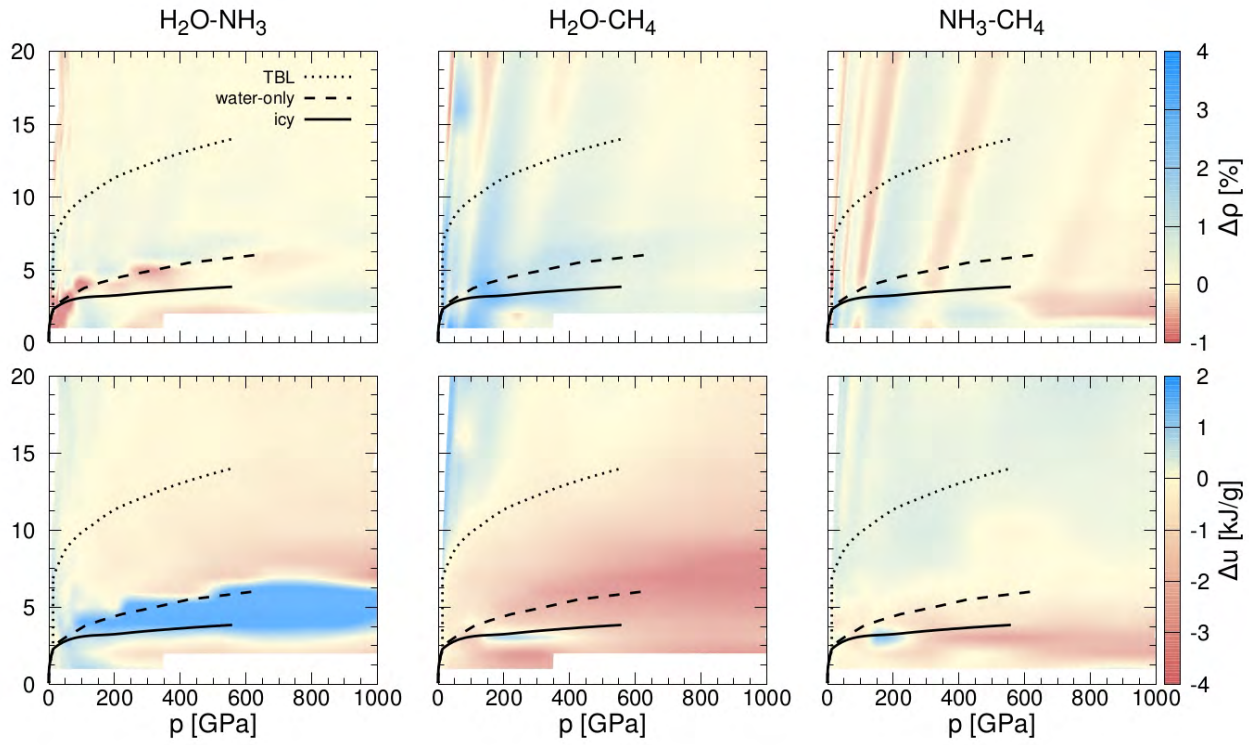

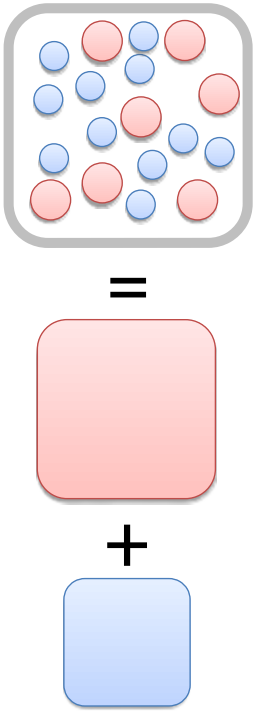

- deviations: density < 4%, energy < 4 kJ/g, diffusion < 20%

  → BUT: phase transitions matter!

Bethkenhagen et al., Astrophys. J. **848**, 67 (2017).

Improved Uranus models

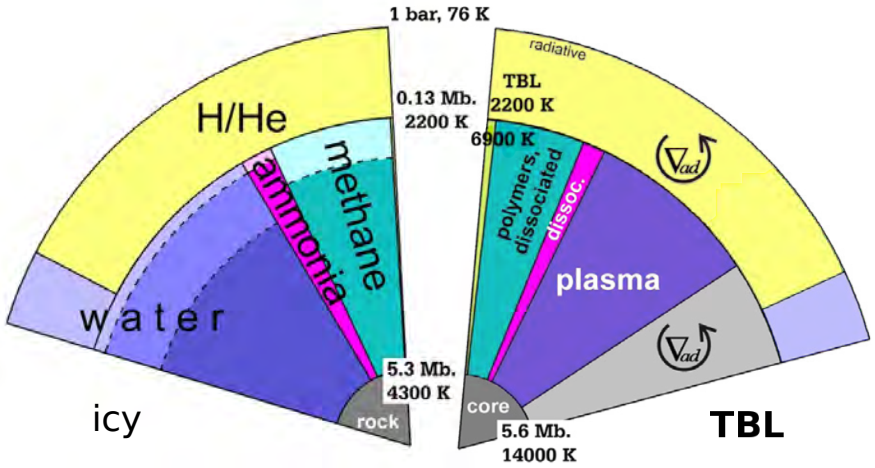

N. Nettelmann et al., Icarus **275**, 107 (2016).
M. Bethkenhagen et al. ApJ **848**, 67(2017).

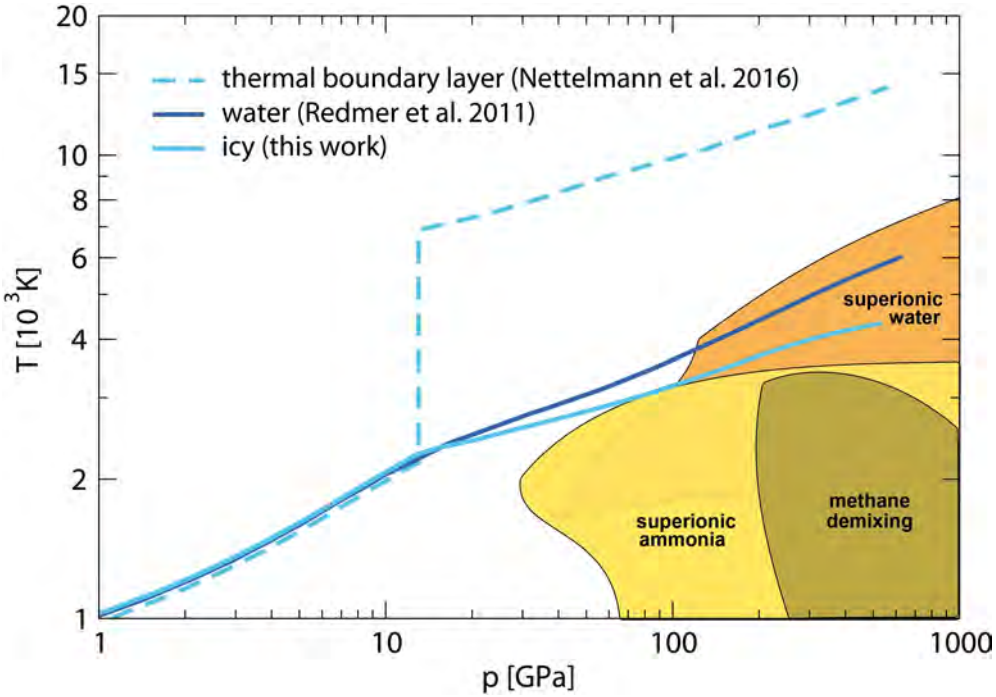

- Uranus models contain DFT-MD EOS for ammonia and methane
- Icy model: ice-richest and coldest model found, very low H/He content in inner mantle
- TBL model: non-adiabatic, thermal boundary layer adjusted to give correct age of Uranus

Future work based on the MLP

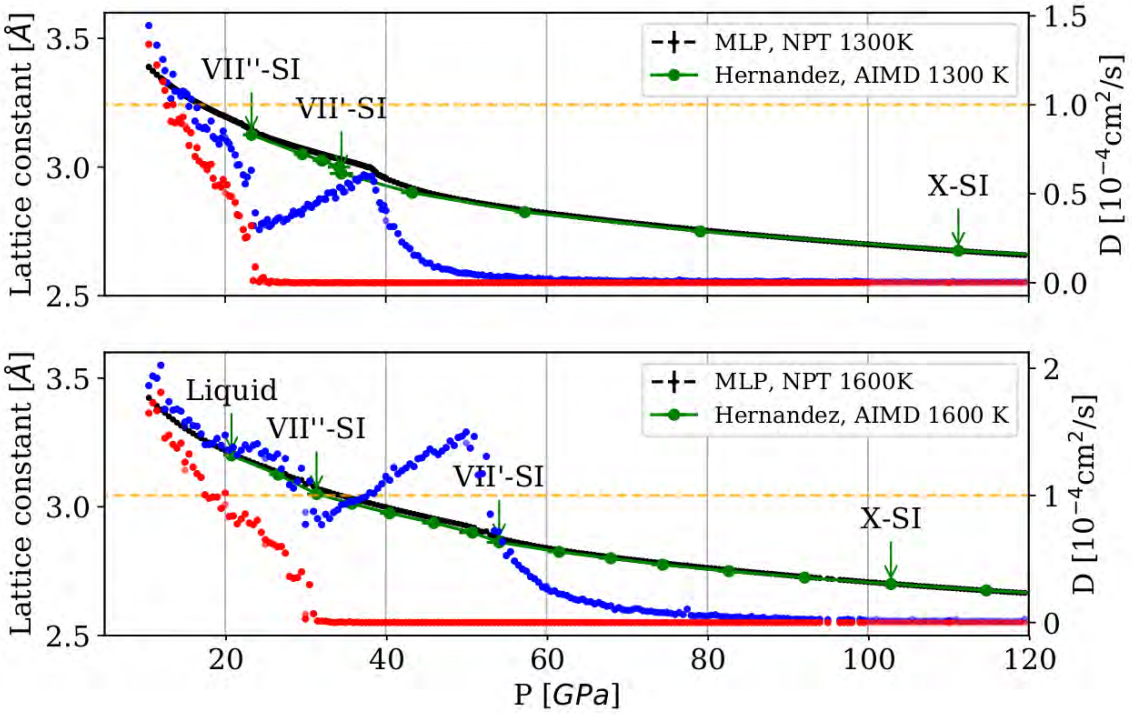

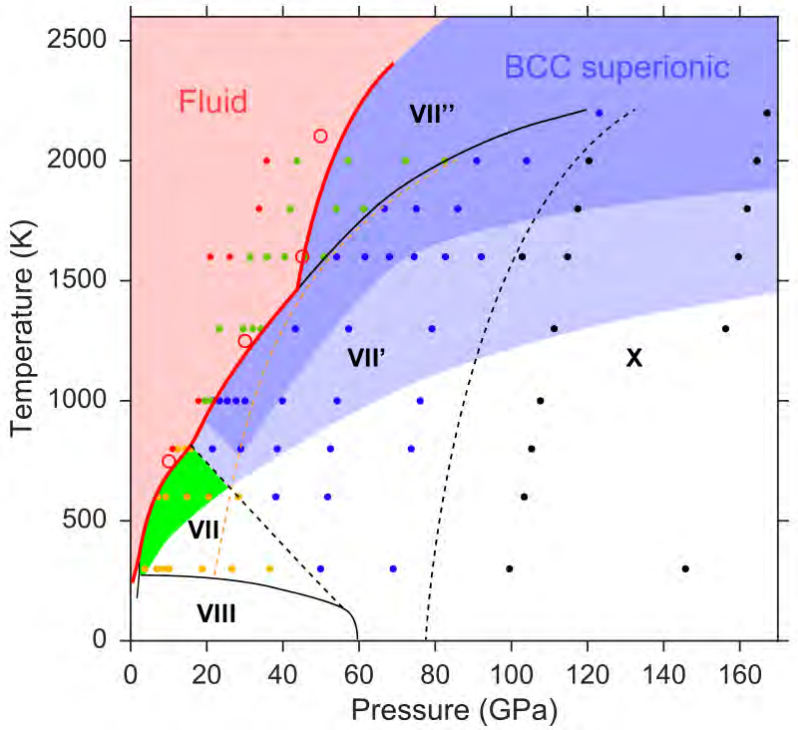

- investigate proposed ice VII' → ice VII'' phase transition with the MLP

Hernandez & Caracas, J. Chem. Phys. **148**, 214501 (2018).
Reinhardt, Bethkenhagen et al., Nat. Comm. **13**, 4707 (2022).

Other structures

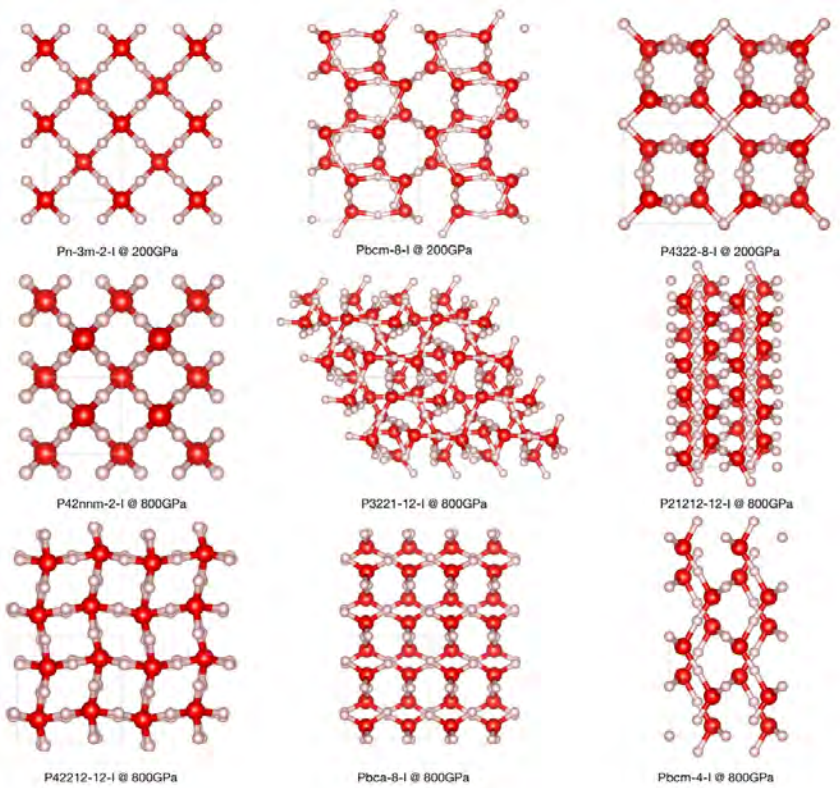

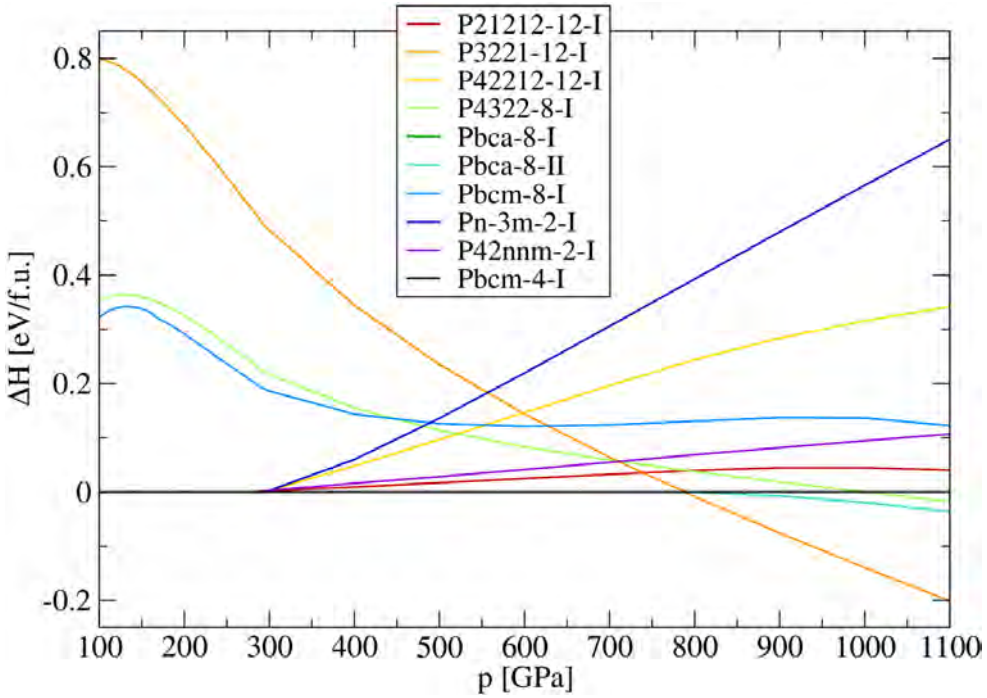

- several other structures (e.g. Pbcm) considered and will be further investigated in the future

Cheng, Bethkenhagen et al., Nat. Phys. **17**, 1228 (2021).

Chemistry – pair distribution functions

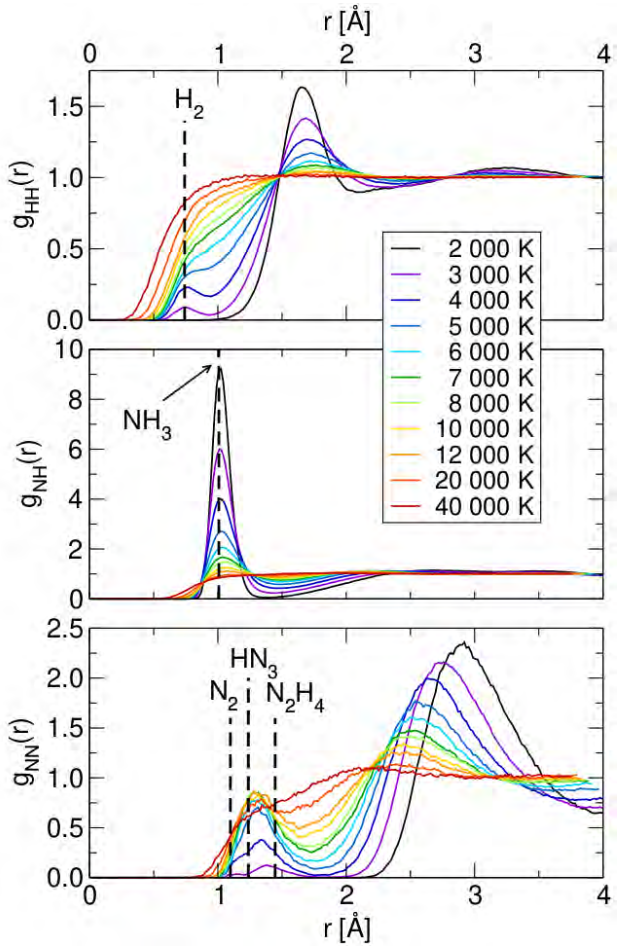

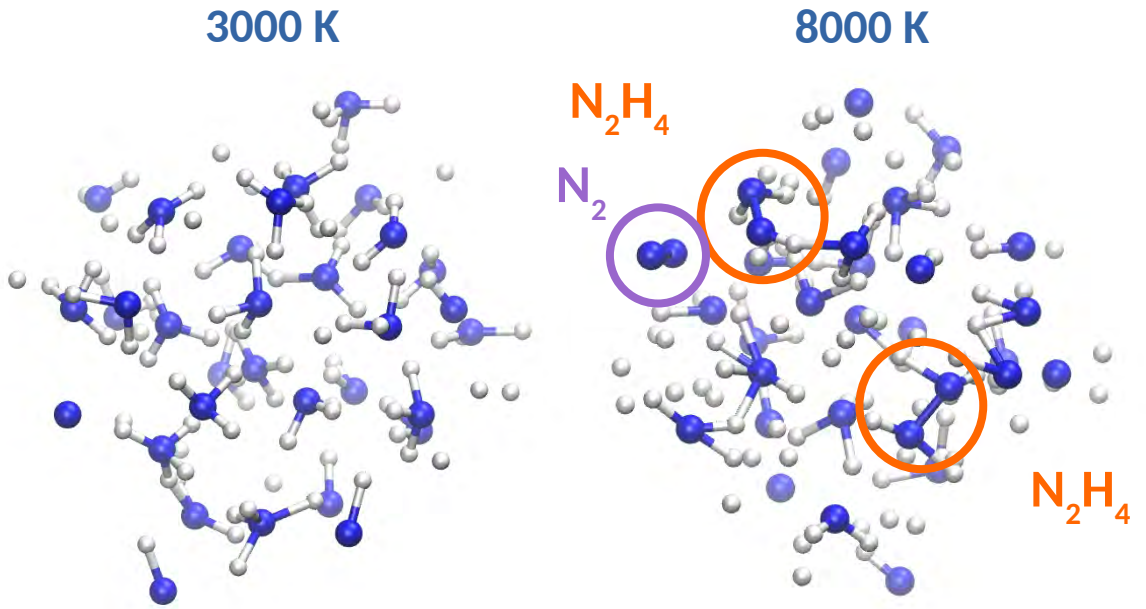

- NH_3 dissociates increasingly above 2000 K into H_2, N_2, hydrazine (N_2H_4) and sometimes even HN_3

Ravasio, Bethkenhagen et al., Phys. Rev. Lett. **126**, 025003 (2021).

Diffusion coefficients

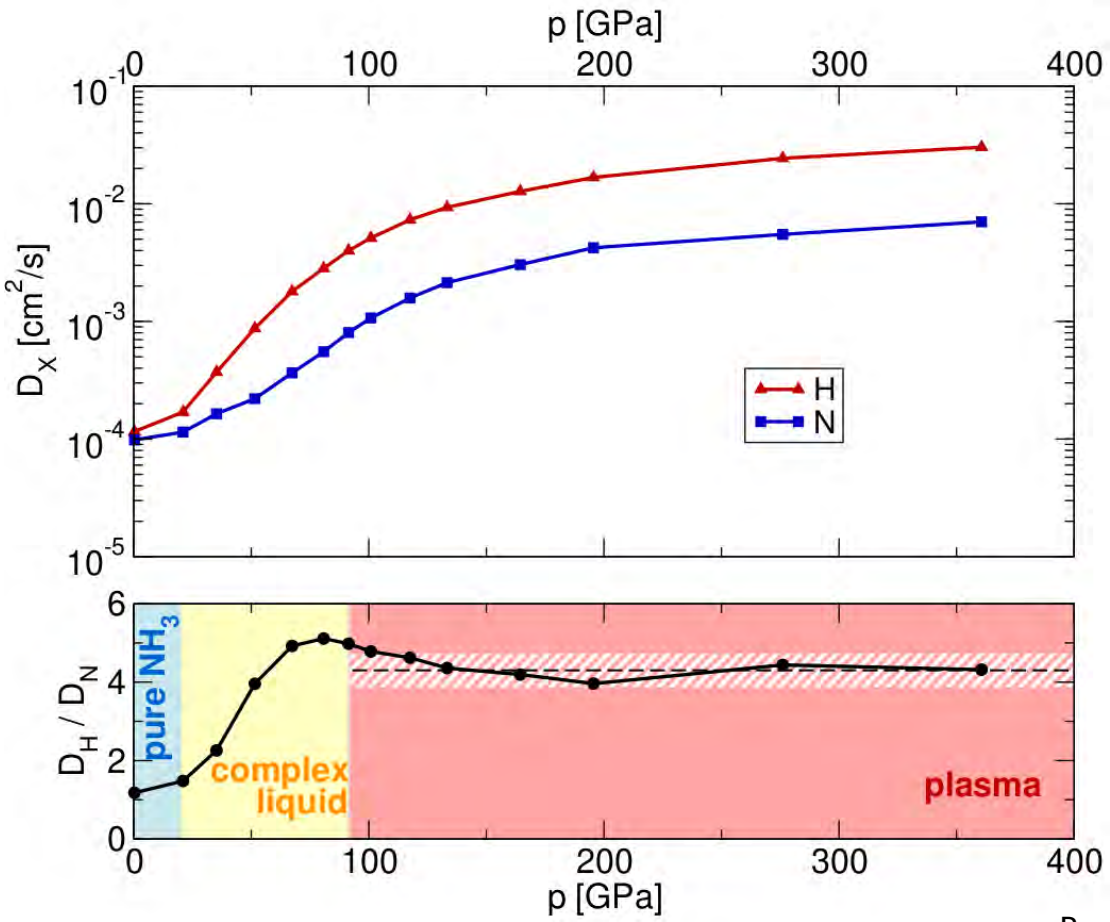

- calculated via velocity auto-correlation function
- diffusion coefficients for both species increase with temperature along Hugoniot
- slope changes slightly at 20 GPa and 90 GPa
- ratio of diffusion coefficients becomes almost constant in plasma

Ravasio, Bethkenhagen et al., Phys. Rev. Lett. **126**, 025003 (2021).

Electrical conductivity

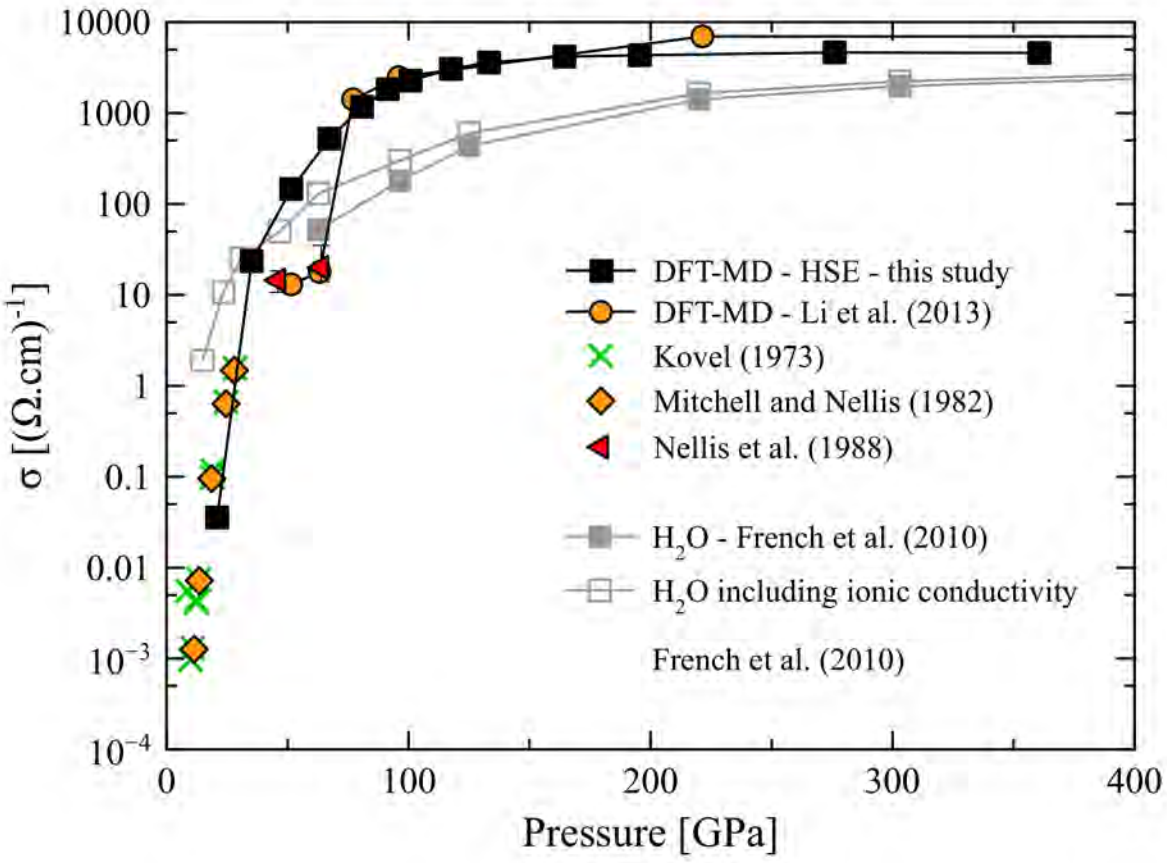

- lowest point in good agreement with previous shock-compression experiments
- significantly higher values than Li et al. (2013) ~ 70 GPa

  → superionic phase?
- overall: find larger conductivity compared to water Hugoniot

  → NH_3 conductivity 1 order of magnitude higher compared to H_2O at ~100 GPa

Kovel, PhD thesis (1973).
Mitchell & Nellis, J. Chem. Phys.**76**, 6273 (1982).
Nellis et al., Science **240**, 779 (1988).
French et al., Phys. Rev. B **82**, 174108 (2010).

Ammonia hydrates (AHH)

Phase diagram

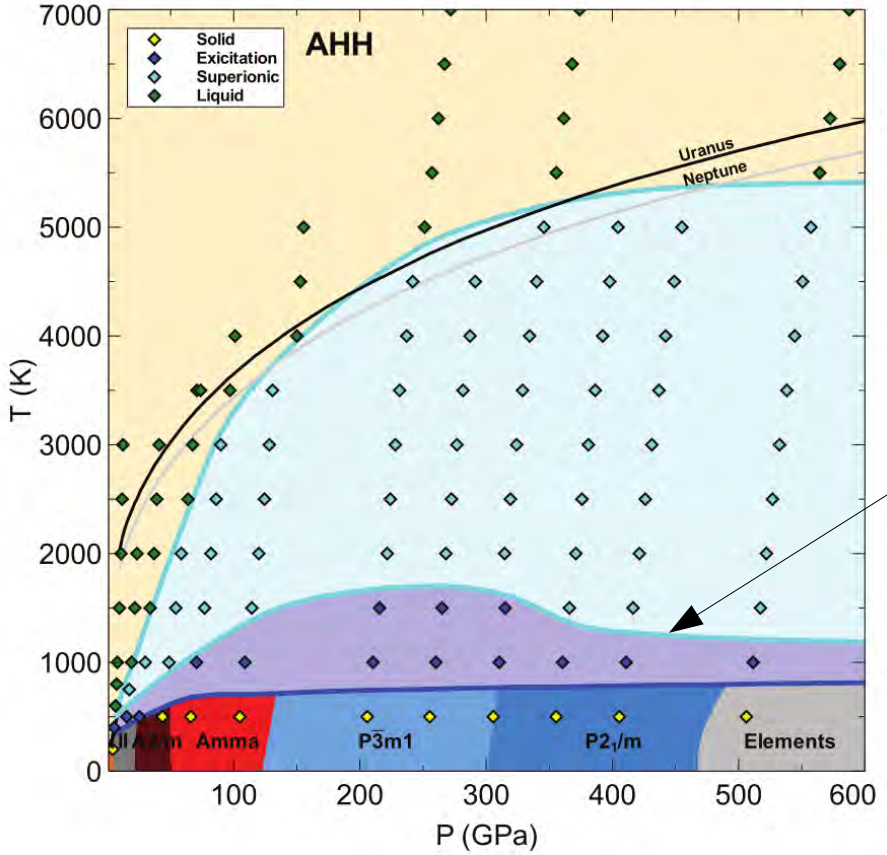

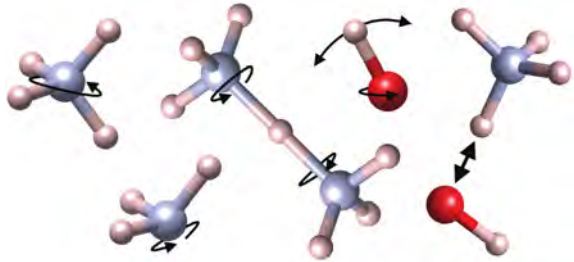

Hydrogen dynamics

excitation

Disordered Molecular Alloy

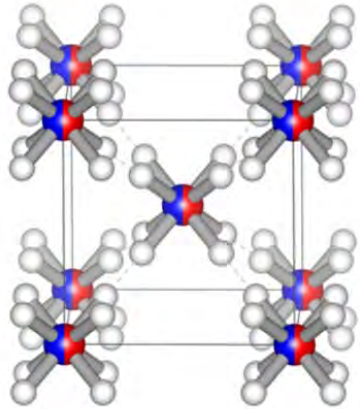

- AHH = 2:1 ammonia-water mixture

  → transitory phase between superionic and solid phases

  → disorder in the heavy ion lattice

Naden Robinson et al., PNAS **114**, 9003 (2017).
Liu et al., Nature Comm. **8**, 1065 (2017).

Zoo of superionic ammonia hydrates

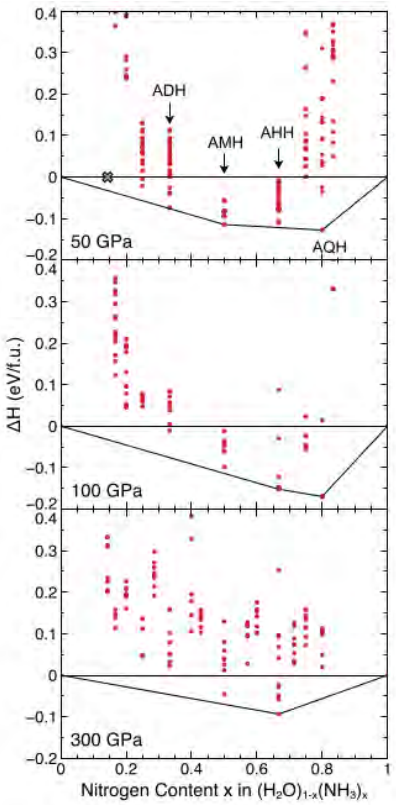

- ammonia-rich phases more stable at high pressures (AQH and AHH)
- extent of superionic region depends ammonia content
- NH_3 might be very concentrated in planetary layer, but masses very similar:

  H_2O 18 g/mol

  NH_3 17 g/mol

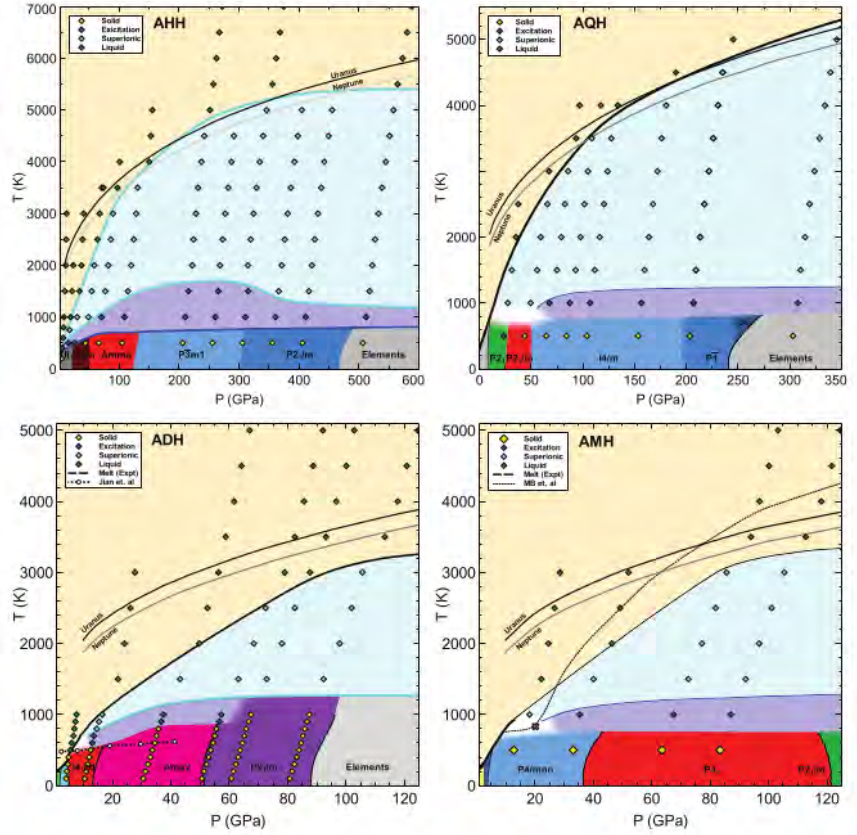

Bethkenhagen et al., J. Phys. Chem. A **119**, 10582 (2015).
Naden Robinson et al., J. Chem. Phys. **149**, 234501 (2018).
Naden Robinson & Hermann, J. Phys.: Condens. Matter **32**, 184004 (2020).

EOS and phase diagram for methane

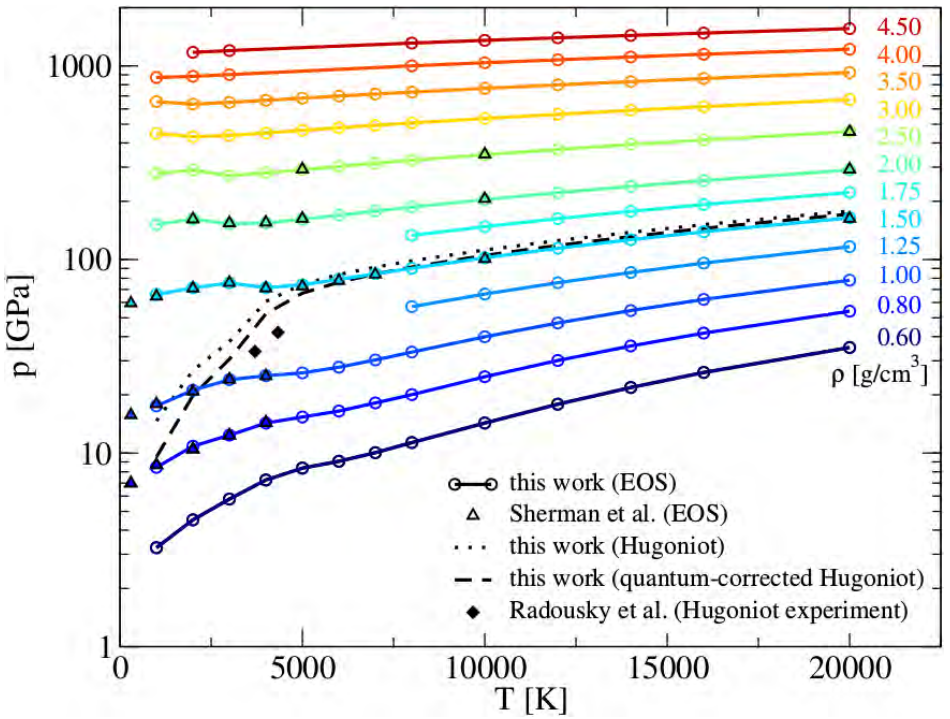

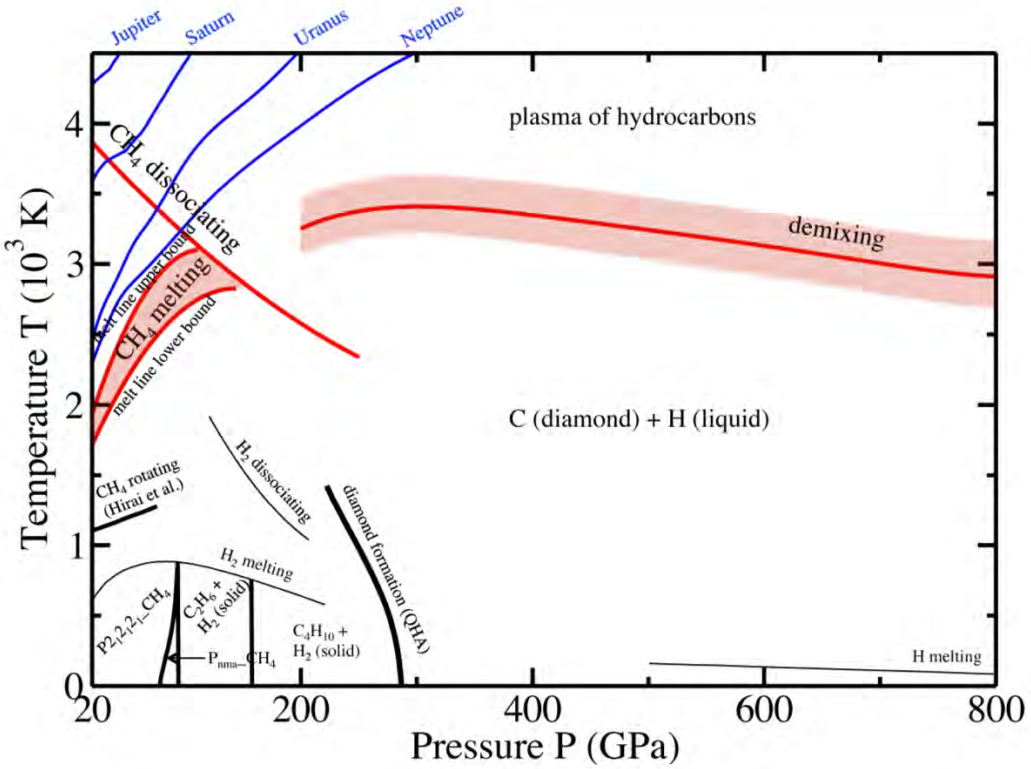

Sherman et al., Phys. Rev. B **86**, 224113 (2012).
Radousky et al., J. Chem. Phys. **93**, 8235 (1990).
Bethkenhagen et al., Astrophys. J. **848**, 67 (2017).

EOS and phase diagram for methane

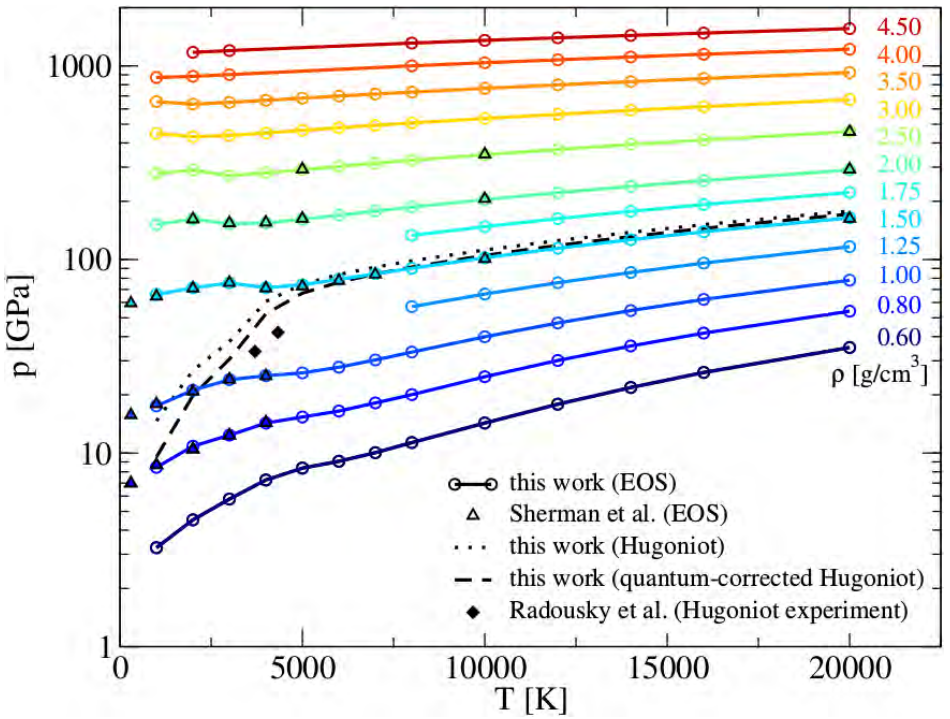

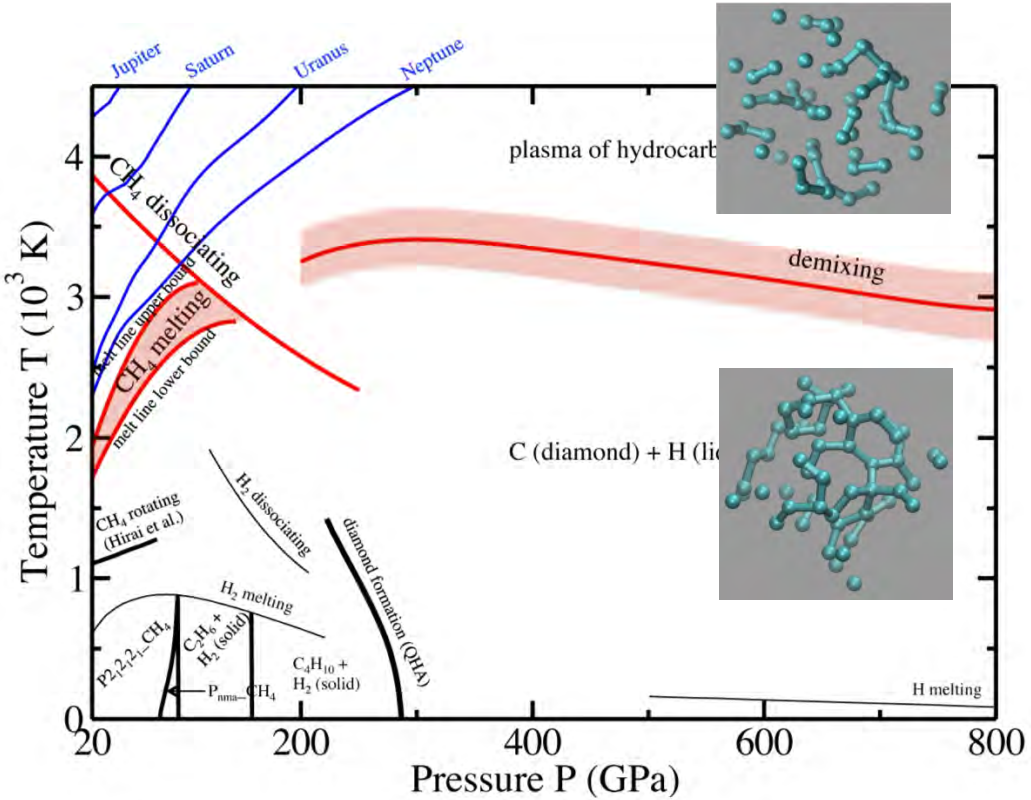

Sherman et al., Phys. Rev. B **86**, 224113 (2012).
Radousky et al., J. Chem. Phys. **93**, 8235 (1990).
Bethkenhagen et al., Astrophys. J. **848**, 67 (2017).

IV. Are superionic phases stable to the addition of rocky material?

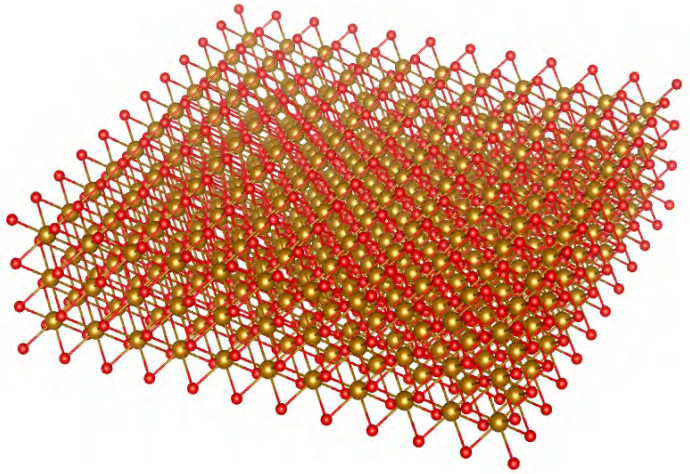

Uranus models with compositional gradients

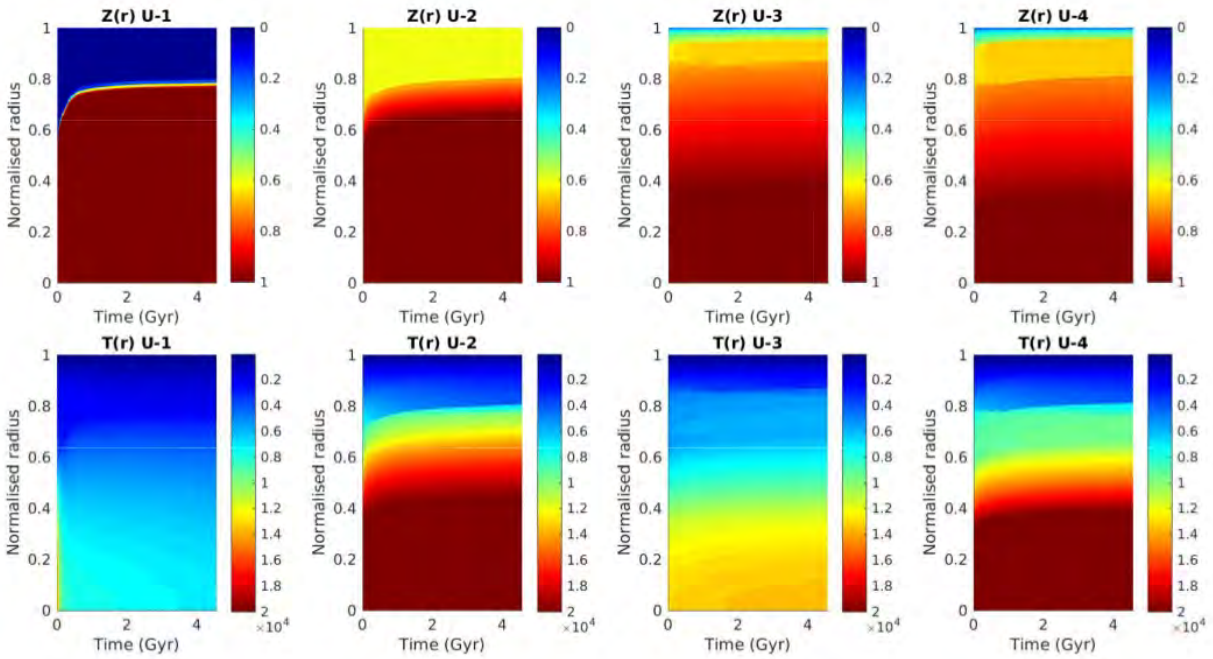

U1 – adiabatic 2-layer model (only ice)

U2 – steep Z gradient

U3 – shallow Z gradient

U4 – shallow Z gradient (rock-rich)

- compositional gradient naturally explains Uranus' low luminosity without artificial thermal boundary layer
- hot, non-adiabatic models with mixture of ice and rock in interior rather than differentiated layers plausible

A. Vazan & R. Helled, A&A **633**, A50 (2020).

Needs for more realistic models

Helled et al., Space Sci. Rev. **216**, 38(2020).

1) TBL/compositional gradients?
2) constrain the ice:rock ratio

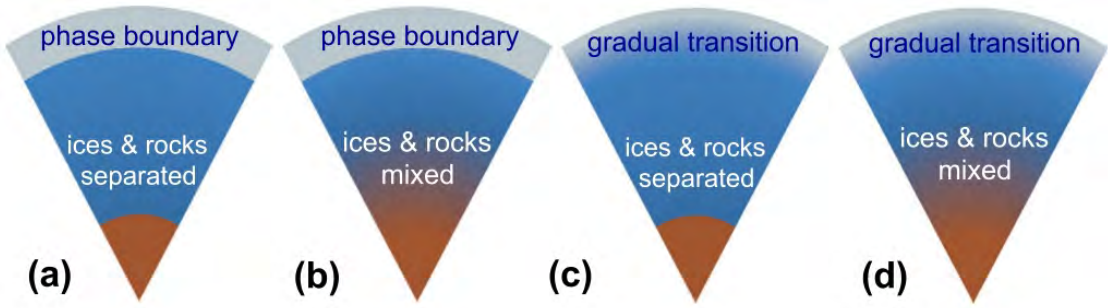

- wide-range EOS dataset for ices, rocks and their mixures based on experiment & DFT-MD
- electrical conductivity + reflectivity → mixing model for transport properties?!
- explore phase transitions (interfaces?) with classical MD with potentials derived from DFT

interface: MgO + superionic water

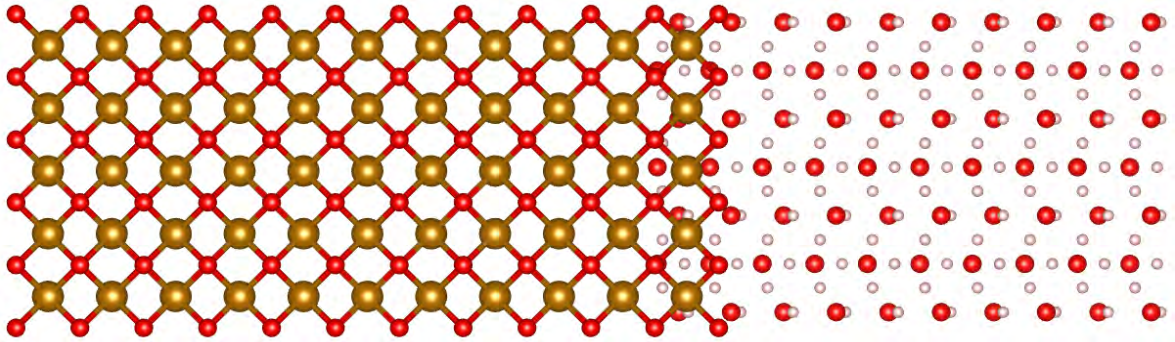

Superionic ice-rock mixtures

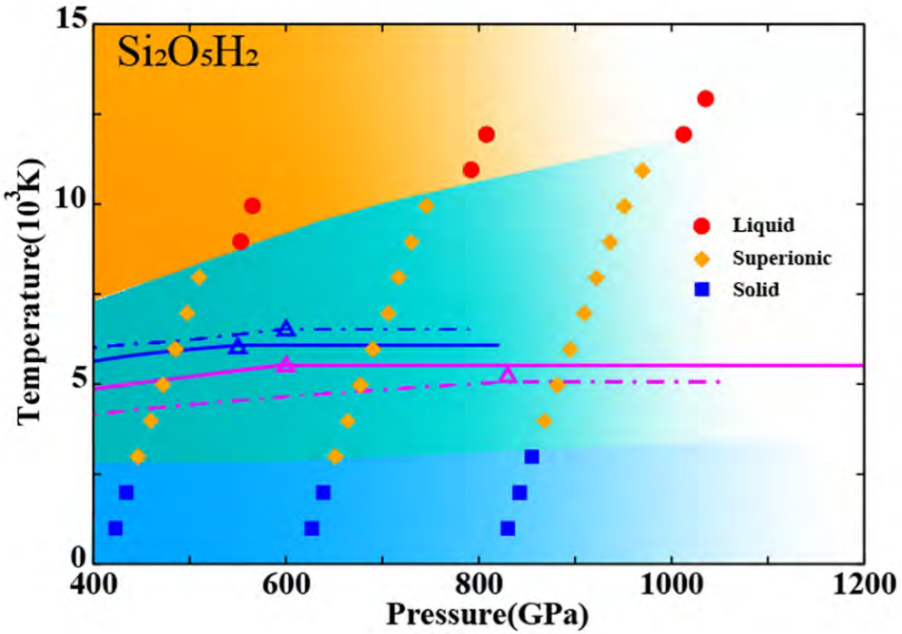

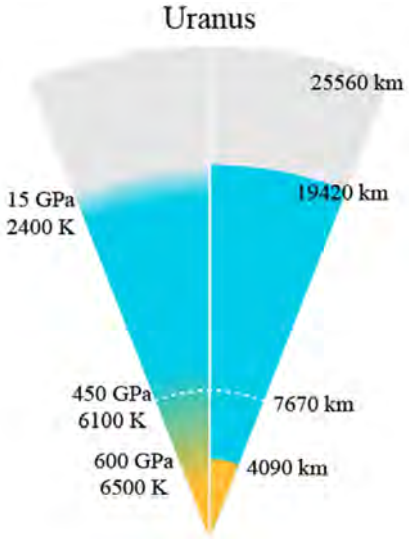

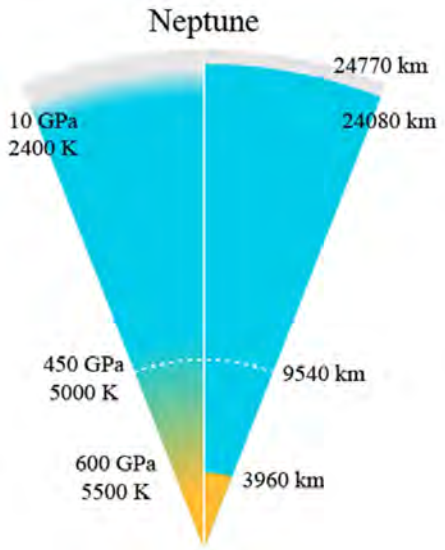

- mixtures $SiO_2 + H_2$ and $SiO_2 + H_2O$ are predicted to be superionic as well
- superionic phase seems to be stable to addition of rocky material → but thermodynamics need to be checked!

Gao et al., Phys. Rev. Lett. **128**, 035702 (2022).